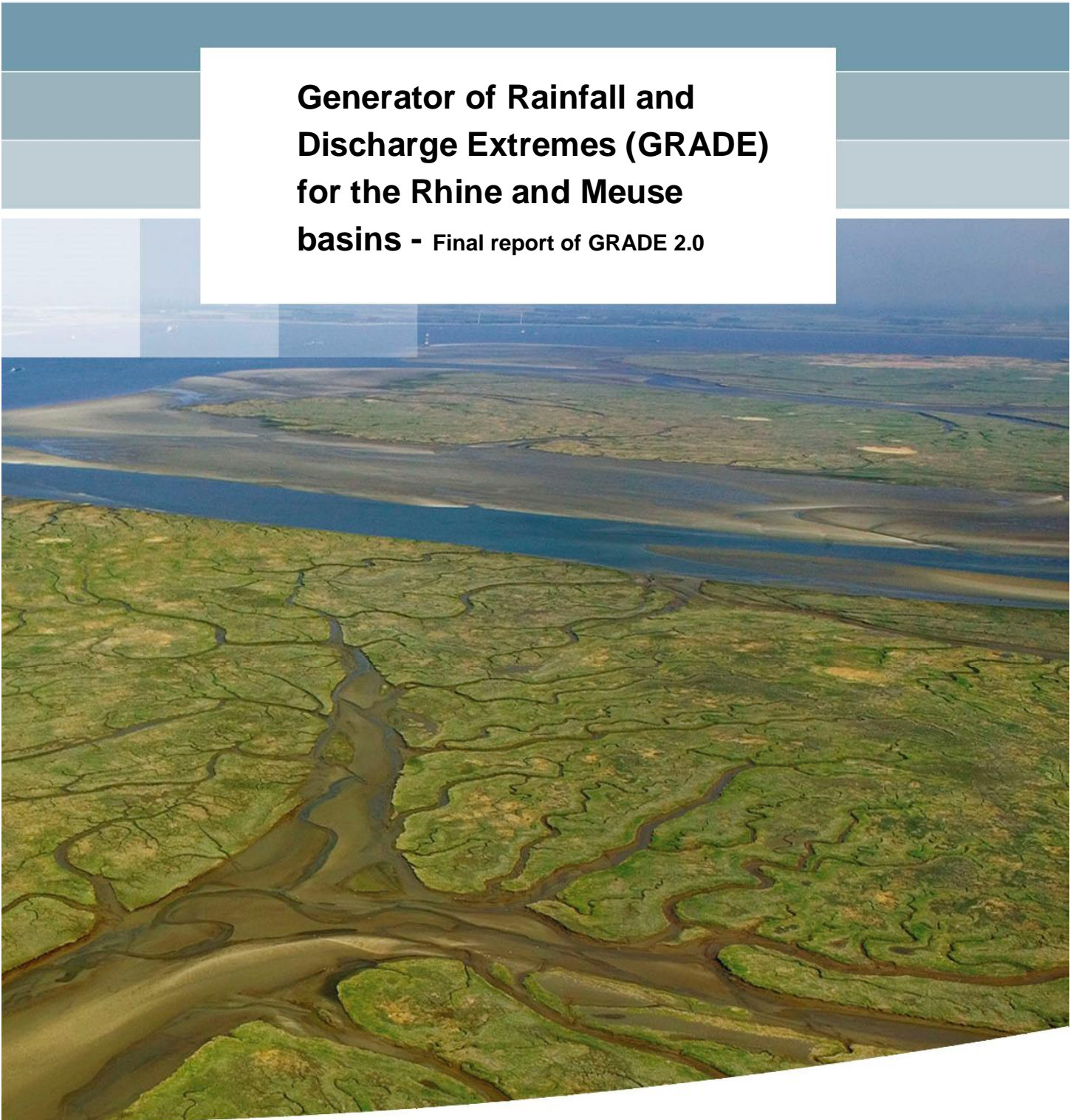


**Generator of Rainfall and
Discharge Extremes (GRADE)
for the Rhine and Meuse
basins - Final report of GRADE 2.0**



Generator of Rainfall and Discharge Extremes (GRADE) for the Rhine and Meuse basins

Final report of GRADE 2.0

M. Hegnauer (Deltares)
J.J. Beersma (KNMI)
H.F.P. van den Boogaard (Deltares)
T.A. Buishand (KNMI)
R.H. Passchier (Deltares)

1209424-004

To the memory of

Marcel de Wit

a great expert of the Meuse basin
and supporter of GRADE

Title

Generator of Rainfall and Discharge Extremes (GRADE) for the Rhine and Meuse basins – Final report of GRADE 2.0

Client	Project	Reference	Pages
Rijkswaterstaat (WVL)	1209424-004	1209424-004-ZWS-0018	84

Keywords

GRADE, river discharge statistics, weather generator, hydrology, hydraulics, Rhine, Meuse, uncertainty analysis, flooding

Summary

Currently the design discharges for the rivers Rhine and Meuse are based on a statistical analysis of observed discharges.

A new method has been developed to derive the design discharges and associated flood hydrographs for the rivers Rhine and Meuse. Stochastic simulation of the weather and hydrological/hydrodynamic modeling are the key elements of this method. The new instrument, called GRADE (Generator of Rainfall And Discharge Extremes), is meant to provide an alternative, more physically based method for the estimation of the design discharge. The GRADE method includes the following components:

Component 1: Stochastic weather generator

The stochastic weather generators used for the Meuse and Rhine basins produce daily rainfall and temperature series. The stochastic weather generator is based on nearest-neighbour resampling and produces rainfall and temperature series that preserve the statistical properties of the original series.

Component 2: HBV model

The HBV rainfall-runoff model calculates the runoff from the synthetic precipitation and temperature series. Temperature is needed to account for temporal snow storage as well as evapotranspiration losses.

Component 3: Hydrologic and hydrodynamic routing

This component of GRADE routes the runoff generated by HBV through the main river. For the Meuse the Sobek hydrodynamic model is used for the main river stretch between Chooz (on the French/Belgian border) and Borgharen, and for the Rhine for the main stretch from Maxau to Lobith. For the Rhine, two models are used, one where the effect of flooding of the dikes in Germany is incorporated in the model and one without flooding behind dikes.

The individual GRADE components were tested extensively. The precipitation series simulated by the weather generator preserve the statistical properties of observed daily precipitation, in particular the distributions of multi-day winter precipitation. The HBV models were calibrated using a GLUE (Generalized Likelihood Uncertainty Estimation) analysis and validated for historical flood events. For small sub-basins of the river Rhine, with a response to precipitation of less than a day (with many of these in Switzerland), the HBV-models perform less well. For larger sub-basins however, and for the whole Rhine and Meuse basins, the simulated discharges fit well to the corresponding observed discharge series for many gauging stations. The hydrodynamic routing component was tested for the same historical period as for the HBV model. The simulated discharge series were compared with the observed discharges at the gauging stations at Lobith (Rhine) and Borgharen (Meuse). Annual discharge maxima are satisfactorily reproduced.

Title
 Generator of Rainfall and Discharge Extremes
 (GRADE) for the Rhine and Meuse basins

Client Rijkswaterstaat (WVL)	Project 1209424-004	Reference 1209424-004-ZWS-0018	Pages 84
--	-------------------------------	--	--------------------

Long simulations with GRADE (of length 50,000-year) are performed and frequency discharge curves and flood hydrographs are derived. The frequency discharge curves reproduce the distributions of the observed annual maximum discharges well. Extreme discharge peaks on the Rhine are substantially reduced by upstream flooding. As a result of flooding the flood hydrograph becomes flatter. The effect of flooding cannot be taken into account in the current method of deriving design discharges and corresponding flood hydrographs.

The uncertainty in the components of GRADE as well as the overall uncertainty in the GRADE simulations is quantified. Two major sources of uncertainty are evaluated, which are the uncertainty in the current precipitation climate (owing to the limited length of the historical precipitation series used in the weather generator) and the uncertainty in the hydrological modeling. For the latter use is made of the results from the GLUE analysis. The combined uncertainty is obtained for return periods up to 100,000 years. As a result of upstream flooding in the Rhine the width of the uncertainty band for the frequency-discharge curve is reduced considerably. The uncertainty of flooding parameters is not taken into account. A sensitivity analysis showed that the impact of flooding is most sensitive to variations in the dike height.

Altogether, GRADE provides a more physically based (and thus more realistic) assessment of extreme discharge statistics and corresponding hydrographs, compared to the current method especially for the Rhine at Lobith in the discharge range where upstream flooding occurs as a result of the current hydraulic conditions.

GRADE has a large potential for applications in wider sense. The method can, for example, also be used for "what-if" scenario analysis. The effect of changes in river geometry (e.g. retention measures), differences in land use or climate change can be taken into account relatively easy. Although this report mainly shows the results at the Dutch border gauging stations Lobith and Borgharen, with GRADE it is also possible to provide the same (statistical) information for other locations in the river basins.

Version	Date	Author	Initials	Review	Initials	Approval	Initials
	nov. 2014	M. Hegnauer (Deltares)		J.C.J. Kwadijk		G. Blom	
		J.J. Beersma (KNMI)					
		H.F.P. van den Boogaard (Deltares)					
		T.A. Buishand (KNMI)					
		R.H. Passchier (Deltares)					

State
 final

Contents

1 Introduction	1
1.1 Scope of the report	1
1.2 The need for the development of GRADE	1
1.3 Short description of the components in GRADE	3
1.4 Presentation of GRADE in this report	5
2 Hydrological background	7
2.1 The hydrology of the Meuse basin	7
2.2 The hydrology of the Rhine basin	8
3 Stochastic Weather Generator	11
3.1 Description of the weather generator	11
3.2 Weather generator for the Rhine basin	12
3.3 Weather generator for the Meuse basin	14
3.4 Limitations of the weather generator	16
4 Hydrological modelling	19
4.1 Description of the HBV model	19
4.2 HBV in GRADE	20
4.2.1 Concept	20
4.2.2 The river Meuse	20
4.2.3 The river Rhine	21
4.3 Calibration	22
4.3.1 The GLUE method	23
4.3.2 The GLUE method applied for the Meuse	24
4.3.3 The GLUE method applied for the Rhine	25
4.3.4 Results HBV model for the Meuse	27
4.3.5 Results HBV model for the Rhine	27
4.4 Limitations of the HBV model	31
5 Flood routing	33
5.1 Description of the flood routing	33
5.2 Flood routing Meuse	33
5.3 Flood routing Rhine	34
5.4 Simulation of historical floods in the river Meuse	38
5.5 Simulation of historical floods in the river Rhine	41
5.6 Limitations of the routing module in representing extreme floods	45
6 Construction of frequency-discharge curves and flood hydrographs	47
6.1 Frequency discharge curve	47
6.1.1 Methodology	47
6.1.2 Results	47
6.2 Shape of the flood hydrograph	49
6.2.1 Methodology	49
6.2.2 Results	51

7 Uncertainty analysis	55
7.1 Uncertainty in stochastic weather generation	55
7.2 Uncertainty in hydrological modelling	59
7.3 Uncertainty in hydrodynamic modelling	63
7.3.1 Uncertainty in Sobek	63
7.3.2 Uncertainty in flooding	63
7.4 Combining uncertainties	63
7.4.1 Reduction of computation time	63
7.4.2 Procedure for combining uncertainties	65
7.5 Frequency discharge curve with uncertainty band	66
7.6 Limitations of the uncertainty analysis	67
8 Final results of the GRADE simulations	69
8.1 Frequency discharge curves	69
8.2 Flood hydrographs	73
9 Conclusions	75
Acknowledgements	77
Relevant GRADE reports	79
Literature	81

1 Introduction

1.1 Scope of the report

A large part of the Netherlands is situated in the delta of the rivers Rhine and Meuse. Flood protection is therefore an important issue in the Netherlands. By law, periodically the flood protection system in the Netherlands is assessed, meaning an evaluation of the current state of the flood protection for the primary flood defences, the design discharges and the corresponding flood hydrographs. Currently the design discharges for the rivers Rhine and Meuse are based on a statistical analysis of observed discharges. Probability distributions are fitted to the observed discharge peaks and used to extrapolate to discharges for long return periods. The observed hydrographs are upscaled to obtain a representative shape of the flood hydrograph.

A new method has been developed to derive the design discharges and associated flood hydrographs for the rivers Rhine and Meuse. Stochastic simulation of the weather and hydrological/hydrodynamic modelling are the key elements of this method. The new instrument, called GRADE (**G**enerator of **R**ainfall **A**nd **D**ischarge **E**xtrêmes), is meant to provide an alternative, more physically based method for the estimation of the design discharge. The output of GRADE also fulfils the requirements of methods for new flooding standards that will be implemented in the coming years.

This report gives an overview of GRADE and the results of the application of this new instrument to determine flood peaks and corresponding flood hydrographs for the rivers Rhine and Meuse. The objectives of the report are to provide:

- An extensive summary of the GRADE system and its components.
- An overview of the overall performance of GRADE as well as for the individual components.
- The strong points and the limitations of the GRADE instrument.
- A discussion of the uncertainties in the GRADE components and the combination of uncertainties.

1.2 The need for the development of GRADE

In the Netherlands the design and evaluation of the flood protection system along the non-tidal part of the rivers Rhine and Meuse is currently based on the estimated discharge corresponding with a return period T of 1250 years (the 1250-year return level) at or near the point where these rivers enter the Netherlands (Lobith for the Rhine and Borgharen for the Meuse) and the flood hydrograph associated with this peak discharge (Ministerie van Verkeer en Waterstaat, 2007).

The current method for the determination of the design discharges uses four types of probability distributions. These are fitted to the (flood) peaks in the discharge records starting at the beginning of the 20th century and the resulting return levels are then simply averaged. Though the computational procedure is relatively simple and straightforward, it has severe limitations.

These limitations include:

- The observed series is not representative of floods, in particular when upstream flooding has a considerable effect on the resulting flood wave. The current method cannot take this into account.
- Use of arbitrarily selected probability distribution functions with diverging extrapolations.
- Large sensitivity to addition of extreme events.
- Inhomogeneity of the long discharge series due to changes in the river geometry and upstream basin.
- Lack of flexibility to incorporate land use changes and interventions in the hydraulic infrastructure (such as retention measures) and effects of climate change.

The design flood hydrograph in the current method is based on upscaling of selected observed hydrographs to the peak value corresponding with a return period T of 1250 years. Shortcomings of this procedure include scaling effects, effect of arbitrary cut off criteria and extrapolation procedures, which lead to unrealistic flood hydrograph shapes. The effect of upstream flooding, which results in wider hydrographs, is not incorporated in the current method.

The shortcomings of the current method have been recognized in the early 1990s during the study of the first Boertien Commission (Waterloopkundig Laboratorium en EAC-RAND, 1993a,b). They suggested that the use of hydrological and hydrodynamic models in combination with extreme meteorological conditions would provide a better understanding of extreme river discharges and their probabilities. The former Institute of Inland Water Management and Waste Water Treatment (RIZA) adopted this idea in a possible alternative to determine the design discharge (Parmet and Van Bennekom, 1998). Besides a hydrological/hydrodynamic model, the development of a stochastic weather generator was foreseen to produce long (i.e., thousands of years) synthetic rainfall series. The development of the new method started with the Rhine basin (Parmet et al., 1999; Eberle et al., 2002). The weather generator for the Meuse basin was completed in 2004 (Leander and Buishand, 2004b) and used for discharge simulations (Aalders et al., 2004) in the same year. In the following years, the weather generator was explored further, the hydrological model was recalibrated, and river routing modules were added under the name GRADE.

GRADE provides discharge series with a length of up to 50,000 years, based on precipitation and temperature series from a weather generator. The weather data is fed into rainfall-runoff models from which the output is routed through the river by a hydrodynamic model. The latter model represents the physical characteristics of the hydraulic infrastructure. The advantage of incorporating these models is that effects of the existing, or planned, hydraulic infrastructure on the flood waves can be taken into consideration. Because of the long time series there is no longer a need for extrapolation of distributions and upscaling of hydrographs.

However, in GRADE, a part of the shortcomings of the current method is shifted to the climatic series created by the weather generator and to the transformation of these series into river discharges, but in principle all limitations in the hydraulic infrastructure can be taken into consideration. In addition, with GRADE it is easier to assess the effect of changes in the river geometry and in the upstream basin as well as the impact of climate change on floods.

The difference between GRADE and the current method is schematically shown in Figure 1.1.

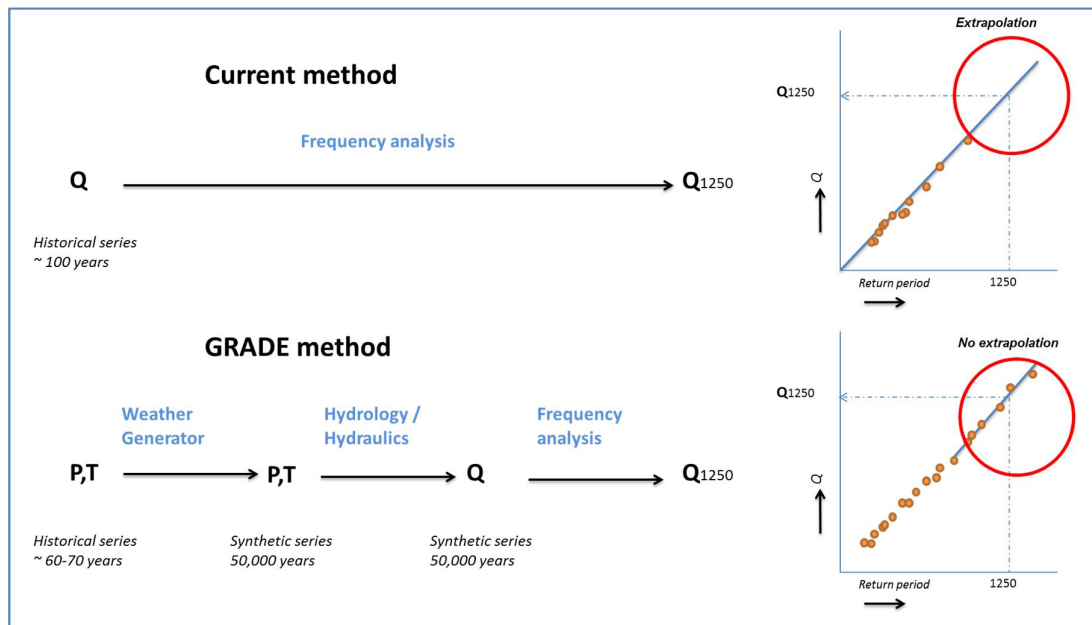


Figure 1.1 Comparison of the current method with the GRADE method. P , T and Q denote precipitation, temperature and discharge respectively. Q_{1250} is the 1250-year discharge

1.3 Short description of the components in GRADE

The GRADE method includes the following components (Figure 1.2):

Component 1: Stochastic weather generator

The stochastic weather generators used for the Meuse and Rhine basins produce daily rainfall and temperature series. The stochastic weather generator is based on nearest-neighbour resampling and produces rainfall and temperature series that preserve the statistical properties of the original series.

Component 2: HBV model

The HBV rainfall-runoff model calculates the runoff from the synthetic precipitation and temperature series. Temperature is needed to account for temporal snow storage as well as evapotranspiration losses. HBV is a conceptual hydrological model of interconnected linear and non-linear storage elements. It is widely used internationally under various climatic conditions and it forms also the basis for the flood forecasting system in the Netherlands of the rivers Rhine and Meuse.

Component 3: Hydrologic and hydrodynamic routing

This component of GRADE routes the runoff generated by HBV through the river stretches. For both the rivers Meuse and Rhine, a simplified hydrologic routing module is used in HBV, but this does not simulate well the physical processes such as retention and flooding. Therefore a hydrodynamic routing component is added. For this purpose, the Sobek hydrodynamic model is used for the Meuse starting from the station of Chooz on the French/Belgian border and for the Rhine from Maxau on the main river. However, only the largest flood waves are simulated with the Sobek model. These flood waves are selected from the results with the simple built-in routing in the hydrological model. This is done, because a full hydrodynamic simulation of the synthetic series is computationally not feasible.

The stochastic weather generator is a stand-alone application which currently runs at the Royal Netherlands Meteorological Institute (KNMI). The output of the weather generator and the other components of GRADE are built into a software package of Deltares, called Delft-FEWS. This environment allows the user to work with pre-programmed workflows for most of the steps in the application of GRADE.

During the development of GRADE a vast number of studies have been done to test the performance of both the method as a whole as well as the individual components.

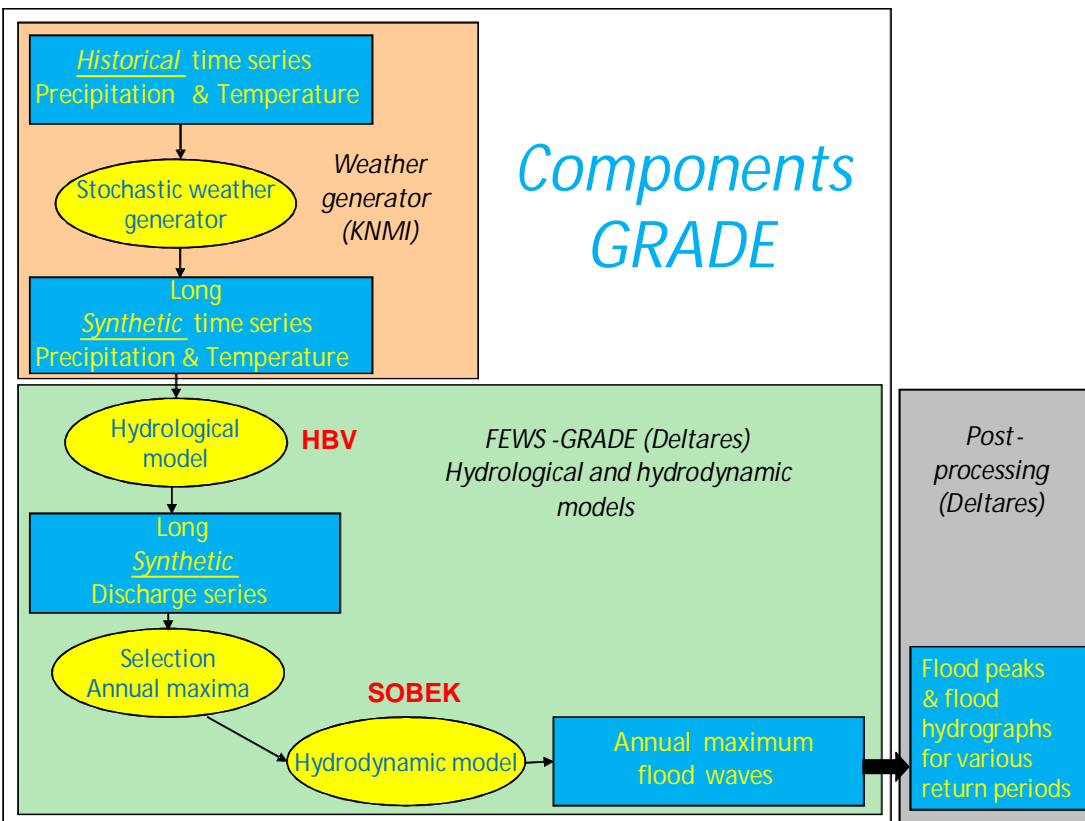


Figure 1.2 Components of GRADE

1.4 Presentation of GRADE in this report

This report presents the GRADE method for the derivation of discharge statistics and associated flood hydrographs for the rivers Meuse and Rhine. In Chapter 2, the physical behaviour of the Rhine and the Meuse basins in relation to high discharges is briefly explained. In the next chapters the separate components are discussed. Chapters 3, 4 and 5 describe the stochastic weather generator, hydrological modelling and flood routing respectively.

Frequency discharge curves based on the annual maxima of the 50,000 year GRADE simulations are given in Chapter 6. The corresponding flood hydrographs are also discussed in this chapter. Chapter 7 deals with the uncertainty analysis for the individual components and the total uncertainty of the GRADE method. The final results are presented in Chapter 8 and conclusions are given in Chapter 9.

2 Hydrological background

Floods are in general caused by heavy rainfall, sometimes in combination with snowmelt. The characteristics of a flood are determined not only by the precipitation, but also by the topography, the soil, the vegetation and the hydrological state of a catchment (e.g. whether the catchment is already wet or is still dry). This chapter gives background information about the hydrology the Rhine and Meuse basins, specifically with respect to the origin of high discharges.

2.1 The hydrology of the Meuse basin

The Meuse is a rain-dominated river. Upstream of Borgharen the basin can be divided into two regions: the part upstream of Chooz (called the Lorraine) and the part between Chooz and Borgharen, where the river flows through the Belgian Ardennes (see Figure 2.1).

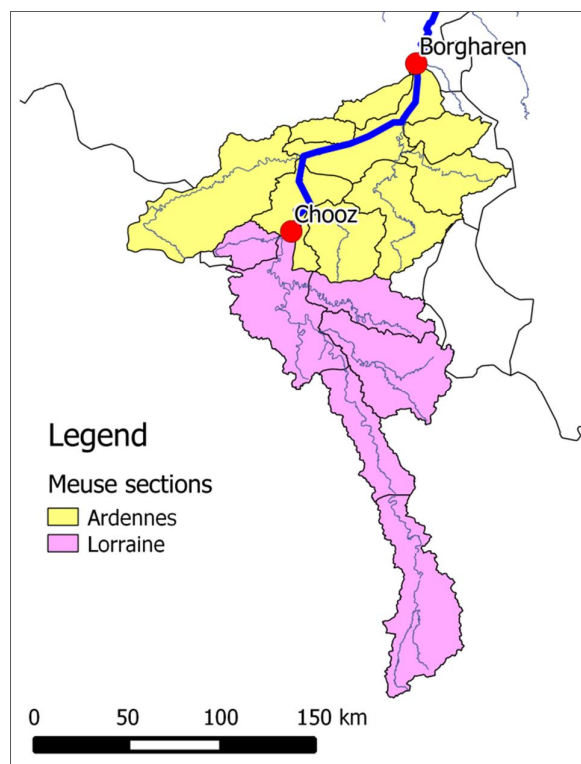


Figure 2.1 Overview of the different regions in the Meuse basin

The Lorraine is characterized by a broad river valley having wide flood plains and a gently sloping river and covers approximately 45% of the total Meuse basin upstream of Borgharen. The other part of the basin is covered by the area between Chooz and Borgharen. The contribution to the discharge at Borgharen is different from event to event. On average, both areas contribute for about 50% to the discharge at the Belgian-Dutch border. The annual pattern is similar for both regions (De Wit, 2008).

Although the contribution to the discharge at Borgharen of both areas is more or less equal, the response to precipitation is completely different for both regions. The Lorraine reacts relatively slowly to rainfall events, while the Ardennes region responds very fast to precipitation. Rainfall that falls in this area can reach Borgharen within a day. The difference between these regions has two main causes:

1. The slope of the Meuse (and its contributing streams) in the Lorraine area is much lower than the slope of the important tributaries in the Ardennes region.
2. The soil properties differ for the two regions. The Lorraine area consists primarily of porous soils, which results in a larger capacity to temporarily store precipitation in the ground, whereas the soil in de Ardennes region mainly consists of hard rock (such as slate) that impedes fast infiltration.

As a result of the difference in characteristics of the two regions and the long shape of the basin, a single large-scale rainfall event over the basin often leads to a double discharge peak at Borgharen. The first peak comes from the fast responding Ardennes regions, while the second peak comes from the slow responding Lorraine region. The difference in timing is typically in the order of a day (De Wit, 2008). This often reduces the maximum peak at Borgharen. However, in the case of multiple large-scale rainfall events on successive days, the peak flows from the different streams and regions may coincide and cause extreme flood events. An analysis by Tu (2006) has shown that the flood events in the Meuse are mainly caused by multi-day precipitation events rather than single events. Tu (2006) shows that the discharge of the Meuse correlates best with multi-day precipitation events between 5 and 15 days.

There is a predominance of the flood peaks in the winter season in the Meuse which is due to the occurrence of consecutive large-scale rainfall, in combination with wet initial soil conditions due to the limited evapotranspiration during winter. The contribution of snow melt to the discharge of the Meuse is small due to the relatively low elevation of the basin. The limited snowpack generally already melts during the winter season (De Wit, 2003), thereby potentially contributing to discharge peaks in winter.

2.2 The hydrology of the Rhine basin

Geographically the Rhine basin, upstream of Lobith, can be divided into five regions (Belz et al., 2007): the mountainous Alpine Rhine and High Rhine upstream of Basel, the Upper Rhine and Middle Rhine between Basel and Bonn which comprises the low mountain ranges and hilly areas in Germany and France and the Lower Rhine, between Bonn and Lobith which comprises the lowland region in Germany (see Figure 2.2).

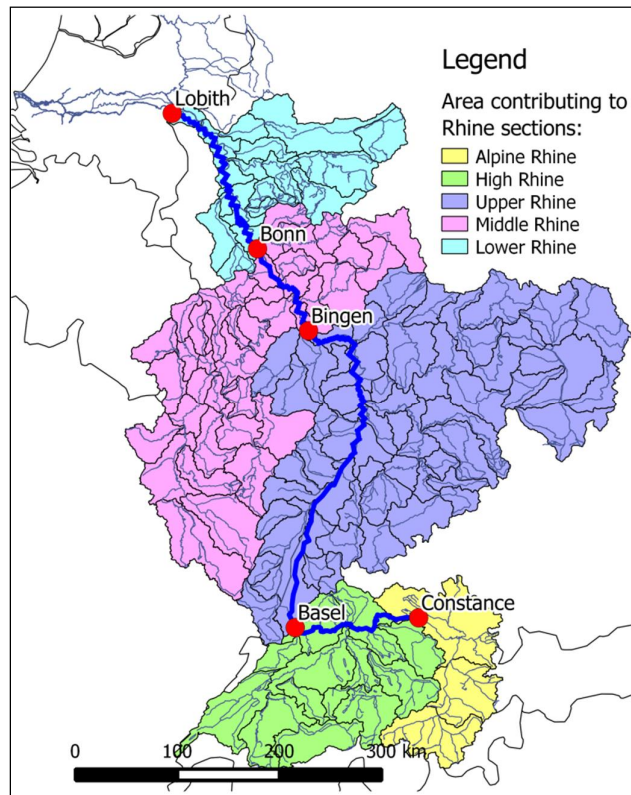


Figure 2.2 Overview of the different regions in the Rhine basin and their corresponding gauging stations

The discharge of the Rhine is determined by the amount and distribution of precipitation and evapotranspiration in the basin. A typical characteristic of the discharge of the Rhine is the change in the annual cycle of the discharge from upstream to downstream. This is illustrated in Figure 2.3 for the discharge regime of the Rhine at Basel and Lobith. The average discharge at Basel peaks at a different moment in the year than at Lobith. This shift in time is caused by the snowmelt in the Alps in spring. During the winter months, snow is stored in the Alps and runoff is limited during winter.

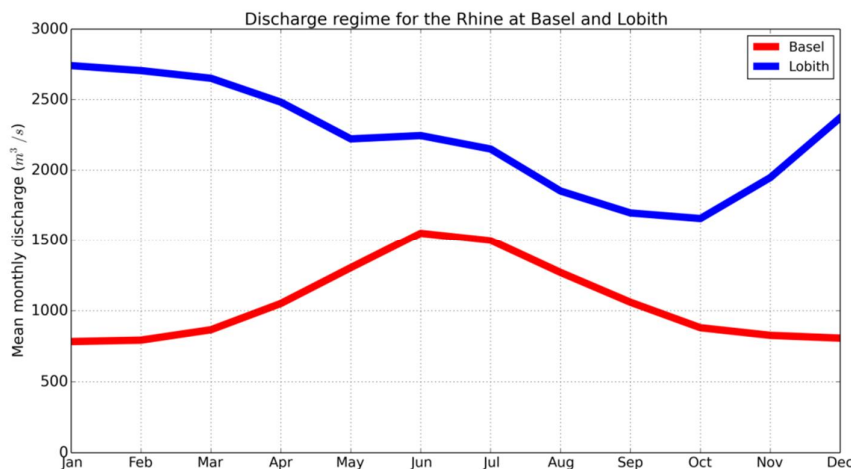


Figure 2.3 Discharge regime of the Rhine at Basel and Lobith

As for the Meuse, (extreme) flood events in the Lower Rhine typically occur during the winter and early spring. They are caused by successive large-scale rainfall events in combination with saturated soils. The coincidence of the peak flows from different tributaries is important. Flood wave travel times from Basel and Koblenz to Lobith are respectively about 5 and 2 days (Diermanse, 2000).

Snow melt, especially in combination with frozen soils, occasionally leads to more extreme runoff. Due to the size and shape of the basin, the volume as well as the height of the discharge peak strongly depends on the spatial extent and the succession of rainfall events. Different flood events show therefore quite different genesis.

As said, extreme floods on the Lower Rhine are often associated with multi-day precipitation events in winter. For example the discharge peaks during the 1993 and 1995 flood events can be related to the 10-day precipitation amounts in a large part of the basin (Disse and Engel, 2001; Ulbrich and Fink, 1995).

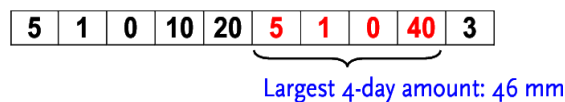
In its delta (The Netherlands) as well as those areas where the Rhine flows through a very wide valley, dikes protect the floodplains. Very high discharges, however, may locally cause overflow and/or breaking of these dikes, leading to uncontrolled flooding. Simulations of such events have shown that flooding attenuates the peak flow in the river further downstream, resulting in lower, but wider flood peaks (Lammersen, 2004).

3 Stochastic Weather Generator

3.1 Description of the weather generator

The weather generator is the first component of GRADE (Figure 1.2). This instrument is used to simulate long records of daily weather data (20,000 – 50,000 years). It is based on a nonparametric resampling technique. Daily rainfall amounts are resampled from the historical record with replacement. Although this does not give new information about the characteristics of the 1-day rainfall amounts, different temporal patterns are generated. Therefore, multi-day rainfall amounts can take values that are not observed in the historical data (Figure 3.1). The long simulated records of daily weather data provide a more accurate estimation of the statistical properties of multi-day extreme events. Buishand (2007) showed this for the estimation of the 100-year return level of 10-day rainfall from a short record of 20 years, assuming no temporal correlation of the daily values. Resampling of the daily values resulted in a reduction of the standard error by a factor of 4 compared to fitting a Generalized Extreme Value (GEV) distribution to the 10-day annual maxima. Likewise, Beersma and Buishand (2007) found a reduction of a factor 2 in the standard error of the estimated 50-year return level of the cumulative (potential) rainfall deficit for resampling of the 10-day rainfall deficits in a 95-year sequence compared to fitting a GEV distribution to the annual maximum cumulative rainfall deficits.

Recorded rainfall series



Rainfall series produced by resampling



Figure 3.1 Schematic representation of resampling. The multi-day values in the generated sequences can take values that are not observed in the historical sequence, due to the reordering of historical days. Single-day values in the generated sequences do not exceed the observed values in the historical record

The weather generators for the Rhine and Meuse basins do not generate rainfall at a single site but rainfall and temperature at multiple locations simultaneously. A major advantage of resampling historical days at multiple locations simultaneously is that both the spatial association of daily rainfall over the drainage basin and the dependence of daily rainfall and temperature are preserved without making assumptions about the underlying joint distributions. To incorporate autocorrelation, one first searches the days in the historical record with similar characteristics as those of the previously simulated day, i.e. the nearest neighbours. One of the k nearest neighbours is randomly selected and the observed values for the day subsequent to that nearest neighbour are adopted as the simulated values for the next day. A feature vector is used to find the nearest neighbours in the historical record.

This vector summarizes the temperature and precipitation over the basin and is determined for each day.

The effect of seasonal variation on the choice of nearest-neighbours is reduced by standardizing the daily precipitation amounts and temperatures and by restricting the search for nearest neighbours to days within a moving window, centred on the calendar day of interest. Standardization eliminates the annual cycle in the mean. The moving window is particularly needed to account for the seasonal variation in the dependencies between variables (e.g., relatively strong spatial correlation of precipitation in winter and weak spatial correlation in summer).

3.2 Weather generator for the Rhine basin

This weather generator generates daily precipitation and temperature simultaneously over 134 sub-basins of the Rhine upstream of Lobith, using observed daily rainfall and temperature data for the 56-year period 1951-2006. Two gridded daily precipitation data sets were used: the HYRAS 2.0 dataset (Rauthe et al., 2013) that was made available by the German Weather Service (DWD) via the Federal Institute of Hydrology (BfG), and the E-OBS dataset (Haylock et al., 2008). The HYRAS dataset has a spatial resolution of 5 km × 5 km. The E-OBS data are available on various spatial grids. For the weather generator the E-OBS data on a rotated 0.22° × 0.22° polar grid (approximately 25 km × 25 km) were used. Apart from the finer spatial resolution of the HYRAS data, the number of rainfall stations used for gridding is much larger for the HYRAS data. See Figure 3.2. Schmeits et al. (2014a) compared the two datasets with respect to mean winter and summer rainfall and 10-day maximum rainfall. The differences are small over the entire Rhine basin, but for the Swiss part of the basin the mean summer rainfall and the mean 10-day maximum rainfall in summer are about 7% larger in the HYRAS dataset. The E-OBS dataset is updated and incremented in a semi-annual cycle. For the weather generator of the Rhine basin version 7 was used, which was available from September 2012.

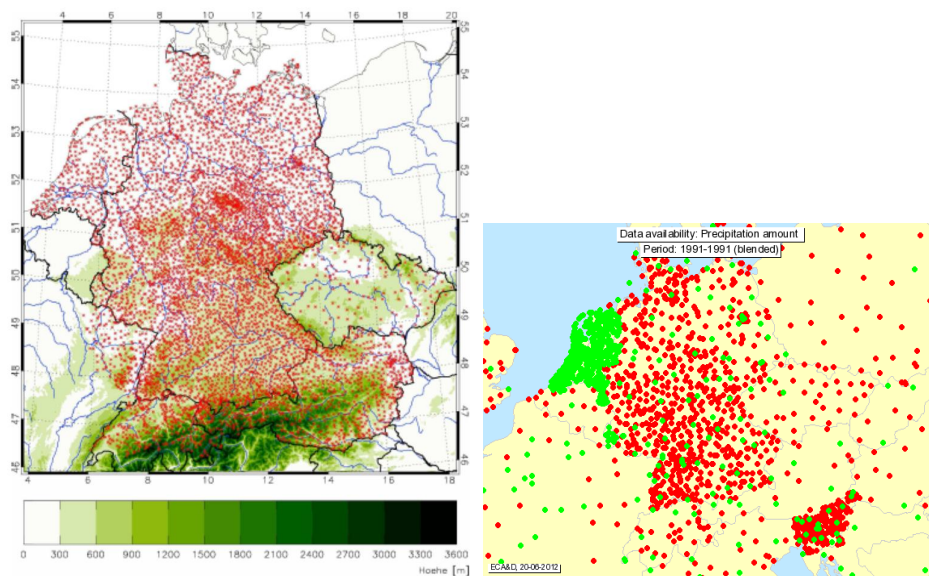


Figure 3.2 Locations of rainfall stations used for the HYRAS (left) and E-OBS (right) data. The green colour-coded stations in the right panel indicate the stations of which the data are publicly available, whereas the data of those in red are not

It is unclear to what extent the HYRAS dataset will be updated with observations after 2006. For daily temperature the E-OBS dataset was used on the same spatial grid as the E-OBS rainfall data. The daily gridded rainfall observations from HYRAS and E-OBS and the daily gridded temperature observations were converted to the 134 sub-basins of the Rhine.

Though the spatial detail of the precipitation fields from the E-OBS data may be limited for hydrological simulations in the Rhine basin, the update of these data is much more ensured than for the HYRAS data. This makes the E-OBS precipitation data attractive for driving the resampling process. First long sequences of daily precipitation and temperature were generated for the 134 sub-basins by resampling the E-OBS data, and then the resampled historical daily precipitation data were replaced by the historical HYRAS precipitation data of the same day. This second step has been indicated as passive simulation because the HYRAS data do not drive the generation of the long sequences. Such an indirect simulation may be necessary in future simulations if the data on the finer grid are not updated. For each sub-basin the daily potential evapotranspiration was derived from the simulated daily temperature. For the Rhine this is accounted for by the HBV model (see Section 4.3.3).

Figure 3.3 compares the distribution of maximum 10-day basin-average rainfall in the winter half-year (October – March) in two 50,000-year simulations, one in which the HYRAS data were directly resampled and one in which they were passively simulated. The winter half-year is considered here because extreme discharges at Lobith are often associated with large multi-day precipitation in winter (see Section 2.2). The differences between the two simulations are small. There is also a good correspondence with the distribution of the observed 10-day winter maxima. The reproduction of this distribution does not become worse when the E-OBS data are used for driving the resampling process. Note that the largest simulated 10-day rainfall amounts are much larger than the largest observed 10-day rainfall amount.

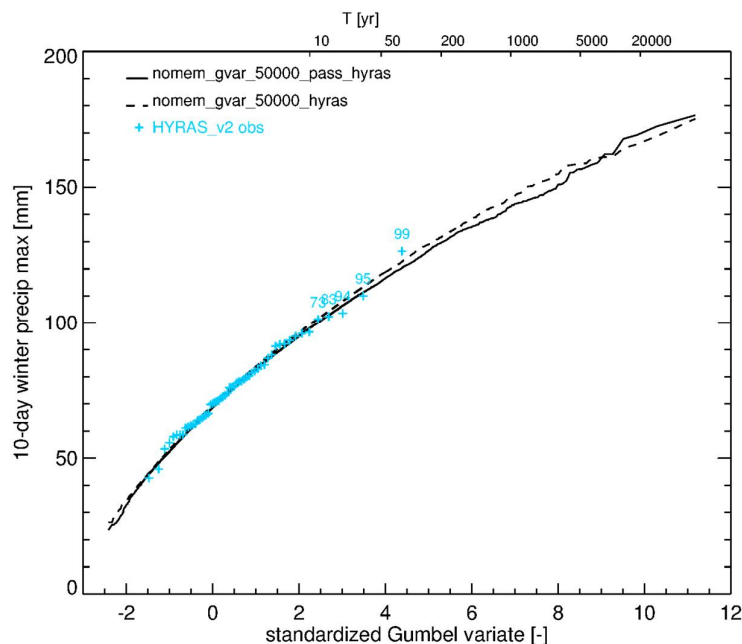


Figure 3.3 Gumbel plots of the maximum 10-day average precipitation over the Rhine basin in the winter half-year for direct resampling of the HYRAS data (dashed line) and passive simulation of the HYRAS data (solid line). The pluses indicate the ordered 10-day observed maxima for the period 1951-2006. The names of the simulations are explained in Schmeits et al. (2014a)

The weather generator for the Rhine basin uses a feature vector of three elements to find the nearest neighbours in the historical data:

- The standardized daily temperature, averaged over the 134 sub-basins.
- The standardized daily precipitation, averaged over the 134 sub-basins.
- The fraction of sub-basins with daily rainfall > 0.3 mm.

Other feature vector compositions have been explored, in particular feature vectors giving more detail of the rainfall fields (Buishand and Brandsma, 2001, Beersma, 2011). This did not result in a better simulation of multi-day extreme rainfall events.

The number k of nearest neighbours was set to 10. Larger values of k generally worsen the reproduction of the autocorrelation coefficients, in particular for the daily temperature. A very small value of k , e.g. $k = 2$, may lead to repetitive sampling of the same historical days with large rainfall in a short period, resulting in exceptionally large 10-day and 20-day values (Buishand and Brandsma, 2001). The search for nearest neighbours was restricted to a window of width $W = 61$ days. Since the historical record has a length of 56 years, the nearest neighbours are generally selected from $56 \times 61 = 3416$ days. Further details of the latest version of the weather generator for the Rhine basin can be found in Schmeits et al. (2014a).

3.3 Weather generator for the Meuse basin

This weather generator generates daily precipitation and temperature over 15 sub-basins of the Meuse upstream of Borgharen. Four of these sub-basins are situated in France, ten in Belgium, and one (the Sambre catchment) partly in France and partly in Belgium. Unlike the weather generator for the Rhine basin, the simulations for the Meuse basin are driven by station data. Long sequences of daily precipitation and temperature are simultaneously generated by resampling from the daily precipitation of Chaumont, Nancy, Vouziers, St Quentin in France, Chiny-Lacuisine and Uccle in Belgium and Aachen in Germany, and daily temperature of Uccle and Aachen for the period 1930-2008 (excluding 1940-1945). The locations of these stations are given in Figure 3.4. The seven precipitation records were selected after an extensive homogeneity analysis of the data for the period 1930-1998 (Leander and Buihand, 2004a). A homogeneity analysis of the data for the complete period 1930-2008 resulted in adjusted precipitation records of Chaumont and Vouziers (Buishand and Leander, 2011). Resampling from the E-OBS data has not been explored for the Meuse basin. The use of E-OBS is less obvious than for the Rhine basin, because the density of the rainfall stations used for the E-OBS data is low over northeast France and Belgium (see Figure 3.2).

The daily average rainfall over the 15 sub-basins, as used in GRADE, was generated in an indirect way, using the historical daily average rainfalls of these sub-basins for the period 1961-2007. For the French part of the Meuse basin, the historical values were derived from daily station data by inverse squared distance interpolation on a $2.5 \text{ km} \times 2.5 \text{ km}$ grid. The number of stations involved in the interpolation varies over the years from 55 to 63 (for details about the stations used, see Buishand and Leander, 2011). For the Belgian part of the Meuse basin, area-averaged rainfall was derived from the daily values of 31 sub-basins that were routinely calculated by the Royal Meteorological Institute of Belgium (RMIB). The resampled data from the seven rainfall stations were replaced by the sub-basin average rainfall for the same historical day if these data originated from the period 1961-2007. For the resampled station data referring to a day in the period 1930-1960 or the year 2008 the sub-basin average rainfall of the closest neighbour of that day in the period 1961-2007 was used (Leander et al., 2005).

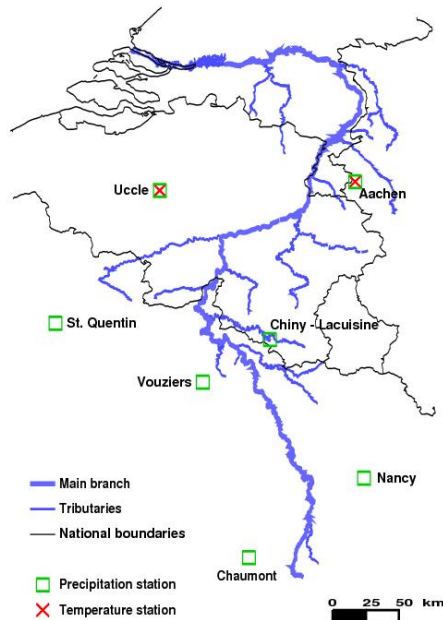


Figure 3.4 Location of rainfall and temperature stations used for driving the resampling process for the Meuse basin

Daily average temperature of the 15-sub-basins was generated in a similar way, using estimated daily temperatures of the sub-basins for the period 1967-2008. These estimates were obtained by inverse squared distance interpolation of the daily temperature data from eleven stations (Buishand and Leander, 2011).

Daily potential evapotranspiration was obtained by multiplying the long-term monthly average potential evapotranspiration of the sub-basin by a factor of $1 + \text{eff} \times T'$ where T' is the difference between the simulated daily temperature and the long-term monthly average temperature. The proportionality constant eff ranges from an average of approximately $0.08 \text{ } ^\circ\text{C}^{-1}$ in summer to $0.13 \text{ } ^\circ\text{C}^{-1}$ in winter (Leander and Buishand, 2007). For the Belgian part of the basin, the long-term monthly average potential evapotranspiration was derived from the daily values for the sub-basins as obtained from RMIB, whereas for the French sub-basins the average monthly potential evapotranspiration of the Belgian sub-basins was used.

The feature vector in the resampling algorithm for the Meuse basin consists of three elements:

- The average standardized daily temperature of Uccle and Aachen.
- The average standardized daily precipitation of the seven rainfall stations.
- The average standardized daily precipitation of the seven rainfall stations, averaged over the four preceding days.

The third element leads to a slower decay of the autocorrelation function (Figure 3.5), which results in a much better reproduction of the standard deviation of the monthly totals in the winter half-year (Leander et al., 2005). The distribution of multi-day rainfall extremes in the winter half-year is also better preserved through the use of this memory element (Figure 3.6).

As for the weather generator for the Rhine Basin the number k of nearest neighbours was set to 10, but the width W of the moving window was set to 121 days (instead of 61 days) for the weather generator of the Meuse basin to improve the simulation of extreme multi-day precipitation amounts (Leander and Buishand, 2004b, 2007). This window width was also used in the additional nearest neighbour step for generating the daily mean rainfalls and temperatures over the sub-basins. The 4-day memory element was not considered in that nearest neighbour step. Further details of the latest version of the weather generator for the Meuse basin can be found in Buishand and Leander (2011) and Schmeits et al. (2014b).

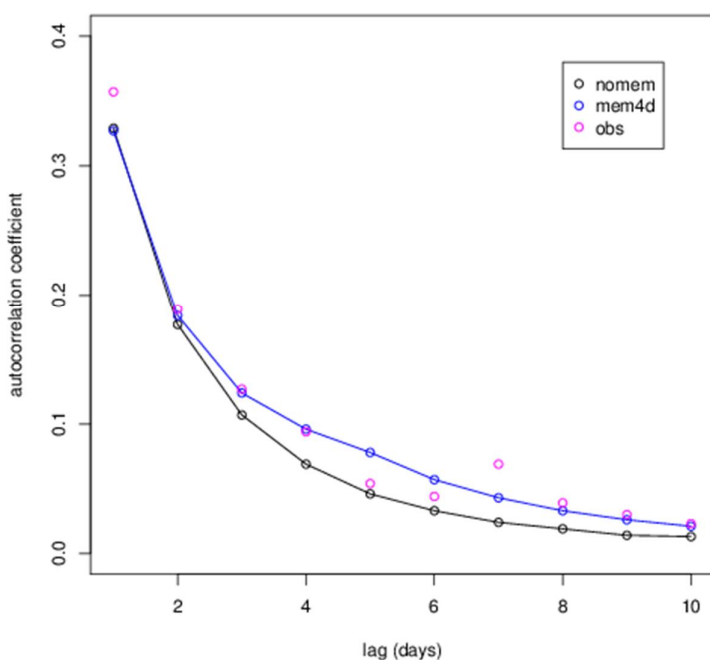


Figure 3.5 Autocorrelation coefficients of daily precipitation in the Meuse basin for the winter half-year. The basin-average autocorrelation coefficients of the observations are compared with those of a 50,000-year simulation with the 4-day element in the feature vector and a 50,000-year simulation where this element was replaced by the fraction of rainfall stations with daily rainfall > 0.3 mm

3.4 Limitations of the weather generator

The nearest-neighbour resampling algorithm cannot generate daily rainfall amounts outside the range of the historical data. The implications of this limitation for the simulated extreme river discharges have been explored by Leander and Buishand (2009). They developed a two-stage resampling algorithm that was capable of generating larger daily rainfall amounts than those observed. This two-stage resampling algorithm was compared with the traditional nearest-neighbour resampling algorithm for the Ourthe catchment upstream of Tabreux (located in the Belgian part of the Meuse basin). It was found that the larger extreme daily rainfall amounts generated by the two-stage resampling algorithm had no discernible effect on the distribution of the simulated discharge maxima in winter. This was also the case if the largest values generated by the traditional nearest-neighbour resampling algorithm were replaced by random values from the tail of an exponential distribution. Therefore this theoretical limitation is not regarded as a practical limitation.

Sequences up to 50,000 years have been generated. Nevertheless, the uncertainty of return values of multi-day rainfall extremes and simulated discharges is considerable owing to the limited length of the baseline series used for resampling. Resampling from a relatively wet baseline series will result in relatively wet long-duration series. Because precipitation exhibits a large year-to-year variability the limited length of the baseline series is a major source of uncertainty. The determination of this uncertainty is discussed in Chapter 7.

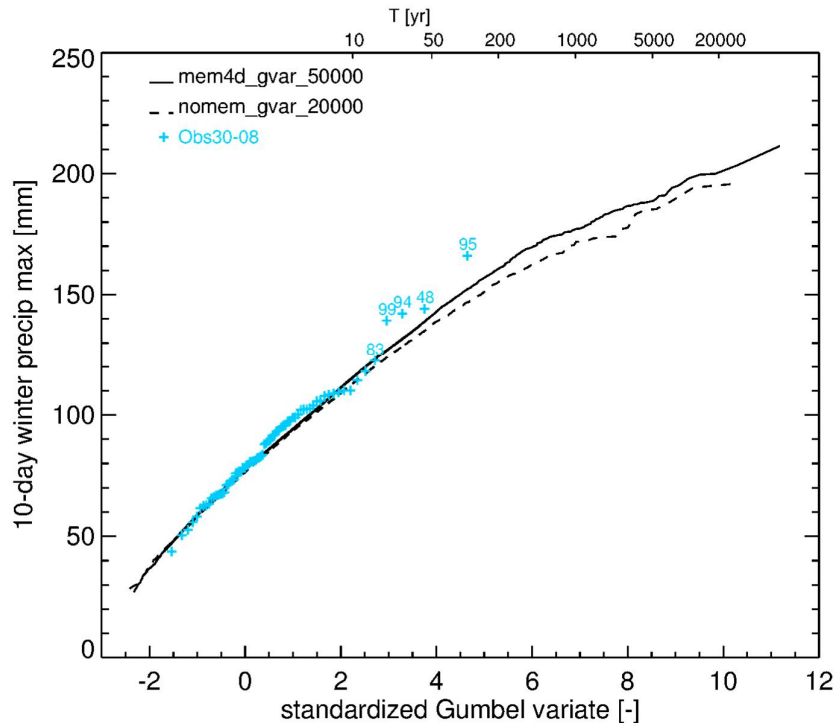


Figure 3.6 Gumbel plots of the maximum 10-day average precipitation over the Meuse basin in the winter half-year for the 50,000-year simulation with the 4-day memory element (solid line) and a 20,000-year simulation without 4-day memory element (dashed line). The pluses indicate the ordered 10-day maxima for the period 1930-2008. Note that the basin averages for the years 1930-1960 and 2008 refer to the closest nearest neighbour in the period 1961-2007 for each day. The names of the simulations are explained in Schmeits et al. (2014b)

Though the autocorrelation of daily precipitation shown in Figure 3.5 is too weak (< 0.35) to obtain an accurate prediction of daily rainfall from the rainfall amounts on previous days, this correlation has a rather strong impact on extreme multi-day rainfall. Ignoring the autocorrelation leads to an underestimation of the return levels of 10-day maximum winter rainfall of 20-25% (Brandsma and Buishand, 1999; Buishand, 2007). It is therefore important to reproduce the autocorrelation well, or more general, the temporal dependence of daily rainfall. The weather generators for the Rhine and Meuse basins reasonably describe short-range temporal dependence, but there are indications that this is not the case for long-range temporal dependence. For a 3000-year simulation for the Meuse basin, Leander and Buishand (2004b) observed that the largest 30-day precipitation amount in the summer season did not exceed the exceptionally large 30-day precipitation amount in July 1980. In a drought study for the Netherlands, a 4-month memory element was needed to simulate the occurrence of extreme rainfall deficits satisfactorily (Beersma and Buishand, 2007).

These examples indicate that for extremes that can be related to extremely persistent weather conditions (e.g. those leading to low water levels), longer memory elements are needed than currently used in the weather generators for the Rhine and Meuse basins. These situations are, however, more typical for the summer season than for the winter season. The latter is the most important season for high river discharges.

For the Rhine basin, the reproduction of the dependence between the spatial patterns on successive days was studied (Beersma, 2011). Both for precipitation and temperature this pattern correlation was underestimated. The implications of this bias are not clear. The spatial dependence of the multi-day winter maximum precipitation amounts was adequately reproduced for the Rhine basin (Buishand and Brandsma, 2001). Inclusion of the daily rainfall amounts over sub-areas of the Rhine basin improves the reproduction of the pattern correlation, but it also leads to a poorer reproduction of other precipitation characteristics.

4 Hydrological modelling

4.1 Description of the HBV model

A hydrological (or rainfall-runoff) model is used to transform the precipitation, temperature and potential evapotranspiration series into discharges. Within GRADE use is made of the HBV rainfall-runoff model both for the Meuse and Rhine basin. The choice of the HBV model was made after an evaluation of rainfall-runoff models by Passchier (1996).

HBV (Hydrologiska Byråns Vattenbalansavdelning) was developed at the Swedish Meteorological and Hydrological Institute (SMHI) in the early 1970s and has been applied to many river basins all over the world (Lindström et al., 1997). HBV is a conceptual model, which means that the model components represent real-world layout of the basin in such a way that the runoff generating processes are described realistically (Figure 4.1).

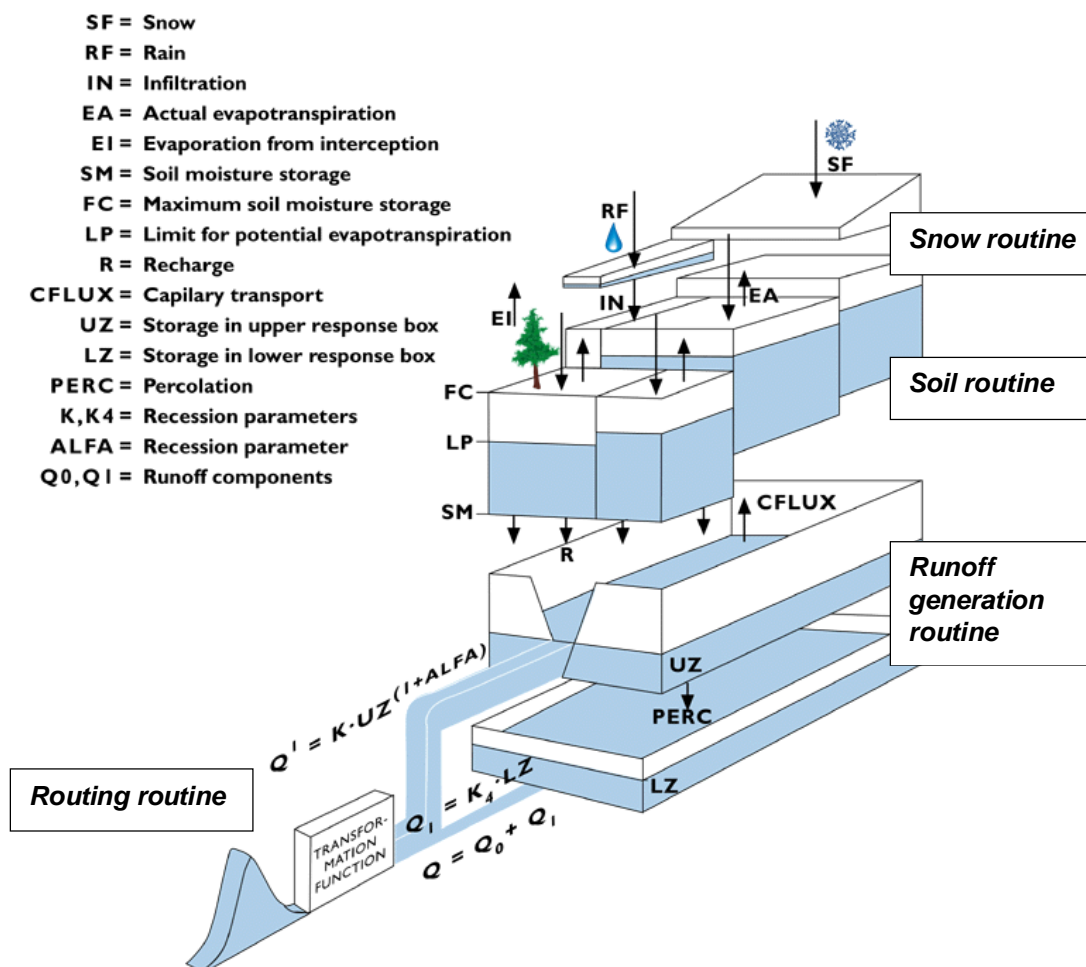


Figure 4.1 Schematic overview of the HBV rainfall-runoff model

There is a difference, though, with physically-based models, which try to mimic the exact physical processes that occur in a river basin by means of physically-based (flow) formulas. Conceptual models rather mimic the behaviour of the runoff generation by using storage compartments and the flows between those compartments. These flows are governed by relatively simple relations, which can be either linear or non-linear (e.g. Beven, 2001).

The model layout can be divided into a number of routines (Figure 4.1). In the “snow routine” accumulation of snow and snow melt are determined according to the temperature. The “soil routine” controls which part of the rainfall and melt water forms excess water and how much is evaporated or stored in the soil. The “runoff generation routine” consists of an upper, non-linear reservoir representing fast runoff components and a lower, linear reservoir representing base flow. Flood routing processes are simulated with a simplified Muskingum approach.

More detailed information on the model structure and the various formulas are given in Lindström et al. (1997).

4.2 HBV in GRADE

4.2.1 Concept

To set up the HBV model the basins of the rivers Rhine and Meuse are subdivided into a number of sub-basins. This division into sub-basins is primarily done to achieve that single values of the model parameters can represent the physical characteristics of the sub-basin. Another important criterion is that precipitation within the sub-basin can be considered as uniform. Small sub-basins will allow for a more detailed fine-tuning of the calibration of the model for the total basin. However, a trade-off between an accurate description of the runoff generating processes and practical limitations (such as a too large number of sub-basins that make the hydrological model too complex to handle) was made. To calibrate the sub-basins on local conditions, discharge data from a gauging station at the downstream end of the sub-basin are needed.

Within each sub-basin different zones are identified for which altitude and land use can be differentiated. For example, within each zone the effect of altitude on the temperature, which is important for snowfall and glacier melt, is taken into account by using a $0.6^{\circ}\text{C}/100\text{m}$ lapse rate.

4.2.2 The river Meuse

The HBV model for the Meuse is a semi-distributed hydrological model that consists of 15 sub-basins, which are shown in Figure 4.2. These sub-basins cover the whole Meuse basin upstream of Borgharen, which has an area of about $21,000\text{ km}^2$. The HBV model runs with a daily time step. The model input consists of daily average precipitation, temperature and potential evapotranspiration for each sub-basin. The model has been calibrated using the GLUE (Generalized Likelihood Uncertainty Estimation) method with emphasis on the reproduction of high flows (see Sections 4.3.1 and 4.3.2). The model for the Meuse is described in more detail in Hegnauer (2013).

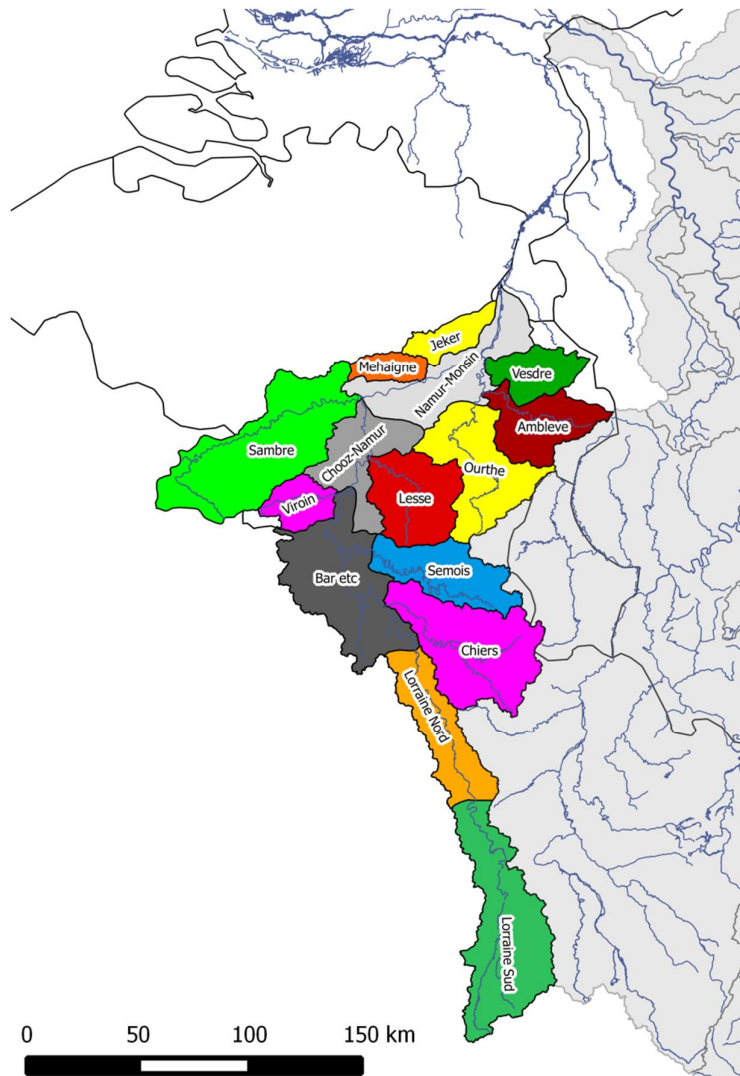


Figure 4.2 Layout of the sub-basins of the Meuse HBV model

4.2.3 The river Rhine

The Rhine basin upstream of Lobith covers an area of about 165,000 km². The lakes in Switzerland have a considerable effect on the discharges. Therefore, four of the initial 134 sub-basins (for which daily precipitation and temperature are provided) were further subdivided to include four large lakes in Switzerland in the HBV setup. This led to the 148 sub-basins (Hegnauer and Van Verseveld, 2013) which are shown in Figure 4.3. The four lakes that are included in the HBV-setup are:

- Lake Constance (German: Bodensee).
- Lake Neuchâtel (French : Lac de Neuchâtel, German : Neuenburgersee).
- Lake Lucerne (German: Vierwaldstättersee).
- Lake Zürich (German: Zürichsee).

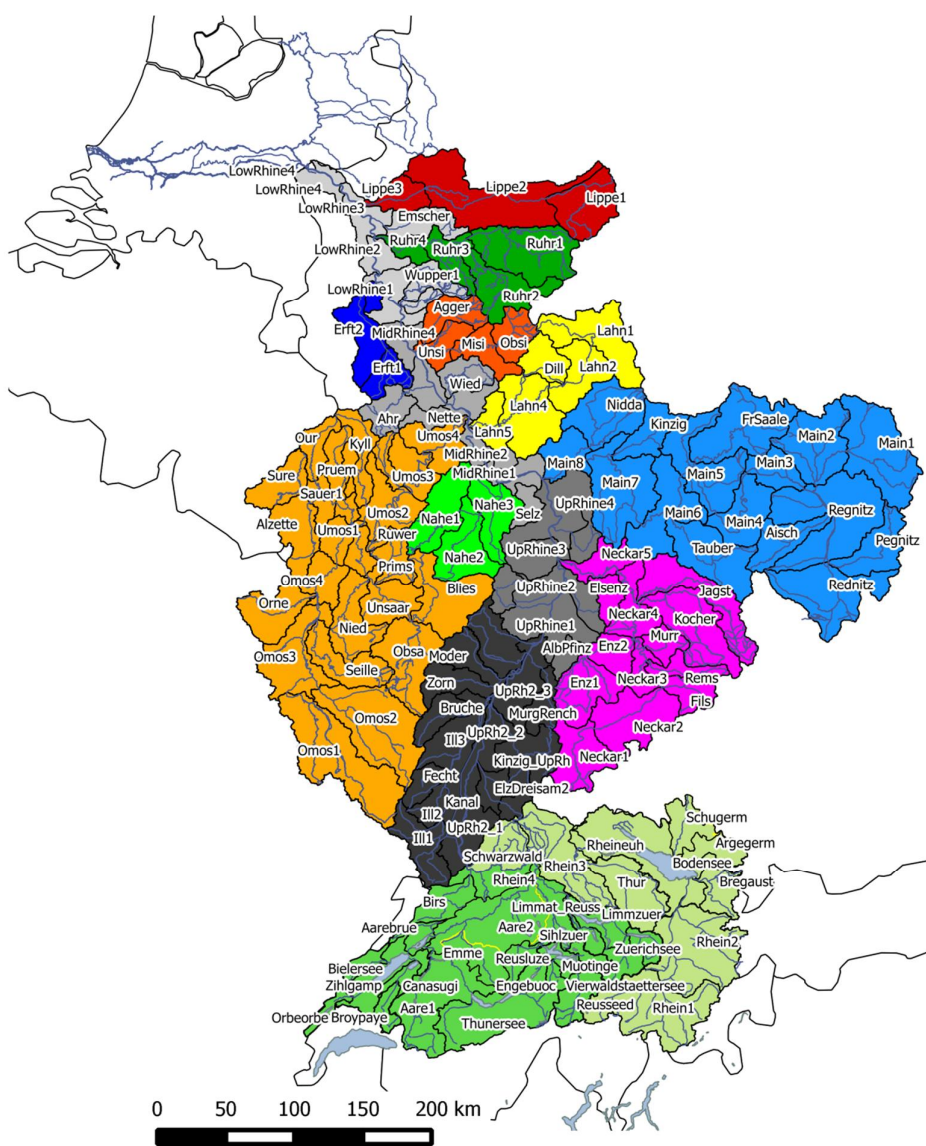


Figure 4.3 Layout of the sub-basins of the Rhine HBV model. The different colours represent the 15 major sub-basins (e.g. the Main, Neckar or Moselle basins)

The HBV model runs with a daily time step. The model input consists of daily average precipitation and temperature for each sub-basin. Daily potential evapotranspiration is calculated from daily temperature by the HBV model (see Section 4.3.3). The model for the Rhine is described in more detail in Hegnauer and Becker (2013).

4.3 Calibration

For the rivers Meuse and Rhine, use is made of a GLUE analysis to calibrate HBV for each sub-basin. The GLUE analysis combines the calibration of the model with an uncertainty estimation of the model parameters, which later on is used in the overall uncertainty analysis (see Chapter 7).

4.3.1 The GLUE method

Working with (complex) models with many parameters introduces the problem of equifinality. This is the effect that multiple parameter sets give approximately the same results. The question is therefore whether one should look for a single “best” parameter set or choose another approach. In GLUE, instead of finding one optimal parameter set, multiple parameter sets are accepted that lead to satisfactory results (Beven and Binley, 1992). By means of multiple model performance criteria, the performance of the parameter sets is analysed. Only the parameter sets that meet the constraints of the chosen performance criteria are selected. Such sets are called “behavioural sets”.

In GRADE, the GLUE method for the calibration of the HBV models for the Rhine and Meuse is applied in three steps, which are illustrated in Figure 4.4:

1. First, the values of six HBV parameters (from hereon called parameter sets) were sampled from a uniform distribution, using a Monte Carlo approach with 5000 samples. The process of sampling starts at the most upstream sub-basins. Only six different parameters were sampled during the GLUE analysis to avoid the problem of equifinality. The parameters that were used in the GLUE analysis are listed in Table 4.1. The values of the other parameters of the HBV model were maintained at their original value (i.e., the values as used in the Berglöv (2009) calibration).
2. Secondly, the behavioural parameter sets were selected. The performance criteria that were used are related to the overall performance (Nash-Sutcliffe efficiency), a volume measure (Relative Volume Error) and the reproduction of extreme peaks (Generalized Extreme Value Error). All behavioural parameter sets (or models) are assumed to be equally likely, which is different from the classical GLUE where different weights for different parameter sets are applied.
3. Next, 5000 parameter sets are sampled for the neighbouring downstream sub-basin. Each of the 5000 parameter sets is combined with a random draw of one of the behavioural parameter sets of the upstream sub-basins. In this way, the information from the upstream calibration is transferred downstream. This process continues in downstream direction until the last downstream gauging station.

See Winsemius et al. (2013) for more details on each of these steps. The result of the GLUE analysis is a set of behavioural parameter sets for each sub-basin.

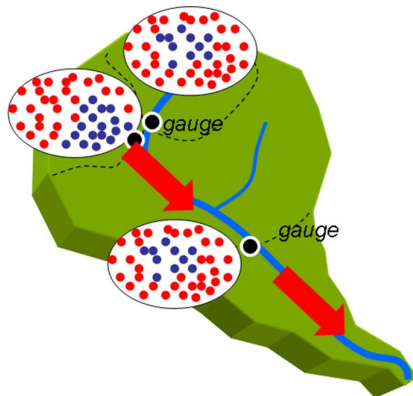


Figure 4.4 Schematic diagram showing the GLUE analysis for a series of sub-basins. All dots within the circle represent the Monte Carlo samples taken from the uniform distribution. The blue dots are the selected behavioural parameter sets, derived from the gauged location. Only the blue sets in the upper basins are passed on to the GLUE analysis of the neighbouring downstream area, which is constrained on the more downstream located gauge

Table 4.1 Parameters that were used for the GLUE analysis

Meuse	Rhine Upstream of Basel	Rhine Downstream of Basel	Parameter	Unit	Name
X	X	X	<i>fc</i>	mm	Maximum soil moisture storage
-	X	X	<i>perc</i>	mm/day	Percolation
X	X	X	<i>beta</i>	-	Soil parameter
X	X	X	<i>khq</i>	1/day	Recession parameter at <i>hq</i>
X	-	X	<i>alfa</i>	-	Measure of non-linearity
X	-	X	<i>lp</i>	-	Limit for potential evapotranspiration (fraction) ¹
X	-	-	<i>hq</i>	mm/day	High flow parameter ²
-	X	-	<i>tt</i>	°C	Threshold temperature
-	X	-	<i>cfmax</i>	mm/day/°C	Melting factor

4.3.2 The GLUE method applied for the Meuse

For the river Meuse, a calibration was made by Van Deursen (2004) based on the work of Booij (2002 and 2005). In this calibration, the high flows were considerably underestimated (up to 300-400 m³/s), which made this model calibration unsuitable for the application in GRADE. For that reason, the relative error in the 20-year return value (the Generalized Extreme Value Error) was included in the evaluation of the HBV simulations during the GLUE analysis (Kramer et al., 2008).

In the GLUE analysis, the model was calibrated on daily discharges for the period 1968-1998 (Kramer et al., 2008), using the same precipitation, temperature and potential evapotranspiration data as in the calibration by Van Deursen (2004). The precipitation and temperature data are the same as those used for the weather generator but the potential evapotranspiration data refer here to the original historical daily potential evapotranspiration data, rather than daily potential evapotranspiration derived from the evapotranspiration – temperature relation discussed in Section 3.3. In Table 4.1 the parameters are given that were included in the GLUE analysis.

For the Meuse, for 500 (out of 2949) behavioural parameter sets at the location of Monsin³, a 3000-year HBV simulation was carried out with synthetically generated rainfall and temperature series (Kramer and Schroevers, 2008). For each of the 500 simulations, the 100-year discharge was determined. From the empirical distribution of this estimated return level, the 5%, 25%, 50%, 75% and 95% quantiles were determined and the corresponding HBV parameter sets were selected for the uncertainty analysis.

¹ *lp* is the soil moisture value above which the actual evapotranspiration reaches its potential value. *lp* is given as a fraction of *fc*.

² *hq* is the high flow level for which the recession rate parameter *khq* is assumed.

³ Monsin is an imaginary measurement station. The discharge at Monsin is calculated from the discharge at Borgharen plus the extractions for the branches between Liège and Borgharen (Albertkanaal, Zuid-Willemsvaart and Julianakanaal). For details, see Bos (1993).

4.3.3 The GLUE method applied for the Rhine

The original HBV models for the sub-basins of the Rhine were set up by the German Federal Institute of Hydrology (BfG) between 1997 and 2004 in cooperation with the Dutch Rijkswaterstaat (see Eberle et al., 2005). A recalibration was carried out by SMHI for the BfG, which aimed at the full flow regime of the river (Berglöv et al., 2009). An examination of the simulation results with this calibration showed that the reproduction of peak values was very poor which would not allow the use of this calibration in GRADE where the emphasis is on the simulation of flood waves beyond any measured discharge values to date. For this reason, another full calibration of the HBV model was made for GRADE, using the GLUE method (Winsemius et al., 2013; Hegnauer and Van Verseveld, 2013). In this new calibration use was made of the HYRAS 2.0 precipitation set (Section 3.2) and the E-OBS 4.0 temperature set⁴ as input of the model and discharge data for the period 1989-2006 from the HYMOG dataset (Steinrücke et al., 2012). In addition, use was made of extra discharge information originally provided by the BfG for the recalibration by SMHI (Berglöv et al., 2009) and discharge data from the FOEN (Swiss Federal Office for the Environment) for the stations located in Switzerland. No discharge data for the Austrian part of the basin was available, so these sub-basins were calibrated using the discharge data of a downstream location provided by FOEN. Daily evapotranspiration was calculated by perturbing monthly average potential evapotranspiration for the period 1961-1995 as derived by Eberle et al. (2005), using daily temperature with an *etf* (see Section 3.3) value of $0.05 \text{ }^{\circ}\text{C}^{-1}$.

A GLUE analysis for the entire Rhine basin at once is computationally not feasible because of the large number of sub-basins. Therefore, the 148 sub-basins of the Rhine HBV model have been grouped into 15 major sub-basins (e.g. Main, Neckar), following the same subdivision as used by SMHI in their calibration report (Berglöv et al., 2009). GLUE has been performed for each of these major sub-basins. An overview of the major sub-basins of the Rhine is given in Figure 4.5. Two of these major sub-basins are located upstream of Basel and 13 are located downstream of Basel.

For practical reasons, the GLUE analysis for the Rhine basin has been carried out in two steps. First an analysis was made for the major sub-basins downstream of Basel (Winsemius et al., 2013), and subsequently an analysis for the two Alpine basins upstream of Basel (Hegnauer and Van Verseveld, 2013). For these two major sub-basins snow is an important component and for that reason two parameters from the HBV snow routine were included in the GLUE analysis. To reduce the degrees of freedom (and avoid the problem of equifinality) two other parameters were excluded from the GLUE analysis upstream of Basel (see Table 4.1).

For each major sub-basin, the number of behavioural sets was reduced to 5. These 5 sets were chosen by running the HBV model for each behavioural set over the period 1985-2006. For each behavioural set, the annual maxima near the downstream end of the major sub-basin⁵ were selected and the discharge associated with a return period of 10 years was derived. The final 5 HBV parameter sets correspond with the parameter sets that represent the 5%, 25%, 50%, 75% and 95% quantiles of the empirical distribution of the 10-year discharges.

⁴ This is an earlier version of the E-OBS data than that used in the weather generator (Section 3.2) in which much less precipitation and temperature stations over Germany were available for gridding.

⁵ This does not apply to the major sub-basins along the main stem of the Rhine, containing many ungauged sub-basins. The 5 parameter sets for these major sub-basins were based on the estimated 10-year discharges near the end of the nearest downstream gauged sub-basin.

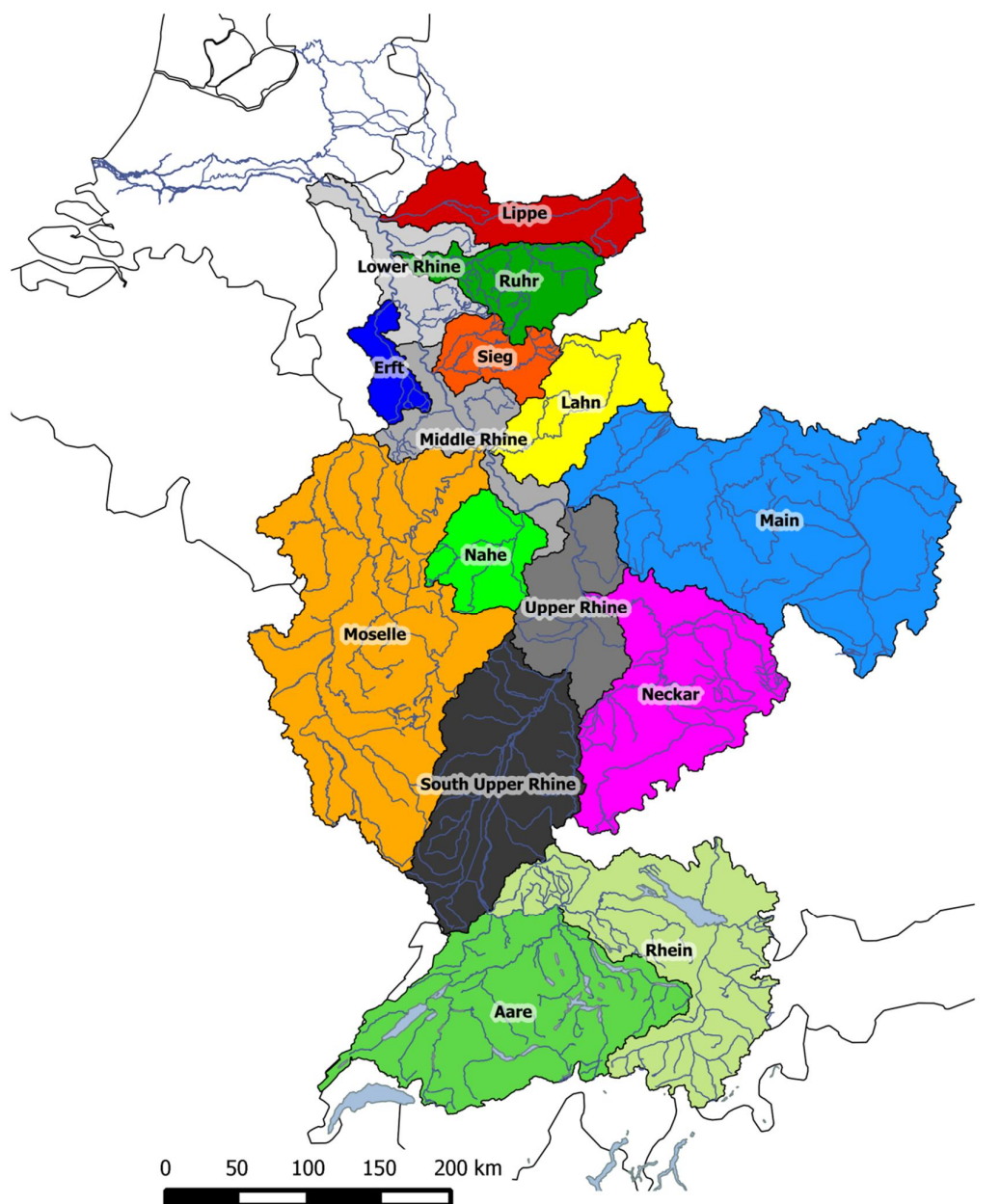


Figure 4.5 Overview of the major sub-basins of the Rhine basin

The 5 representative parameter combinations for each major sub-basin lead to 5^{15} possible combinations of parameter sets for the whole Rhine basin, which is computationally not feasible to use in the uncertainty analysis. For this purpose, only 5 different combinations were considered for the whole Rhine basin, which consist of the 5%, 25%, 50%, 75% and 95% parameter sets of each major sub-basin.

Many sub-basins along the main stretch of the Rhine (see the grey areas in Figure 4.6), the so called ZWE⁶ areas, were not calibrated during the GLUE analysis due to lack of (reliable) discharge data. Instead, the parameters for the ZWE areas were copied from other similar basins. The choice of a similar sub-basin was based on the average slope, because the important hydrological processes in the sub-basin can be related to the slope of the sub-basin. The final 5 parameter sets from the calibrated sub-basin with the average slope closest to the average slope of the ZWE area of interest were selected (see Hegnauer and Becker, 2013).

4.3.4 Results HBV model for the Meuse

The HBV model for the Meuse has been validated on 9 historical floods between 1993 and 2004 of which three major events (Dec '93, Jan '95 and Oct/Nov '98) were also included in the calibration. The average Nash-Sutcliffe efficiencies for each of these floods in Table 4.2 indicate that the GRADE parameter sets perform in general well. Especially for extreme discharge peaks, the GRADE calibration of HBV performs better than the earlier calibrations of HBV. However, the performance of HBV is rather poor for a number of sub-basins (Viroin, Vesdre and Amblève). This poor behaviour could be explained by the presence of reservoirs that have a damping effect on the discharge peaks of the rivers Vesdre and Amblève (Van Vuuren, 2003). More details on the validation procedure, including a sensitivity analysis of the criteria used in the GLUE analysis, are given in Kramer et al. (2008).

Table 4.2 Average Nash-Sutcliffe (NS) efficiencies for the HBV sub-basins of the Meuse for 9 discharge peaks from the period between 1993 and 2004. The highest NS-efficiencies are printed bold

Start event	16/12/93	25/1/95	20/10/98	1/12/99	15/12/00	22/1/02	31/10/02	15/12/02	5/1/04	Mean
End event	26/12/93	4/2/95	26/10/98	15/1/00	15/4/01	30/3/02	30/11/02	29/1/03	31/1/04	
Van Deursen	0.84	0.78	0.89	0.76	0.83	0.84	0.71	0.86	0.76	0.81
GRADE 05%	0.71	0.78	0.78	0.86	0.89	0.91	0.81	0.97	0.92	0.85
GRADE 25%	0.68	0.69	0.70	0.89	0.88	0.87	0.86	0.97	0.92	0.83
GRADE 50%	0.58	0.83	0.91	0.86	0.84	0.85	0.89	0.97	0.92	0.85
GRADE 75%	0.95	0.60	0.75	0.88	0.86	0.88	0.79	0.97	0.94	0.85
GRADE 95%	0.86	0.64	0.76	0.87	0.80	0.82	0.90	0.96	0.93	0.84

4.3.5 Results HBV model for the Rhine

The GLUE analysis of the HBV model for the Rhine basin upstream of Basel turned out to be difficult. For many sub-basins, the results of the GLUE analysis are poor (Figure 4.6) and often no behavioural parameter sets could be found without loosening the criteria thresholds. However, although the performance on sub-basin level is sometimes poor, the overall performance of the HBV model for the whole area upstream of Basel is reasonable. Particularly the damping effect of the Bodensee has a positive effect on the performance. The poor performance on sub-basin level is reflected in the relatively large uncertainty in the modelled results (see for example Figure 4.7). An explanation for the relatively poor behaviour could be: 1) The dominance of processes that occur on a smaller time scales than used in the model (e.g. hours instead of days); 2) The anthropological activities in the sub-basins, such as reservoirs and abstractions; 3) Representativity of the precipitation observations in mountainous areas

⁶ The abbreviation ZWE originates from the German 'zwischen Einzugsgebieten'

The GLUE analysis showed good results for most of the HBV sub-basins downstream of Basel (Figure 4.6). Areas for which the performance is lower are the Erft, two sub-basins in the south-east of the Main basin and a number of sub-basins in the south of the Upper Rhine basin. The lower performance for the Erft is caused by the lignite mining industry that has led to large-scale disturbance of the natural environment. In the other basins the lower performance is probably due to the dominance of processes that occur on a smaller time scale than the (daily) model time step, for example caused by steep slopes or soil types with limited storage capacity. For the Main, anthropogenic activities, including interbasin connectivity, in the Rednitz and Pegnitz sub-basins and the presence of karst in the Aisch basin were suggested as a reason for the rather poor behaviour in these sub-basins (Winsemius et al., 2013).

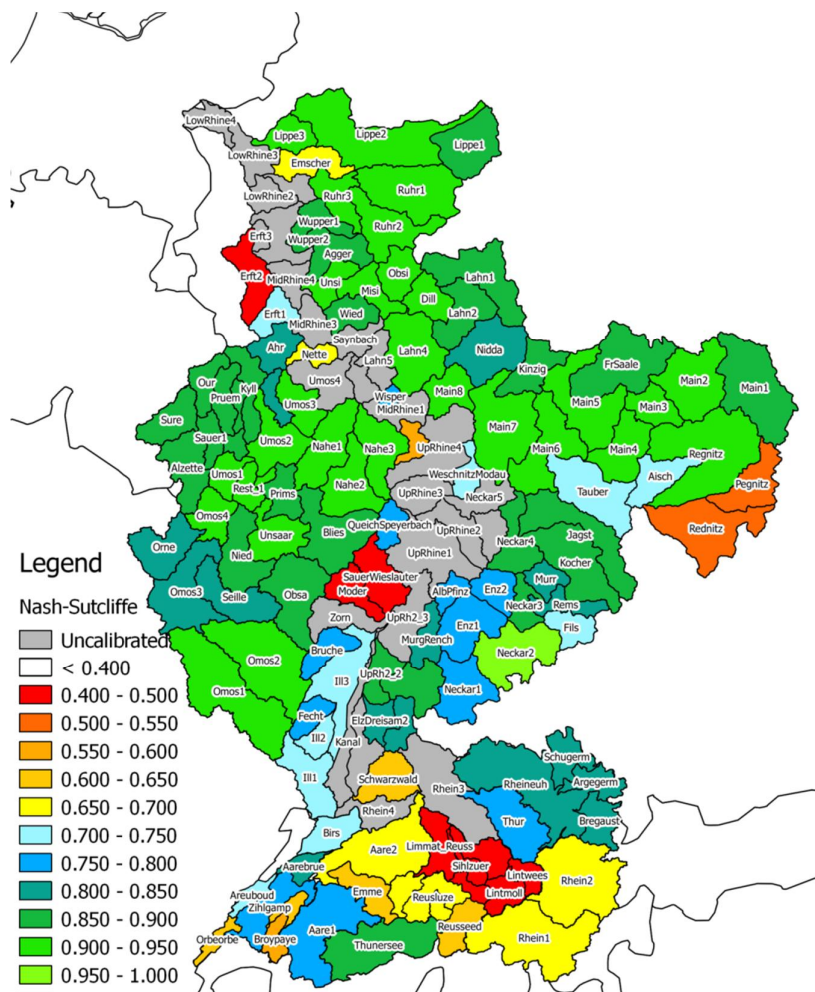


Figure 4.6 Overview of highest obtained Nash-Sutcliffe efficiency during sampling per sub-basin

In Figure 4.7 - Figure 4.9 the hydrographs for two major flood events are shown for the Rhine at Neuhausen (downstream of Lake Constance, Switzerland), the Neckar and the Moselle, respectively. Here the behavioural parameter sets are plotted from which the final 5 parameter sets are selected. As discussed earlier, the large uncertainty in the modelled results in Switzerland (see Figure 4.7) is caused by the poor performance of HBV for many Swiss sub-basins. For the Moselle and the Neckar basins, the uncertainty is much less.

This is also reflected in the relatively good performance for the sub-basins of those rivers as shown in Figure 4.6.

Although the timing of the peaks is often quite good, the height of the peaks is not always well simulated. For the Neckar and the Moselle it seems that the peak flows are often (slightly) overestimated. This could be explained by the fact that no damping of the flood wave is included in the HBV model.

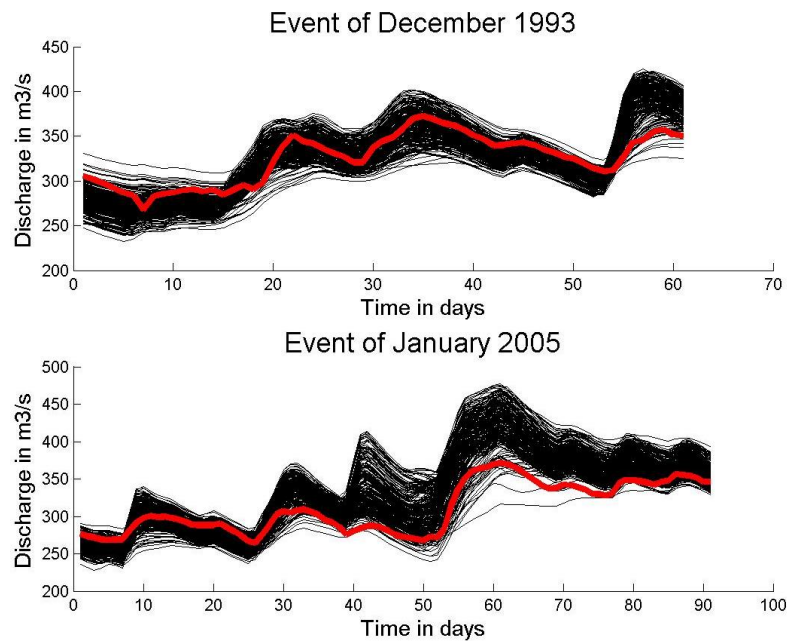


Figure 4.7 Modelled discharges for all behavioural parameter sets (black lines) and observed discharges (red line) for the 1993 and 1995 events at Neuhausen (CH)

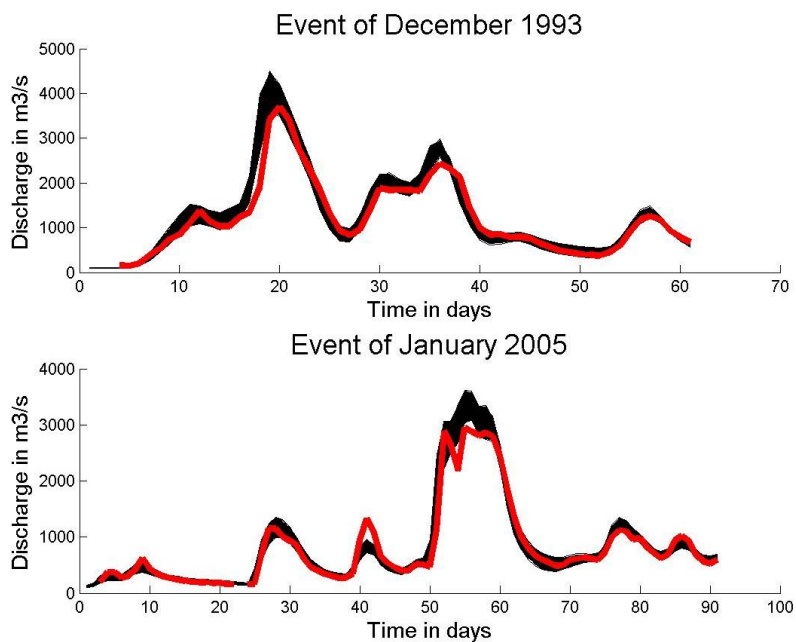


Figure 4.8 Modelled discharges for all behavioural parameter sets (black lines) and observed discharges (red line) for the 1993 and 1995 events at Cochem (Moselle)

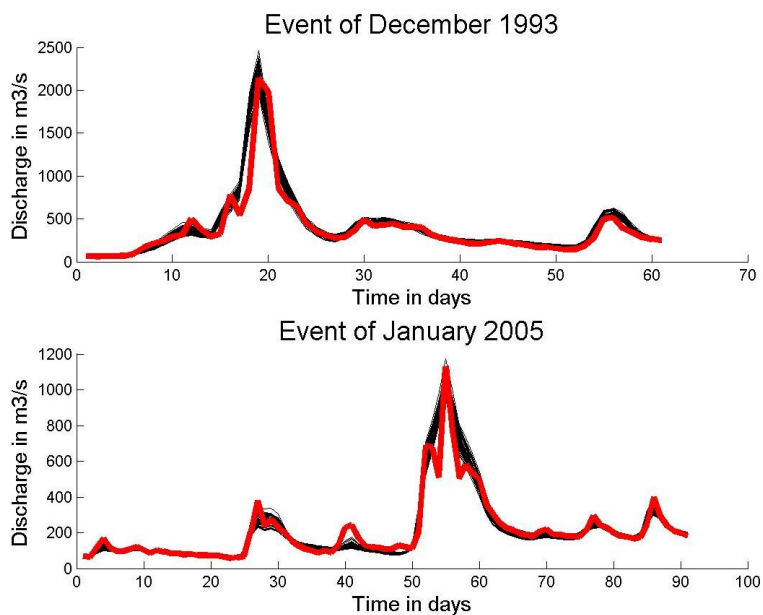


Figure 4.9 Modelled discharges for all behavioural parameter sets (black lines) and observed discharges (red line) for the 1993 and 1995 events at Rockenau (Neckar)

4.4 Limitations of the HBV model

The HBV model belongs to the class of conceptual models, which try to mimic the hydrological processes that govern the generation of flood events by a series of reservoirs and equations describing the exchange between those reservoirs. The level to which this type of models represents reality depends heavily on the layout of these reservoirs and equations. For the most extreme floods that are simulated with GRADE, it is not known whether the processes represented by the model concept are still fully valid. While the uncertainty in the historical discharge range is quantified in the calibration, the model has to be applied in a range of discharges far above the highest recorded discharge. Such difficulties cannot be avoided and are an issue for any type of hydrological model. However, the class of models indicated as 'physically-based' will probably be better able to simulate faithfully the hydrological processes, even in the discharge range beyond the measured values. At present the application of such models is however too complex to consider them as an alternative to the HBV model for a river basin as large as that of the Rhine.

In Kramer et. al. (2010) it was shown that the way flood hydrographs are reproduced, strongly depends on the layout of the model. Spatial lumping and ignoring interception lead to an overestimation of the serial correlation of the daily discharges, resulting in too smooth hydrographs. Introducing hydrological processes that are not yet included in the model, improving existing process descriptions and/or using a fully distributed model will probably result in less serial correlation and thus in a less smooth hydrograph which is expected to better fit the measured hydrographs.

In the models used in GRADE the time step is equal to one day. There are indications that in some parts of the basin(s) (e.g. in Switzerland) the time step of one day is too long for a correct representation of the processes. The current computing power does not allow an hourly time step within GRADE. Besides this, the availability of hourly data is limited.

5 Flood routing

5.1 Description of the flood routing

The routing of the flood waves from the various sub-basins through the main channels can be done by using either the hydrological flood routing module in HBV or flood routing of external hydrological or hydrodynamic models, which are fed by the simulated discharges of the HBV sub-basins.

The most advanced method, hydrodynamic routing, is the preferred type, because it can adequately simulate important hydrodynamic effects, such as backwater effects of the main river on the tributaries (and vis-à-vis) and particularly the impact of inundation on the propagation of the flood wave. Due to the computation time required the hydrodynamic calculations are only done for the flood waves associated with the annual maximum flood peaks. These annual maximum flood peaks are derived from the hydrological routing results using a three-step approach:

1. First the full synthetic series (50,000 years) are simulated with the flood routing in HBV and the annual maximum flood peaks at Borgharen, respectively Lobith, are selected.
2. Subsequently the corresponding annual maximum flood waves are simulated again with the hydrodynamic routing, starting 30 days before the moment of the peak until 20 days after the moment of the peak.
3. The results of the two are combined to get a continuous discharge series.

5.2 Flood routing Meuse

For the hydrodynamic flood routing of the Meuse a Sobek⁷ model is used in GRADE. The Sobek model comprises the Meuse from Chooz at the border between Belgium and France to Keizersveer in the Netherlands, as is shown in Figure 5.1. The model represents the river geometry of 1997 for the Belgian part of the Meuse (from Chooz to Borgharen) and the river geometry of 2006/2007 for the Dutch part of the Meuse (Borgharen to Keizersveer). There are several lateral inflows defined both for the Dutch and the Belgian part of the Meuse. The model includes retention areas and groundwater interaction along the Dutch part of the Meuse but not along the Belgian part. The model runs with a time step of 1 hour. More information about the Sobek model can be found in Hegnauer and Becker (2013).

In Kramer et al. (2010) the incorporation of weirs in the model is discussed. For the flood event of 2002, the effect of the weirs on the discharge appeared to be limited. Hence, their effect is ignored in the GRADE simulations.

For the Meuse, the difference between the results of the Sobek routing and the internal HBV routing is small. The Sobek results are slightly higher due to the hourly timestep, compared to the daily timestep of the HBV model. In the future, a different Sobek model could be used that includes retention measures and/or upstream flooding.

⁷ With Sobek we refer to the River/Estuary version of the Sobek software (in short Sobek-RE)

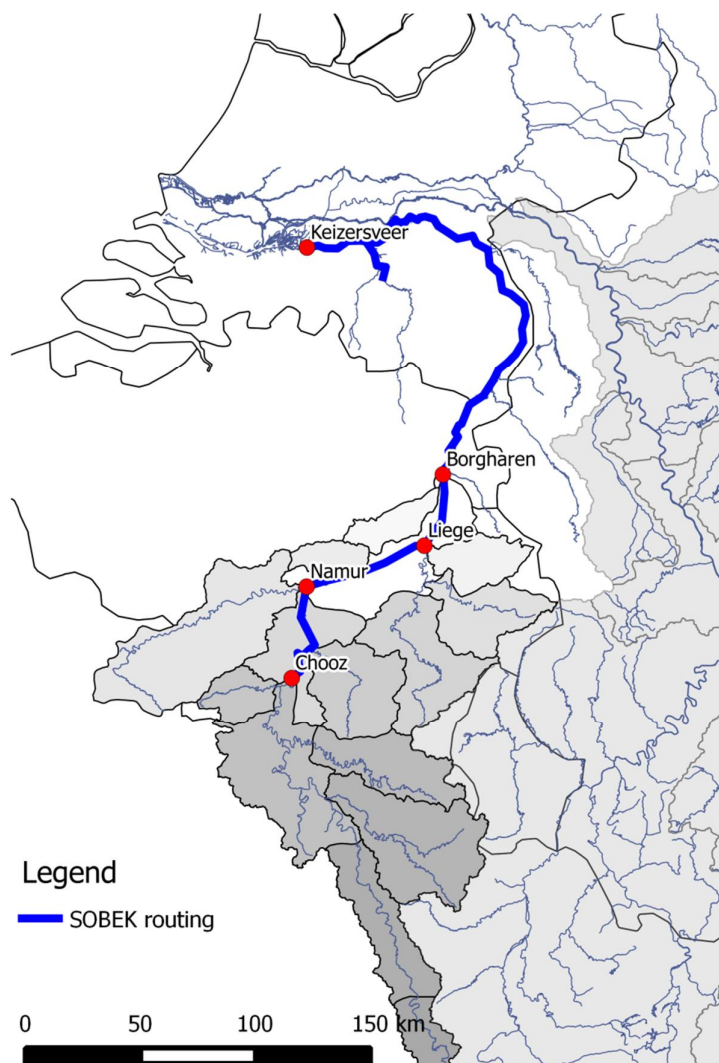


Figure 5.1 Schematization of the hydrodynamic Sobek flood routing in GRADE Meuse, including the gauging stations that correspond to input and output locations of the Sobek model

5.3 Flood routing Rhine

For the hydrodynamic flood routing of the river Rhine, different routing components are used in GRADE:

- 1) Hydrologic routing:
 - a) Muskingum routing Basel – Maxau without flooding areas
- 2) Hydrodynamic routing:
 - a) Sobek routing Maxau – Lobith without flooding areas
 - b) Sobek routing Maxau – Lobith with flooding areas

In Figure 5.2 an overview of the different routing components is presented.

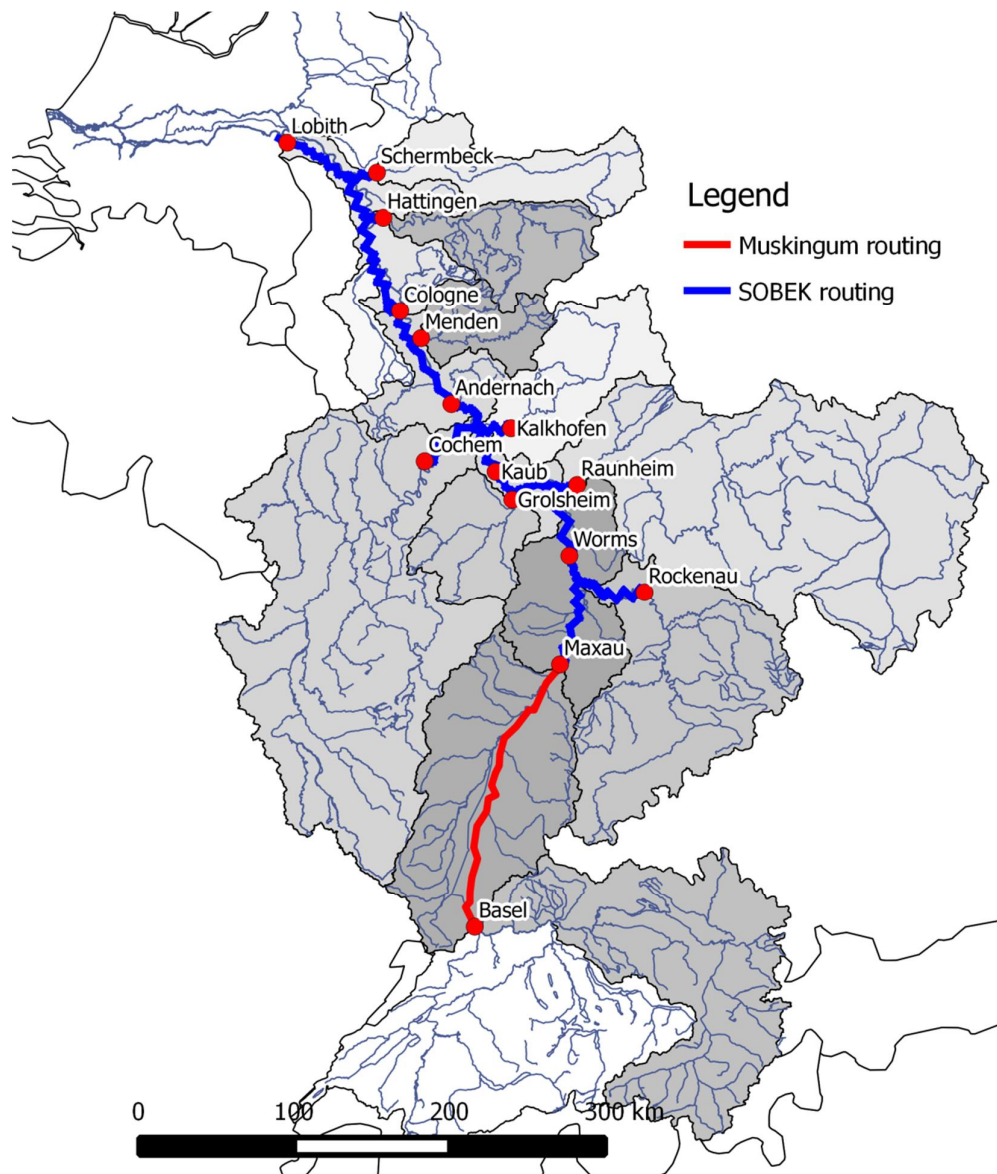


Figure 5.2 Schematization of the hydrologic Muskingum and hydrodynamic Sobek flood routing in GRADE Rhine, including the gauging stations that correspond to input and output locations of the Muskingum and Sobek models

For the main river between Basel and Maxau, the hydrologic routing uses a separate Muskingum routing module (Patzke, 2007) that gives better results on this stretch than the standard HBV routing module. The results of the Muskingum routing at Maxau are used as input for the hydrodynamic Sobek model.

The Sobek models for the Rhine used in GRADE comprise the Rhine from Maxau (Germany) to Lobith (and slightly further on to Pannerdensche Kop in the Netherlands) and the downstream sections of the tributaries Neckar, Main, Nahe, Lahn, Moselle, Sieg, Ruhr and Lippe. Other tributaries are included in the routing models as lateral inflows.

Use is made of two versions of the model, one with and one without flooding areas behind the dikes of the Upper Rhine between Maxau and Kaub and the Lower Rhine (between Bonn and Lobith, see Figure 2.2). The river geometry of 2010 is used in both versions (HKV, 2011) and existing retention areas are included. In the Lower Rhine-part (Andernach – Pannerdensche Kop), groundwater interaction has been incorporated (BfG, 2008).

In the version with flooding, potential flood areas behind the dikes are modelled as retention areas that retain water during a flood and are emptied when the flood recedes. In even more extreme flood situations the flood flows into the retention area, by-passes the river and flows back into the river at a more downstream location. The latter effect is only taken into account for the Lower Rhine (HKV, 2011). The results of 2-D Delft-FLS and Waqua calculations were used for the schematization and calibration of the effects of bypassing of parts of the river (Van der Veen et al., 2004; LANUV NRW, 2010; De Joode, 2007; Wijbenga et al., 2008).

There are no hydraulic structures in the modelled part of the main stem of the Rhine. Hydraulic structures in the downstream stretches of the tributaries Neckar, Main, Nahe, Lahn, Moselle and Ruhr are implemented in the Sobek model, including their operation rules. The way the Sobek models are coupled to the HBV model is described in Hegnauer and Becker (2013).

The Sobek models were calibrated using hydraulic roughness of the main channel as calibration parameter. Calibration was based on a comparison between model results and observations for several steady-state measurements and flood waves (BfG, 2008, Meijer, 2009). The hydraulic roughness of the flood plain was based on land-use data.

Uncertainty in flooding

Flooding is modelled in the Sobek model as overtopping when it concerns a structure like a retaining wall, or as overtopping with breaching when it concerns a dike. The time when overtopping occurs or the way a dike breaches in the model has an effect on the damping of the flood wave. The magnitude of this effect has been investigated through a sensitivity analysis by doing calculations for different flooding “scenarios” (Udo and Termes, 2013). Four parameters that are related to the way flooding is modelled in Sobek were adjusted within certain ranges:

- Var 1: The level of the top of the dike (-0.5m or +0.5m)
- Var 2: The width of the breach in the dike (-25% or +50%)
- Var 3: The volume of the retention area behind the dike (-50% or +50%)
- Var 4: The initial water level behind the dike (-1.0m or +1.0m)

The choices of these parameters and their ranges were based on expert judgement. The results of this sensitivity analysis are shown in Figure 5.3. The figure shows that the level of the top of the dike and the retention volume behind the dike have the strongest influence on the discharge at Lobith. However, the determination of the volume of the area behind the dikes is much more accurate than the + and -50% that is used in this sensitivity analysis. Therefore, the effect of the uncertainty in the retention volume behind the dikes on the discharge at Lobith is much less than Figure 5.3 suggests.

The results that are shown here were obtained by simultaneously adjusting the model parameters for each location in the model where these parameters are used. For example, in the case of 0.5 meter higher dikes, all dikes in the model were adjusted. The results presented in Figure 5.3 should therefore be seen as upper limit of the effects.

It should also be noted that at the Lower Rhine the level of the top of the dike and the volume of the retention area behind the dike were used in the calibration of the Sobek model. By adjusting these parameters, in principle the model should be recalibrated, which was not done during this study. Therefore the results of this sensitivity analysis should be used with caution.

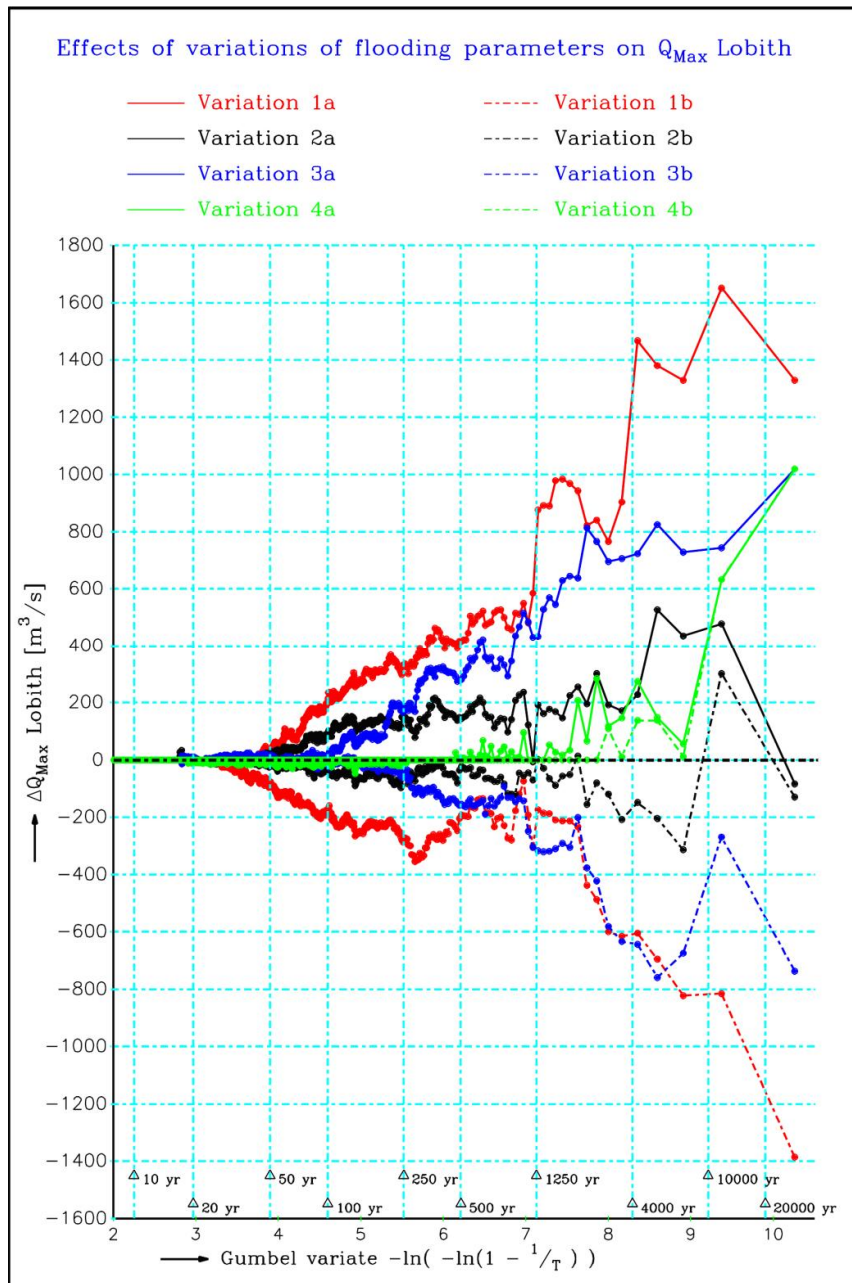


Figure 5.3 Results for different flooding “scenarios” for the Rhine. The results are presented relative to the Sobek model with flooding. Variation 1a: dike top +0.5m; 1b: dike top -0.5m; 2a: breach width -25%; 2b: breach width +50%; 3a: retention behind dike -50%; 3b: retention behind dike +50%; 4a: water level behind dike +1m; 4b: water level behind dike -1m. See main text for details

5.4 Simulation of historical floods in the river Meuse

This section shows some modelling results for the historical period 1967-1998. These results give an impression of the performance of GRADE for the Meuse.

Time series

The hydrograph for the 1993 and 1995 events is shown in Figure 5.4 (Chooz) and Figure 5.5 (Borgharen). These are the second and third highest floods recorded at Borgharen since the start of the observations in 1911. The modelled discharge pattern is in good accordance with the observed discharges. Apart from the magnitude of the Jan/Feb 1995 peak at Borgharen both the magnitude and the timing of the peaks are well simulated. More information about the performance of GRADE for the Meuse can be found in Kramer and Schroevers (2008).

The Nash-Sutcliffe efficiencies for Chooz and Borgharen are listed in Table 5.1. The Nash-Sutcliffe efficiency for Borgharen is slightly better than for Chooz, but for both locations the model is well capable to simulate the flow in this period.

Table 5.1 Nash-Sutcliffe efficiencies of GRADE for different stations along the Meuse for the period 1993-1995

Stations	Chooz	Borgharen
Nash-Sutcliffe	0.83	0.86

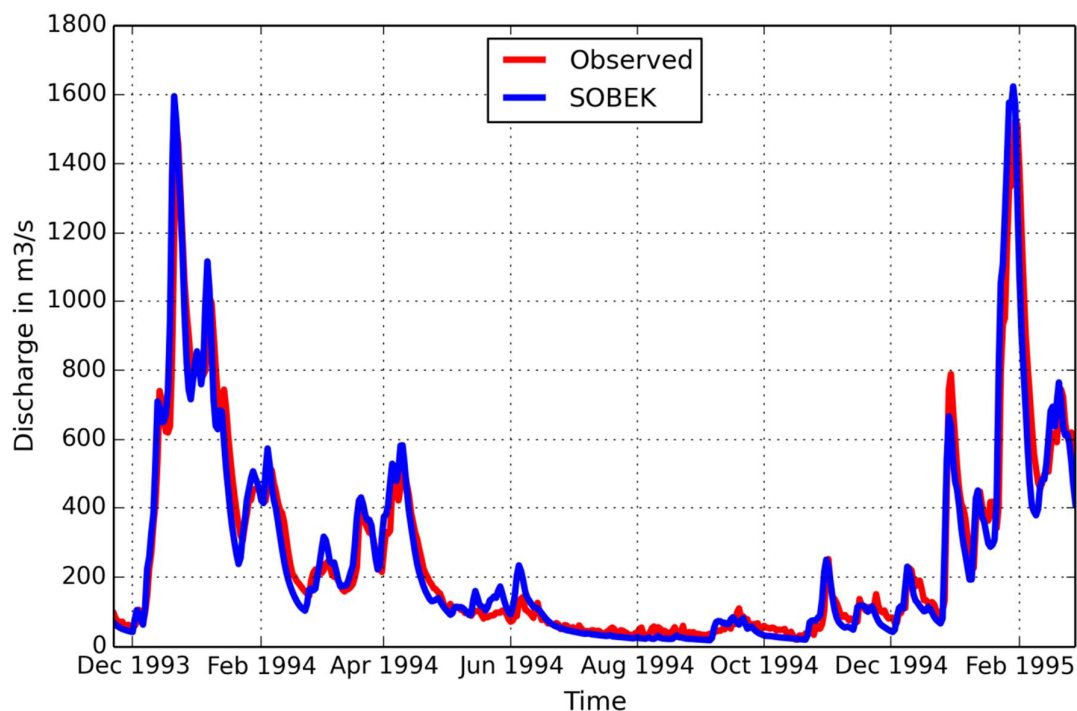


Figure 5.4 Simulation of the flows in the Meuse at Chooz comprising the 1993 and 1995 flood events

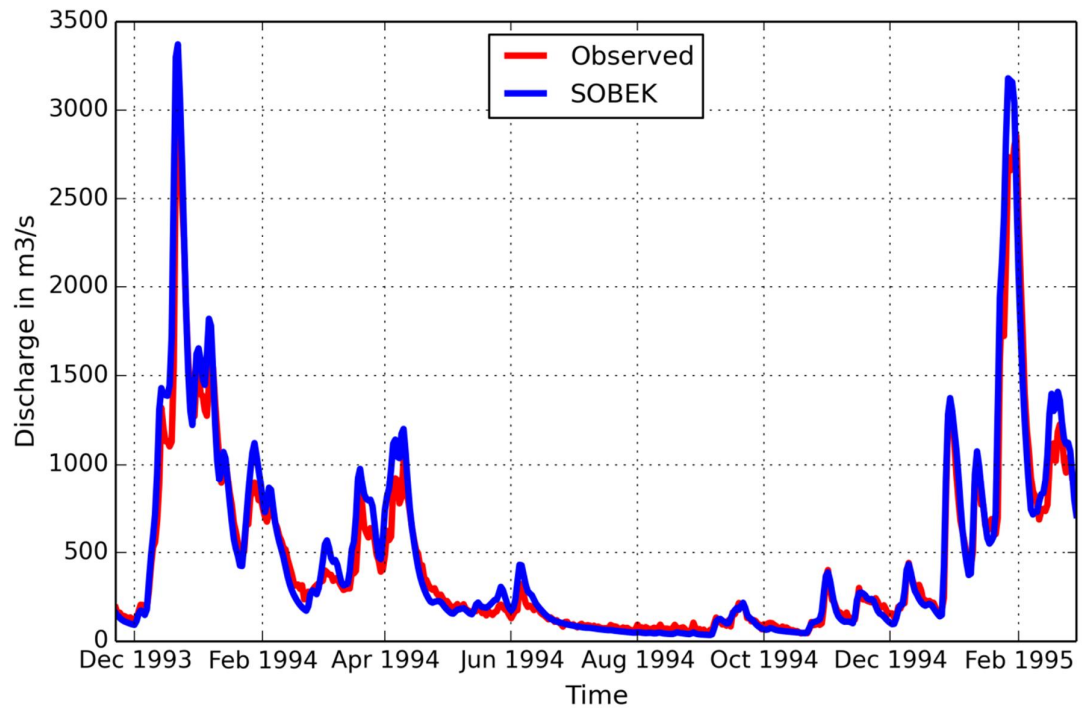


Figure 5.5 Simulation of the flows in the Meuse at Borgharen comprising the 1993 and 1995 flood events

Reproduction of the annual maxima

Figure 5.6 shows the modelled (vertical axis) and measured (horizontal axis) annual maximum discharges for the Meuse at Borgharen. The blue dashed line represents the line of equality. Overall, the simulated discharges seem to overestimate the observed discharges slightly. For Chooz and Borgharen the mean of the annual maxima (MHQ) is shown in Figure 5.7. On average, the simulated discharges are slightly higher than the observed discharges.

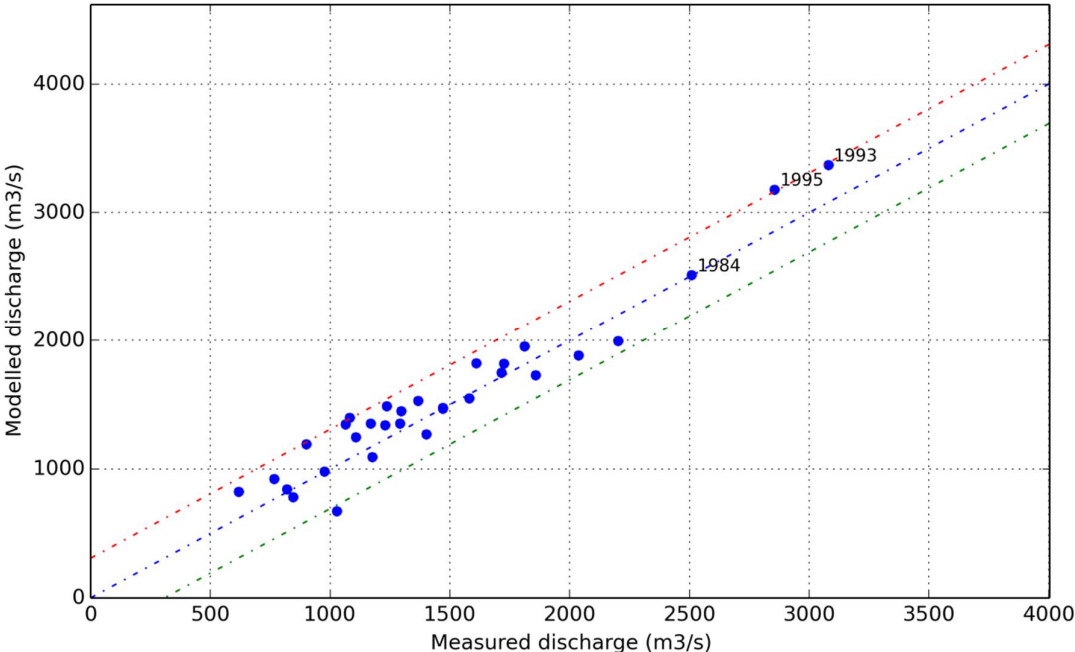


Figure 5.6 Overview of the modelled and measured annual maxima (1967-1998) for the Meuse at Borgharen. The dashed lines represent the line of equality (blue) with its +300 m³/s and -300 m³/s band

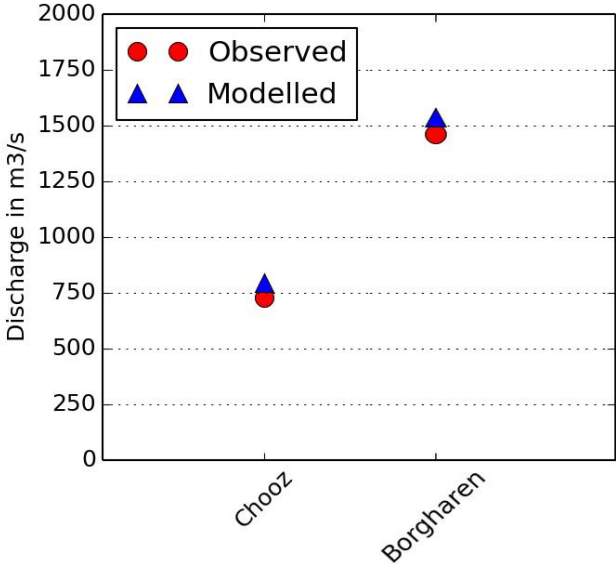


Figure 5.7 Mean annual maximum discharges (MHQ) (1967-1998) for the Meuse at Chooz and Borgharen

5.5 Simulation of historical floods in the river Rhine

This section shows some modelling results for the historical period 1951-2006. These results give an impression of the performance (see also Hegnauer, 2014) of GRADE for the Rhine.

Time series

Figure 5.8 to Figure 5.11 show the hydrographs at 4 gauging stations along the Rhine between Kaub and Lobith for the period December 1993 to February 1995. Also for the Rhine this period contains two of the three highest floods recorded since the start of the observations at Lobith in 1901. The simulated hydrographs are in good accordance with the ones observed. The timing of the peaks is well simulated, but the lowest flows in this period are often slightly underestimated. For 6 stations along the Rhine the Nash-Sutcliffe efficiencies are listed in Table 5.2. The Nash-Sutcliffe efficiency for Lobith is high, meaning that the model is well capable to simulate the flow at Lobith. The reason that the Nash-Sutcliffe efficiency is lower for Basel and Maxau could be that the daily time step used to calculate the runoff is too long to capture the generating runoff forming processes upstream of Maxau.

Table 5.2 Nash-Sutcliffe efficiencies of GRADE for different stations along the Rhine for the period 1993-1995

Stations	Basel	Maxau	Kaub	Andernach	Cologne	Lobith
Nash-Sutcliffe	0.75	0.74	0.84	0.87	0.89	0.91

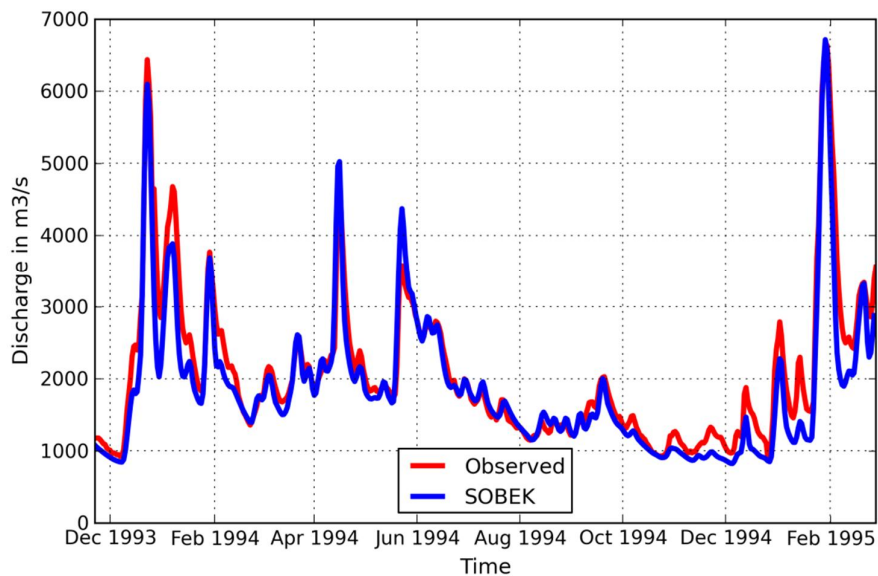


Figure 5.8 Simulation of the flows in the Rhine at Kaub comprising the 1993 and 1995 flood events

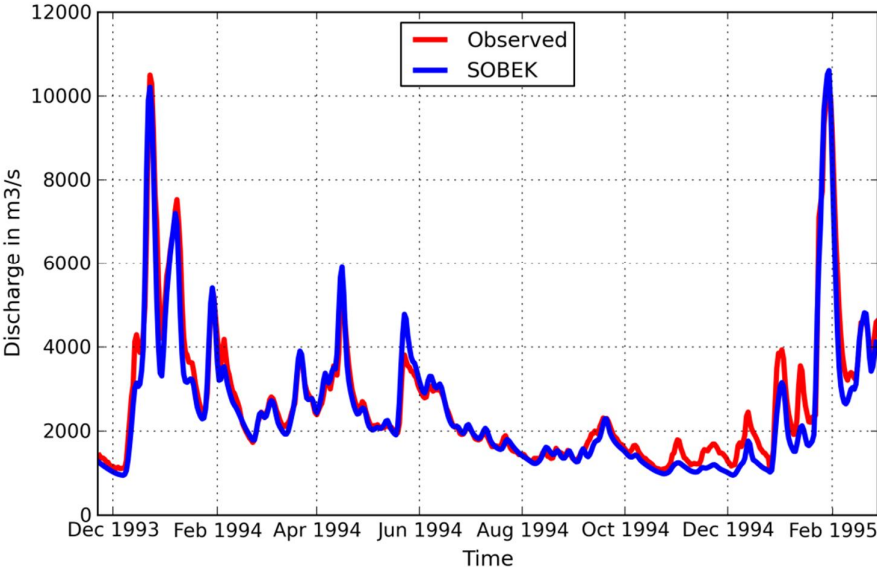


Figure 5.9 Simulation of the flows in the Rhine at Andernach comprising the 1993 and 1995 flood events

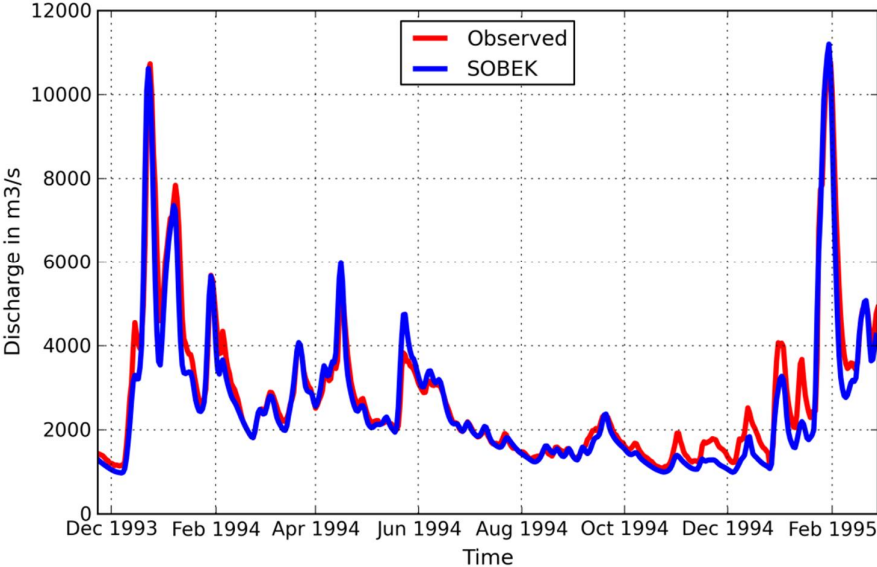


Figure 5.10 Simulation of the flows in the Rhine at Cologne comprising the 1993 and 1995 flood events

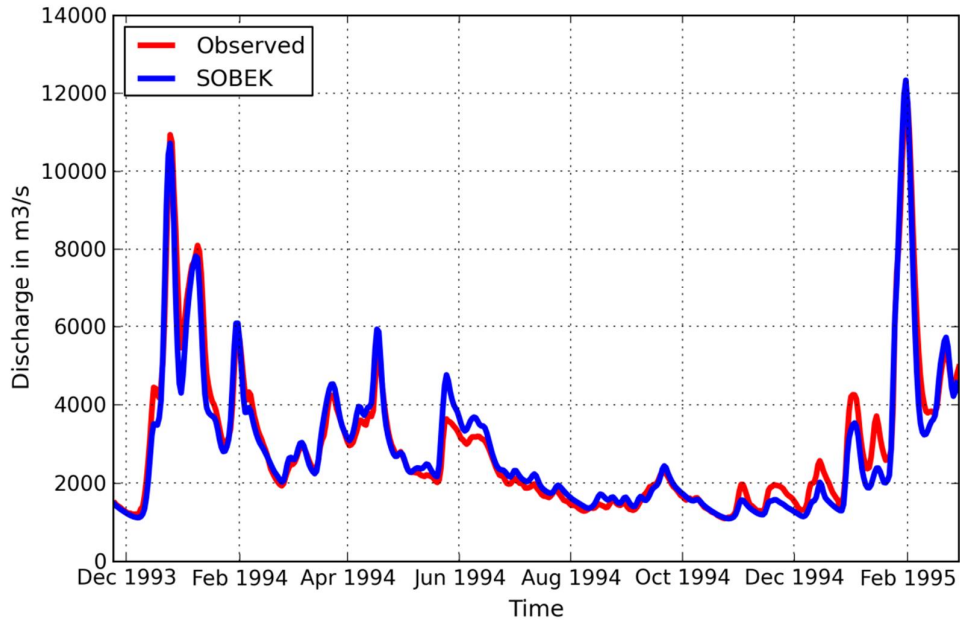


Figure 5.11 Simulation of the flows in the Rhine at Lobith comprising the 1993 and 1995 flood

Reproduction of the annual maxima

Figure 5.12 shows the modelled (vertical axis) and measured (horizontal axis) annual maximum discharges for the Rhine at Lobith. The blue dashed line represents the line of equality. The large deviation of two flood events above the red dotted line is associated with a strong overestimation of the discharges at Maxau. In the Muskingum routing module for the stretch between Basel and Maxau no retention is modelled. For high flow events at Lobith with very high discharges upstream of Maxau (such as the 1988 flood event), the modelled peaks are therefore too high compared to the measured peaks.

Figure 5.13 shows the results for the mean annual maximum for different gauging stations along the Rhine. Only at Maxau a clear deviation from the mean observed annual maximum is found, which is not yet fully understood since no such overestimation is found for Basel or Kaub.

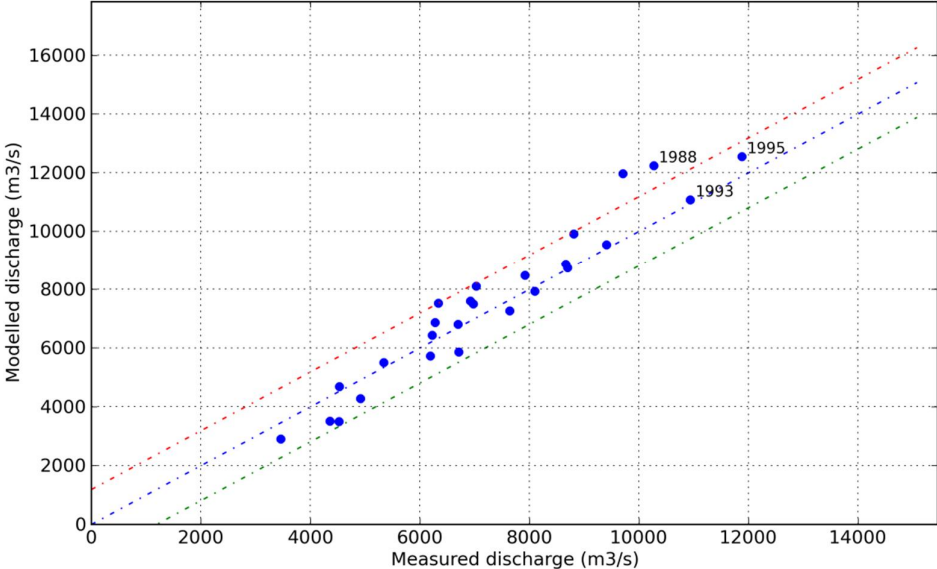


Figure 5.12 Overview of the modelled and measured annual maxima (1951-2006) for the Rhine at Lobith. The dashed lines indicate the line of equality (blue) with its +1000 m³/s and -1000 m³/s band

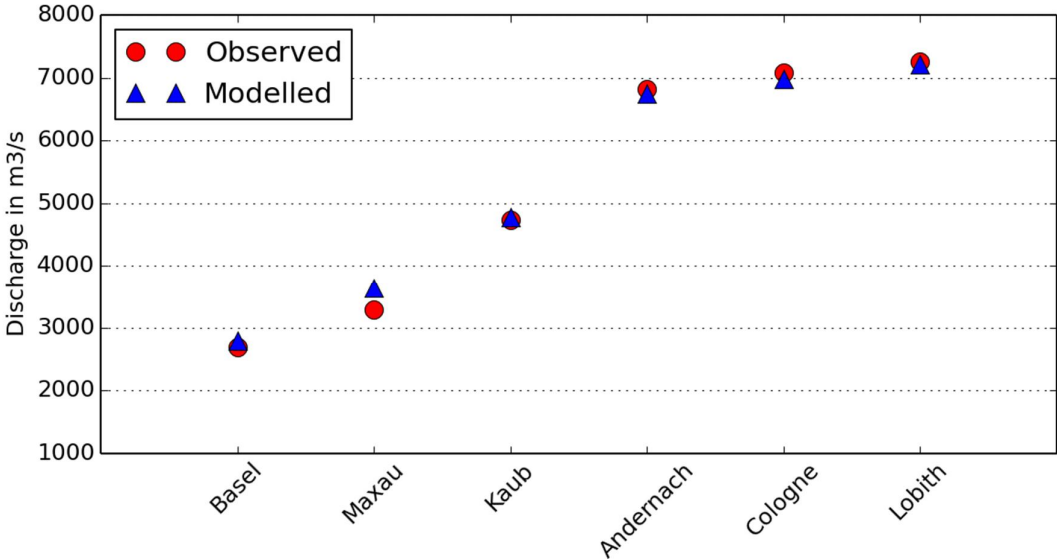


Figure 5.13 Mean annual maximum discharges (MHQ) (1951-2006) for different locations along the Rhine

5.6 Limitations of the routing module in representing extreme floods

There are three main limitations of the routing modules in GRADE. For the Meuse use is made of a Sobek model without flooding areas. Especially in the area around Liège, it is known that flooding will occur during extreme flood events. This will have a profound attenuating effect on the flood wave at Borgharen. A first study on the effect of flooding areas around Liège was performed by Paarlberg and Barneveld (2013). They concluded that the reduction of the flood peak as a result of upstream flooding could be in the order of 5-10%, depending on the magnitude of the discharge. However, the available information on which this conclusion is based is too limited to include upstream flooding of the Meuse in GRADE for this moment.

For the Rhine a limitation is the fact that retention areas between Basel and Maxau are not incorporated in GRADE. For this part, the simplified Muskingum routing is applied, which cannot model the retention areas that are located along this stretch of the river. Extending the Sobek model and including the retention area in the schematization up to Basel could solve this problem.

Finally, there is a difference in the formulation of flooding in the routing between the Upper Rhine and the Lower Rhine. The flooding areas behind dikes are modelled differently for both stretches of the Rhine. For the Upper Rhine a simplistic way is used to describe the flooding in the surrounding region, whereas for the Lower Rhine a complex system of retention and flooding areas is used. The latter is based on a comparison with a 2D hydraulic model. Because of this difference, the modelling results for the Lower Rhine are more accurate than for the Upper Rhine.

6 Construction of frequency-discharge curves and flood hydrographs

Flood peaks and corresponding flood hydrographs for various return periods (including the design discharge with a return period of 1250 years) are calculated with GRADE using the 50,000 year reference simulation. In this simulation the reference synthetic weather series (corresponding to the solid lines in Figure 3.3 (Rhine) and Figure 3.6 (Meuse)) is combined with the 50% HBV-parameter set. To derive flood hydrographs Sobek is used. For the Rhine two model schematizations are considered, one with and one without upstream flooding. For the Meuse, only one model (without upstream flooding) is available.

6.1 Frequency discharge curve

6.1.1 Methodology

A frequency discharge curve is a continuous representation of flood peaks (or annual maximum discharges) as a function of their return period (or exceedance frequency). The flood peaks for the various return periods are obtained by ranking the annual maximum discharges in the generated 50,000-year sequence in increasing order. The rank in this ordered set determines the return period. For the 100 largest discharges, i.e. for return periods ≥ 500 years, the method of Weissman (1978) was used to reduce the effect of random fluctuations in the upper tail of the distribution. This method makes use of the joint limiting distribution of these order statistics. The Weissman fit is also used to extrapolate to return periods of 100,000 years.

For the assessment of the frequency discharge curves, it is important to take into account the possibility of flooding along the river as flooding has a damping effect on the downstream flood peaks. For the Rhine, flooding already has an effect on discharges well below the 1250-year discharge (Figure 5.3), whereas for the Meuse it was found in earlier studies that flooding, especially around Liège, starts around the 1250-year discharge (Dewals et al., 2012; Paarlberg and Barneveld, 2013). As mentioned in Section 0, flooding is not incorporated in GRADE for the Meuse.

6.1.2 Results

The resulting frequency discharge curve for the Meuse at Borgharen and the sorted observed annual maximum discharges are shown in Figure 6.1. For short return periods (up to $T = 20$ years) the frequency discharge curves correspond well to the sorted observed annual maxima. For longer return periods, a (small) deviation from the sorted observed annual maxima is found. The 1250-year flood peak according to the GRADE simulation is $3910 \text{ m}^3/\text{s}$.

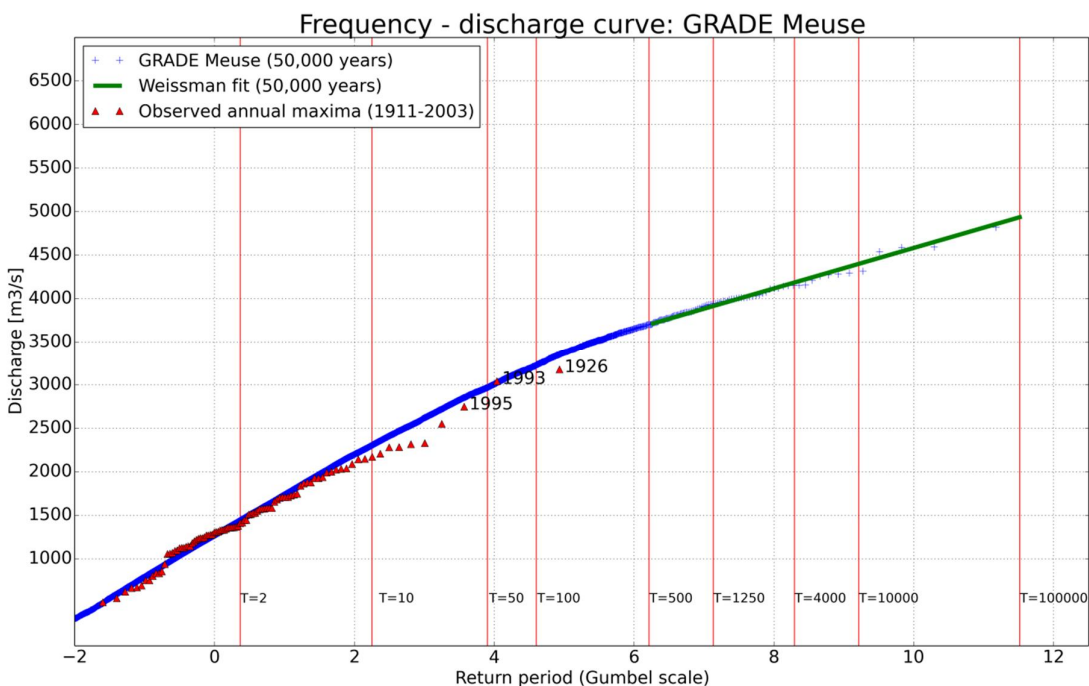


Figure 6.1 Frequency discharge curve for the river Meuse at Borgharen, together with the sorted observed annual maxima

Figure 6.2 shows the frequency discharge curves for the Rhine at Lobith for the situation with upstream flooding in Germany and when there is no flooding. For return periods just below $T = 2$ years, there is a slight “bump” in the sorted annual maxima in the observations which is not reproduced by GRADE. For longer return periods, the frequency discharge curves correspond well to the distribution of the observed annual maxima.

For discharges below $12,000 \text{ m}^3/\text{s}$, both frequency discharge curves coincide. It is shown that below $12,000 \text{ m}^3/\text{s}$, no (significant) upstream flooding occurs and it is therefore no surprise that both routing models give the same results. Since 1901, only the three largest flood events (1926, 1993 and 1995) had peaks near $12,000 \text{ m}^3/\text{s}$. For the case that upstream flooding is ignored, the frequency discharge curve is almost a straight line (on the Gumbel scale), resulting in a 1250-year flood peak of $16,560 \text{ m}^3/\text{s}$. When flooding is taken into account, the flood frequency curve diverges from the curve without upstream flooding (Figure 6.2). The 1250-year flood peak from the GRADE simulation is then $14,350 \text{ m}^3/\text{s}$. For a return period of 1250 years, the absolute difference between the two frequency discharge curves is about $2210 \text{ m}^3/\text{s}$. This difference is caused by the upstream flooding in Germany.

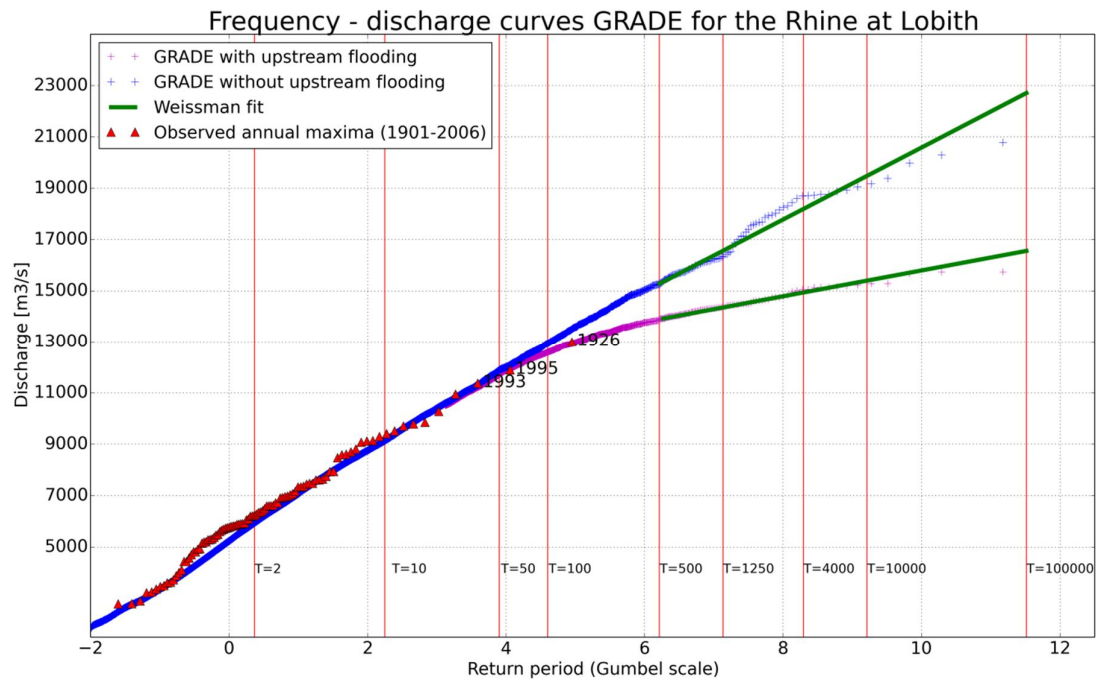


Figure 6.2 Frequency discharge curves for the river Rhine at Lobith, with and without upstream flooding, together with the sorted observed annual maxima

6.2 Shape of the flood hydrograph

6.2.1 Methodology

The methodology for the derivation of the flood hydrograph associated with a given peak discharge is for the Rhine the same as for the Meuse. The description is given here for the Meuse. The method is described in more detail in Kramer (2012).

As for the derivation of the flood peaks, use is made of the entire set of 50,000 synthetic flood hydrographs. These synthetic hydrographs include peak values both in the reach of the historical floods and significantly higher, including values (far) above the present design flood value for a return period of 1250 years. This implies that no upscaling of historical flood hydrographs is necessary as in the current method (Section 1.2) and use can be made of an interpolation of the hydrograph shapes. All synthetic flood hydrographs are grouped into classes corresponding to flood peaks. By averaging the flood hydrograph within a class, an “average flood hydrograph shape” for each return period is obtained. This averaging can be done either in horizontal or vertical direction as is shown in Figure 6.3 for the Meuse at Borgharen.

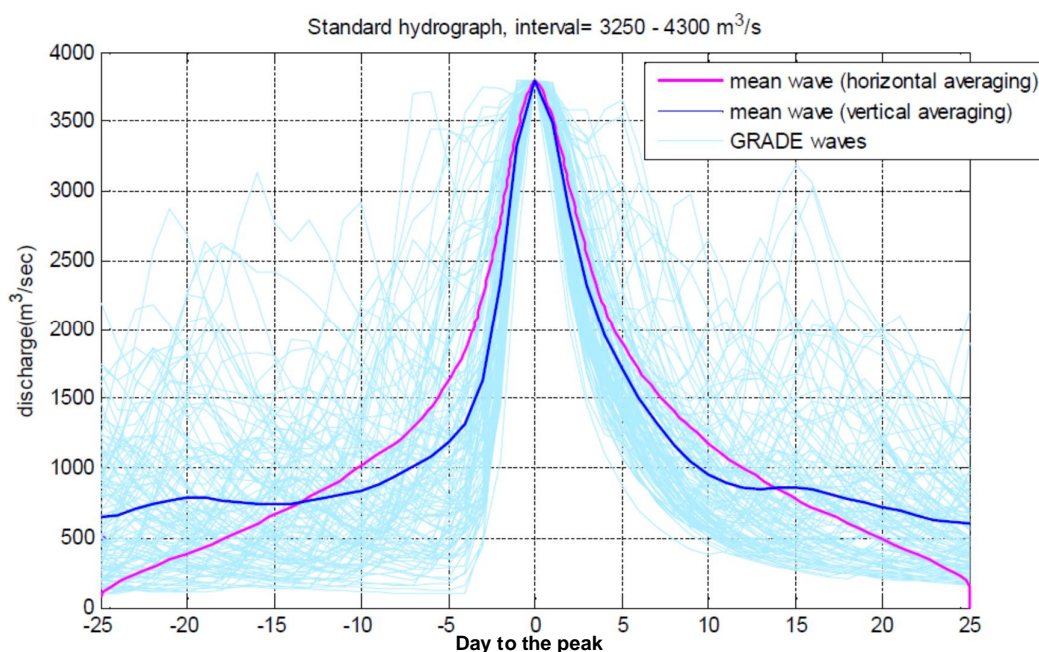


Figure 6.3 Comparison between horizontal averaging (pink line) and vertical averaging (dark blue line) for the river Meuse at Borgharen based on all hydrographs in the class between 3250 m³/s and 4300 m³/s (light blue lines). Source: Kramer (2012)

Vertical averaging corresponds to averaging of the ordinates. An advantage of vertical averaging is that it better preserves the flood volume of all the hydrographs in the same class. However, in GRADE, both options for horizontal and vertical averaging are built in the system and the user can choose which method to apply. All hydrographs presented in this report are based on vertical averaging.

Figure 6.4 shows the shape of the 1250-year hydrograph for the river Meuse at Borgharen based on all hydrographs with peak discharges above 3500 m³/s. All hydrographs within this class are first scaled to the 1250-year peak discharge of 3910 m³/s. After scaling, a beta distribution⁸ is fitted to the ordinates of all scaled hydrographs within the class for each day to the peak (the grey lines in Figure 6.4). From the beta distribution, the mean hydrograph and the pointwise 95% uncertainty band⁹ are derived. The pointwise 95% uncertainty band is calculated from all hydrographs that fall within the discharge class.

⁸ The log-normal distribution in Kramer (2012) is replaced by the beta distribution, because the properties of this distribution fit better to the data.

⁹ The pointwise 95% uncertainty band is constructed by deriving the 2.5% and 97.5% quantile of the ordinate for each 'day to the peak' and by combining these quantiles to one uncertainty band. The 95% probability holds thus pointwise. This is different from a global 95% uncertainty band, which is constructed, such that it captures a whole flood wave with probability 95%. Generally, a global uncertainty band is wider than a pointwise uncertainty band.

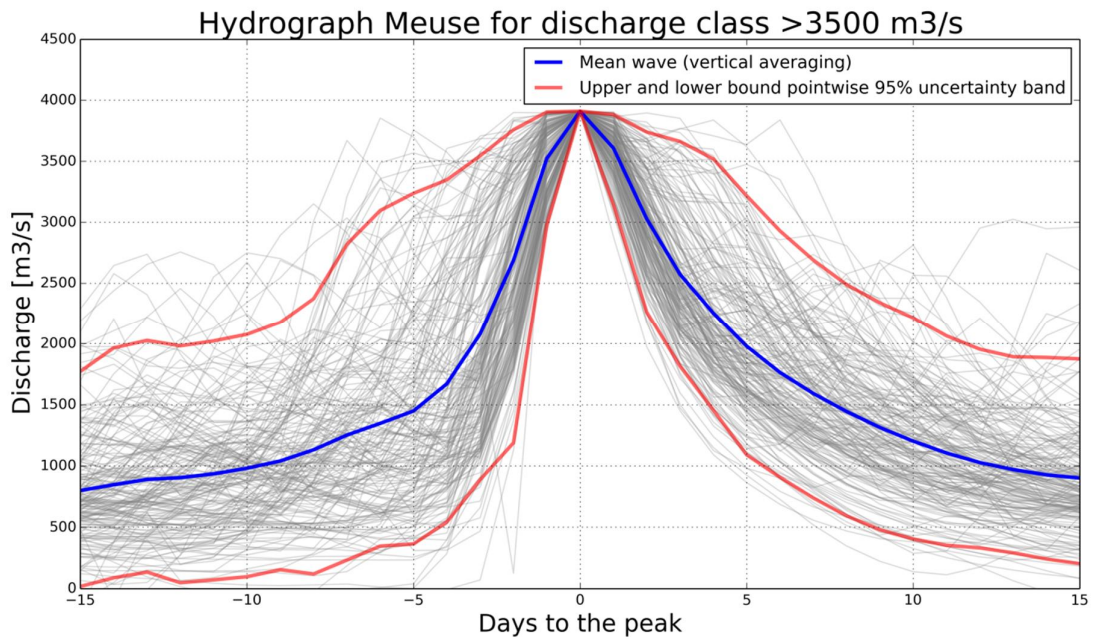


Figure 6.4 Shape of the 1250-year hydrograph for the river Meuse at Borgharen in GRADE (blue line) with the pointwise 95% uncertainty band, based on vertical averaging (red lines). The grey lines represent the hydrographs on which the design hydrograph and the uncertainty band are based

6.2.2 Results

The shape of the hydrograph for the Meuse at Borgharen is shown for different discharge classes in Figure 6.5. The width of the hydrograph increases for higher discharge classes, just as could be expected. However, after scaling with the average maximum discharge in the class, the resulting “relative” hydrograph for the higher peaks is narrower. This is not the case in the current method, where the width of the relative hydrograph stays the same for all peak discharges.

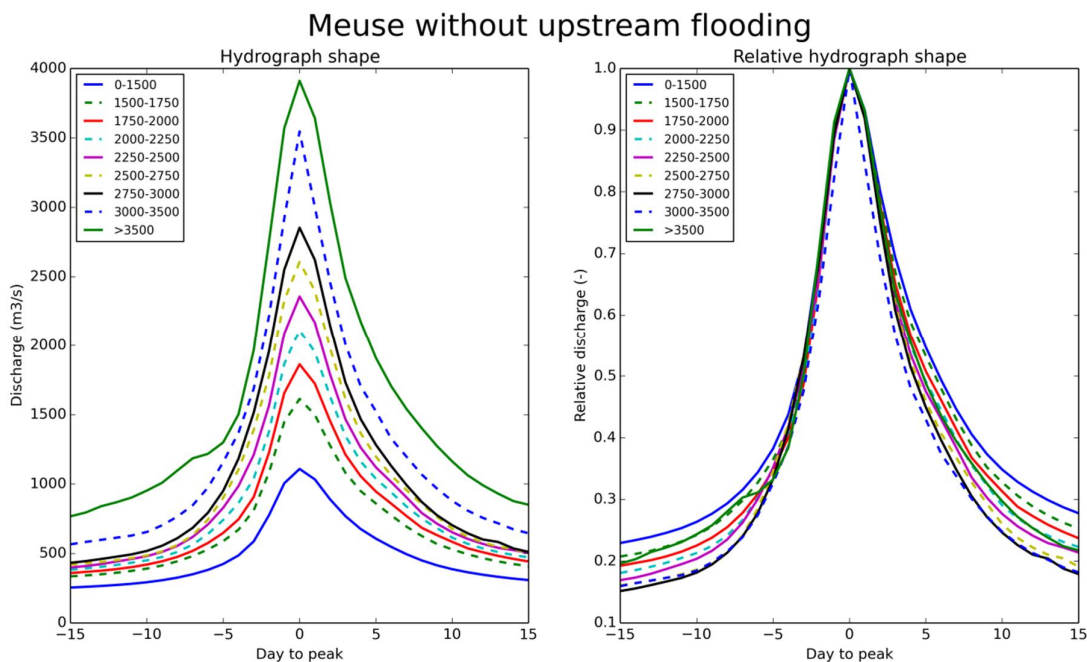


Figure 6.5 Hydrograph shape for the Meuse at Borgharen for different discharge classes based on vertical averaging. The left figure presents ‘absolute’ hydrographs, whereas the right figure shows the ‘relative’ hydrographs which are scaled by the average maximum discharge within a class

In Figure 6.6 the resulting flood hydrographs for the Rhine at Lobith with upstream flooding are presented. Also here, the width of the hydrographs increases for increasing peak discharges, but in the right panel it can be seen that the hydrograph shape for the two highest discharge classes (i.e. the dark blue dashed line and the black line) is different from the other hydrographs. The hydrographs corresponding to the two highest discharge classes are not the smallest anymore after scaling. This is caused by upstream flooding. Water which is temporarily stored in the flooding areas is delayed so that the hydrograph becomes lower, but wider.

Figure 6.7 shows the hydrograph shape for the Rhine at Lobith without upstream flooding. Here the pattern more or less looks like that for the Meuse where upstream flooding is also not taken into account.

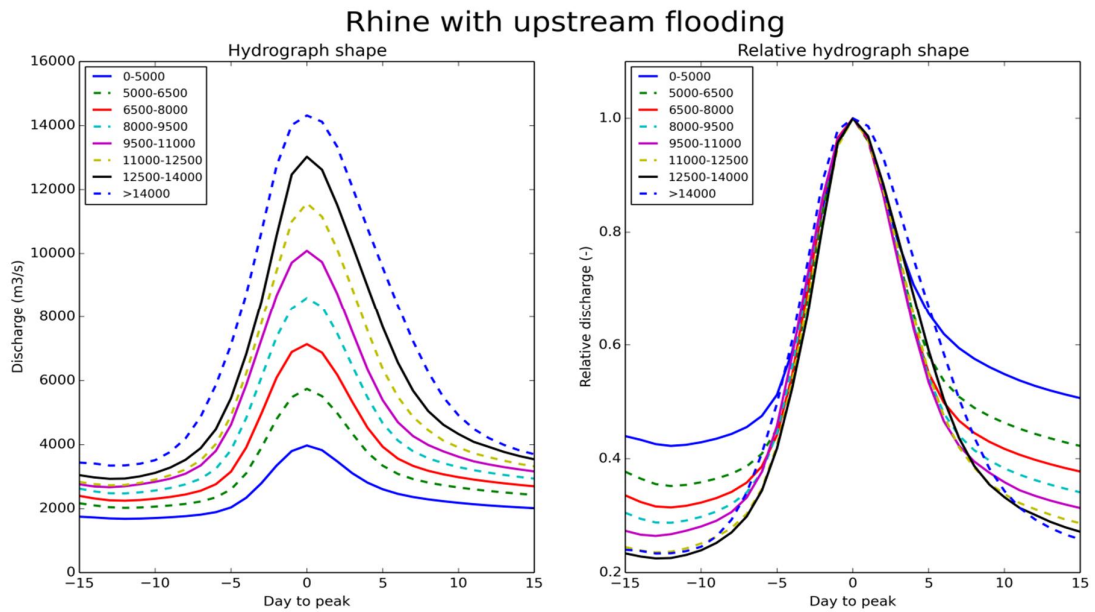


Figure 6.6 Hydrograph shape for the Rhine at Lobith with upstream flooding for different discharge classes based on vertical averaging. The left figure presents 'absolute' hydrographs, whereas the right figure shows the 'relative' hydrographs which are scaled by the average maximum discharge within a class

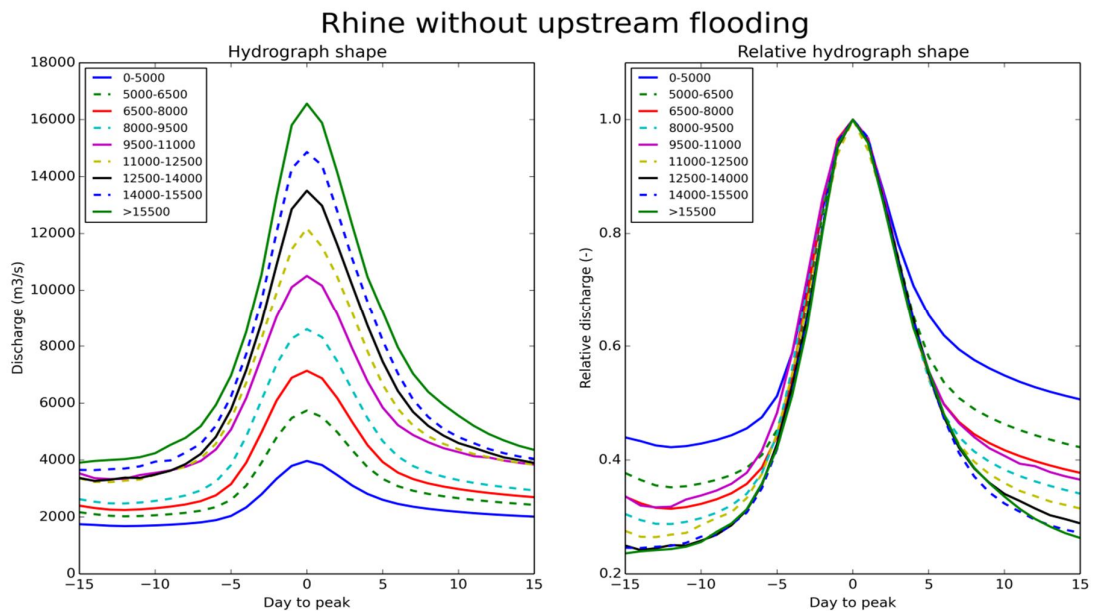


Figure 6.7 Hydrograph shape for the Rhine at Lobith without upstream flooding for different discharge classes based on vertical averaging. The left figure indicates 'absolute' hydrographs, whereas the right figure shows the 'relative' hydrographs which are scaled by the average maximum discharge within a class

A comparison between the situations with and without flooding on the Rhine is presented in Figure 6.8. It is clear that the hydrograph for the situation with upstream flooding is wider than for the situation without flooding. However the flood waves have a similar volume.

The hydrographs for a return period of 1250 years with 95% (pointwise) uncertainty bands are shown in Chapter 8.

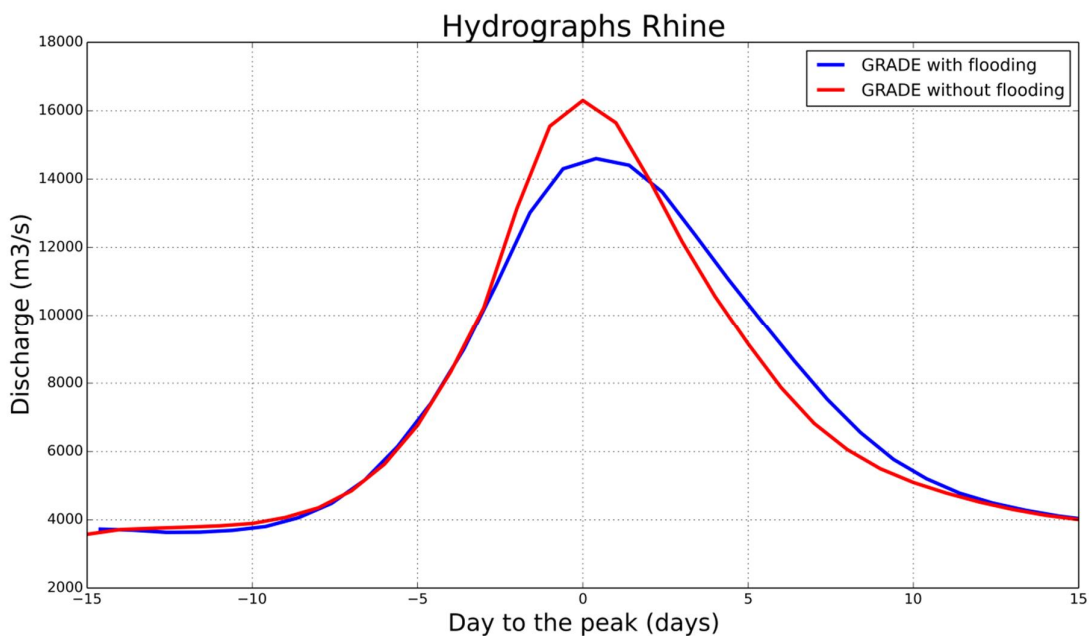


Figure 6.8 Comparison of the 1250-year hydrographs for the Rhine for the situation with and the situation without upstream flooding

7 Uncertainty analysis

In the foregoing chapters some issues about uncertainties in GRADE have already been mentioned. In this chapter the representation of the uncertainties in the GRADE components is more explicitly considered, together with the recipe for the combination of these uncertainties. The uncertainties in the three components of GRADE are discussed in Sections 7.1 - 7.3. The combination of uncertainties is described in Section 7.4 and the results and limitations of the method in Sections 7.5 and 7.6 respectively. For more details on the uncertainty analysis, reference is made to Van den Boogaard et al. (2014) and Schmeits et al. (2014a,b).

7.1 Uncertainty in stochastic weather generation

Daily rainfall and temperature sequences of 50,000 years have been generated for the Rhine and Meuse basins. It was already noticed in Chapter 3 that the limited length of the baseline series is a major source of uncertainty. A jackknife method was used to determine the uncertainty of the return levels of extreme multi-day rainfall and extreme river discharge. In this method subsets or jackknife series were formed by leaving out subsequent non-overlapping i -year blocks from the baseline series. For each jackknife series a 20,000-year simulation was conducted similar to the 50,000-year reference simulation and return levels were estimated. Let $Q_{WG}(i)$ be the estimated T -year return level from the i -th jackknife series. Then the jackknife standard deviation of the estimated T -year return level is given by:

$$s_{WG} = \sqrt{\frac{n-1}{n} \sum_{i=1}^n [Q_{WG}(i) - m_{WG}]^2} \quad (1)$$

where

$$m_{WG} = \sum_{i=1}^n Q_{WG}(i) / n \quad (2)$$

and n is the number of jackknife series. Note that the factor $(n-1)/n$ in Eq. (1) deviates from that in the ordinary expression for the standard deviation because of the dependency between the jackknife series.

To avoid splitting the winter half-year in the jackknife procedure, years run from 1 October to 30 September. There are then 55 complete winter half-years in the baseline series of the Rhine basin and 72 in the baseline series of the Meuse basin. The accuracy of s_{WG} decreases with increasing blocksize, which points towards the use of short blocks. It is, however, not feasible to take blocks as short as one year, because of the enormous computational burden involved. For the Rhine basin a blocksize of 5 years was chosen, resulting in 11 jackknife series. Because there are less computational restraints for the smaller Meuse basin, a blocksize of 3 years was used for this river basin, resulting in 24 jackknife series.

Figure 7.1 presents Gumbel plots of the maximum 4-day and 10-day average precipitation over the Rhine basin in the winter half-year for the 11 simulations based on the jackknife series. These plots are scattered around the plot for the 50,000-year reference simulation. However, the plot of the 4-day maxima for the jackknife series, where the 1987-1991 block was deleted, deviates considerably from the plot for the reference simulation at long return periods. This block contains the winter half-year October 1986 – March 1987 in which the largest basin-average 4-day rainfall is found in the baseline series (74.3 mm, October 1986).

For each jackknife series, the 1250-year return level was estimated from the 100 largest winter maxima in the 20,000–year simulation, using the method of Weissman (1978). For this return level, the use of the jackknife resulted in a relative standard deviation s_{WG}/m_{WG} of 6% for the 4-day rainfall amounts over the Rhine basin and 5% for the 10-day rainfall amounts. This is low compared to the relative standard deviation of the estimated 1250-year return level from fitting a GEV distribution to the 4-day and 10-day maxima, which is about 15%.

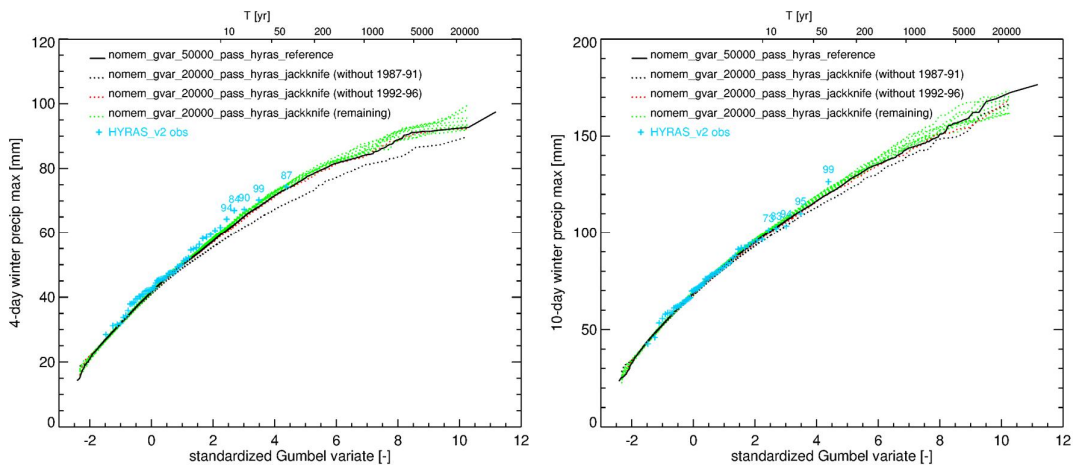


Figure 7.1 Gumbel plots of the maximum 4-day (left panel) and 10-day (right panel) average precipitation over the Rhine basin in the winter half-year for the 50,000-year reference simulation based on the whole baseline series (black solid) and for the 20,000-year simulations based on the jackknife series (black, red and green dotted, see legend). The pluses indicate the ordered observed maxima for the period 1951-2006 (and for the top 5 the year minus 1900 is added, e.g., 87 indicates the winter half-year October 1986 – March 1987)

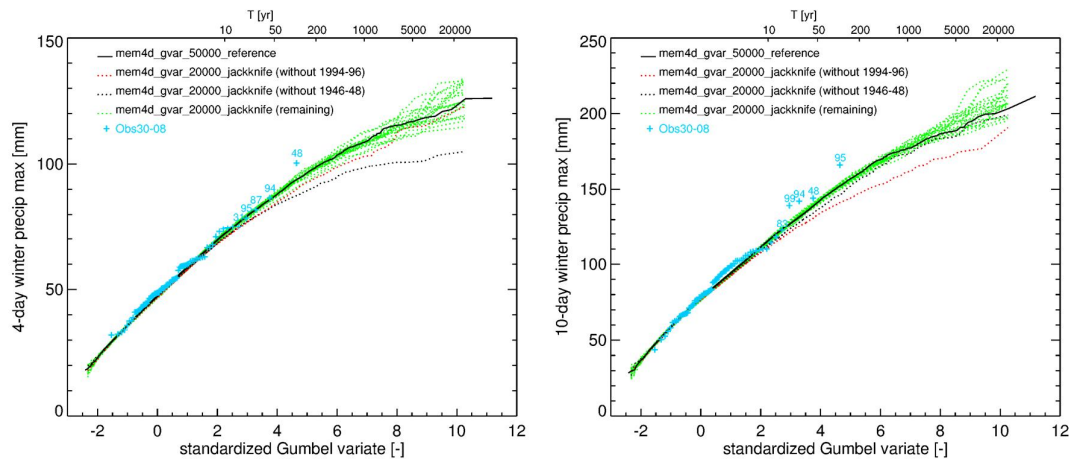


Figure 7.2 As Figure 7.1 but for the Meuse basin. The pluses indicate the ordered 10-day maxima for the period 1930-2008. Note that for the years 1930-1960 and 2008 no daily basin averages were available and that these were replaced by the closest nearest neighbour in the period 1961-2007, cf. Leander and Buishand (2008)

Figure 7.2 presents similar Gumbel plots for the jackknife series of the Meuse basin. Two simulations are highlighted in this figure: the simulation for the jackknife series without the 1946-1948 block (black dotted) and the simulation for the jackknife series without the 1994-1996 block (red dotted). These show the lowest precipitation maxima at long return periods, which is caused by the deletion of a winter period with extreme multi-day rainfall over the Meuse basin (December 1947 or January 1995). These winter periods have a large influence on the simulation of extreme 4-day (December 1947) and 10-day (January 1995) basin-average rainfall. Comparing Figure 7.1 and Figure 7.2, it can be seen that for the Meuse basin the spread between the simulations is larger than for the Rhine basin. The relative standard deviations of the estimated return levels are therefore larger for the Meuse basin. For the 1250-year return level of maximum basin-average rainfall of the Meuse basin, the relative standard deviation is 13% for the 4-day maxima and 11% for the 10-day maxima (compared to respectively 6 and 5% for the Rhine basin). Though there is some evidence that the inclusion of a memory term in the feature vector enhances the influence of certain historical days upon the simulation of extreme multi-day events (Schmeits et al., 2014a,b), this does not explain the large differences between the relative standard deviations of the estimated 1250-year return levels for the Rhine and Meuse basins. Replacing the 4-day memory term by the fraction of sub-basins with daily rainfall > 0.3 mm, reduces the relative standard deviations to 10% for both the 4-day and 10-day maxima, which is still much larger than the values found for the Rhine basin. The estimated 1250-year return levels from different versions of the weather generator for the Meuse basin are, however, more accurate than the estimates from fitting a GEV distribution to the 4-day and 10-day maxima for which a relative standard deviation of about 15% is found.

To transfer the uncertainty of the climate into an uncertainty of the river discharge each of the jackknife series is used as input to the hydrological HBV models for the Meuse and the Rhine basins (see also Section 7.2).

In Figure 7.3 the results for the HBV model for the Meuse for the 24 jackknife series are presented, using the 50% parameter set. This figure shows some similarities with Figure 7.2. For example jackknife series 18 (sub18 in Figure 7.3) corresponds to the red dotted line in Figure 7.2. This is the jackknife series where the 3-year period 1994 - 1996 (which includes the extreme event in January 1995) is left out from the baseline series. Both for the 10-day rainfall extremes and the discharge maxima, omitting this 3-year period shows the most pronounced deviation with respect to the simulations for the other jackknife series.

In Figure 7.4 the resulting frequency discharge curves for the Rhine for all 11 jackknife series are plotted. Two jackknife series (subseries 8 and 9) give considerably lower results than the other series. Subseries 8 is based on the baseline series without the years 1987-1991, whereas subseries 9 is based on the baseline series where the years 1992-1996 are omitted. For the first jackknife series the largest simulated 4-day precipitation amounts were considerably lower than those from the reference series (Figure 7.1), while the second jackknife series does not contain the major precipitation and discharge events of December 1993 and January 1995.

Equations (1) and (2) can also be applied to the resulting discharges of the 11 jackknife series to obtain the relative standard deviation of the estimated 1250-year discharge level. For the Rhine this relative spread is 6.5%, which is 'slightly' larger than the 6% and 5% found for the 4-day and 10-day maxima of basin-average rainfall. For the Meuse the relative spread for the 1250-year discharge return level is 9.7%, which is noticeably smaller than the 13% and 11% for the 4-day and 10-day maxima of basin-average average rainfall. Compared to the Rhine the relative standard deviation for the Meuse is about 1.5 times as large.

The sensitivity of the simulated extreme multi-day events and river discharge to specific extremely wet historical periods is a limitation of the present weather generator. It enhances the uncertainty owing to the limited length of the baseline series. The two-stage resampling algorithm mentioned in Section 3.4 may not suffer from this limitation. In contrast to the present weather generator, the simulated values from that algorithm do generally not correspond to those observed on certain days in the past. However, there is no multi-site version of the two-stage resampling algorithm yet, and this algorithm is much more computer intensive than the present weather generator.

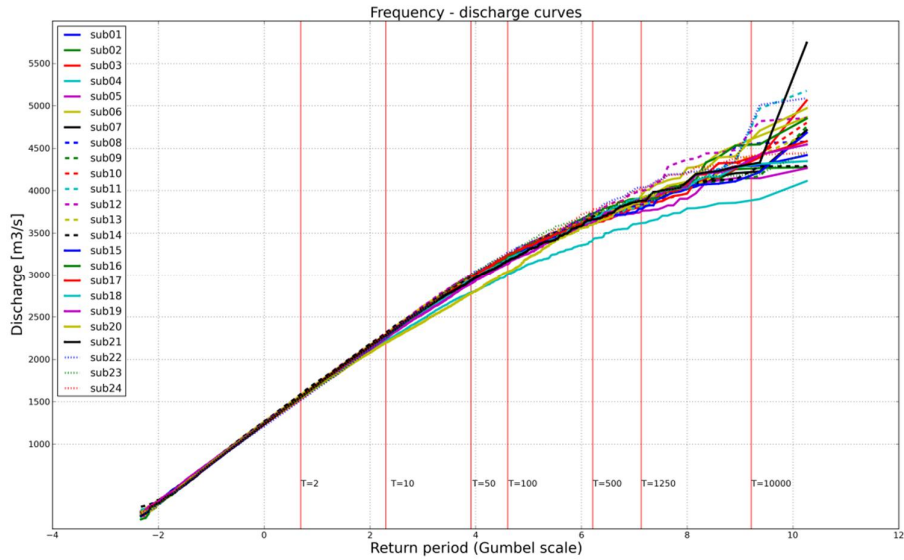


Figure 7.3 Frequency discharge curve of the Meuse for the 50% HBV parameter set for all 24 jackknife series

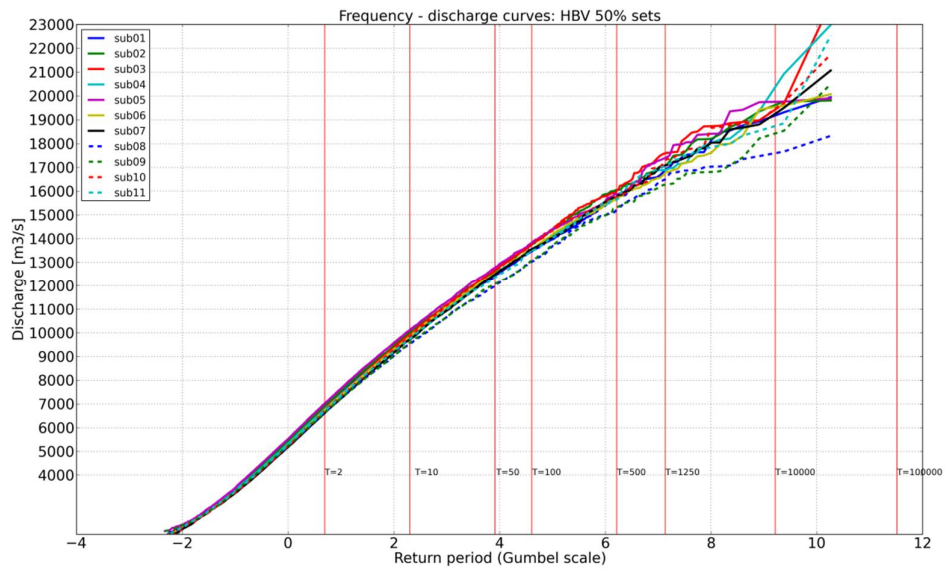


Figure 7.4 Frequency discharge curve of the Rhine for the 50% HBV parameter set for all 11 jackknife series

7.2 Uncertainty in hydrological modelling

The hydrological HBV models in GRADE represent another source of uncertainty in the system. The HBV uncertainty analysis is limited to the model parameter uncertainty. Other sources of uncertainty, such as the model concept and model schematization, are very hard to quantify and were therefore not included in the analysis.

For the Meuse basin and the major sub-basins of the Rhine five representative HBV parameters were selected. This selection was based on the 5%, 25%, 50%, 75% and 95% quantiles of the computed 10-year (Rhine) or 100-year (Meuse) discharges for a large number of behavioural HBV-parameter combinations (see Chapter 4). These quantiles are denoted by q_1, \dots, q_5 , respectively.

As the five representative parameter sets are not equally likely, a weight or probability w_j is assigned to each of these sets ($j = 1, \dots, 5$). This weight has to be proportional to $f(q_j)$, with $f(\cdot)$ the density of the distribution of the generated 10-year or 100-year discharges in the selection procedure of the five representative parameter sets. To obtain a sound estimate of $f(q_j)$ an analytical probability distribution had to be derived for these extreme discharge events. For the Rhine this was carried out for two major sub-basins: the Neckar and the Moselle. For both basins a Reversed Weibull probability distribution function provided the best fit among various candidate distributions. Moreover, for these basins virtually the same weights were found: 0.0678, 0.221, 0.300, 0.277 and 0.134. These weights were then also used for the other major sub-basins as well as for the five 'over all' representative sets for the entire Rhine basin.

For the Meuse the weights were not separately identified and the same weights were used for the five representative HBV-parameter combinations as those derived for the Neckar and the Moselle, because of the similarities between the Meuse and Moselle basins. No more effort was made to determine precisely the values of the weights, as it was found that the overall uncertainty in GRADE's estimates of the extreme discharges at Lobith and Borgharen is hardly sensitive to the setting of the weights.

To obtain the *HBV-induced* uncertainty in GRADE's estimate of an extreme discharge event (e.g. the 1250-year discharge) the system must be simulated for each of the five representative parameter sets. For a given (i.e. synthetically generated) weather series this yields five estimates of the desired discharge event, $Q_{\text{HBV}}(1), \dots, Q_{\text{HBV}}(5)$. Using the weights w_j , the mean m_{HBV} and the standard deviation (or spread) s_{HBV} of the extreme discharge event are estimated:

$$m_{\text{HBV}} = \sum_{j=1}^5 w_j Q_{\text{HBV}}(j) \quad (3)$$

$$s_{\text{HBV}} = \sqrt{\sum_{j=1}^5 w_j [Q_{\text{HBV}}(j) - m_{\text{HBV}}]^2} \quad (4)$$

The spread s_{HBV} provides a quantitative measure of the HBV-induced uncertainty in the extreme discharge event. The mean and the spread can also be used to derive a 95% confidence interval.

This procedure is illustrated with some results obtained from GRADE simulations for the Meuse and Rhine using the first 20,000 years of the reference weather generator (WG) series. For each of the five HBV-parameter sets the extreme discharges at Borgharen and Lobith were derived. The discharges (according to the HBV model) corresponding to a 1250-year return period are listed in the bottom rows of Table 7.1. In the last two columns of this table the (weighted) mean and spread are given.

Table 7.1 Discharges at Borgharen and Lobith for a return period of 1250 years, computed with GRADE for the 5 HBV parameter sets, based on the first 20,000 years of the 50,000 years reference run. The uncertainty in the discharge estimate is given by the spread in the last column

HBV-parameter set	HBV discharge [m^3/s] for $T=1250$ years					Weighted Mean (m_{HBV})	Weighted Spread (S_{HBV})
	5%	25%	50%	75%	95%		
Meuse at Borgharen	3654	3759	3933	3949	4050	3896	112
Rhine at Lobith	16673	16218	16702	16999	16354	16629	295

Frequency discharge curves for the five HBV-parameter sets are shown in Figure 7.5 for the Meuse and Figure 7.6 for the Rhine. The relatively small width of the five curves for the Rhine indicates that the sensitivity of the discharge to the HBV parameters is considerably smaller for this river than for the Meuse. Nevertheless, the relative standard deviation s_{HBV}/m_{HBV} is no more than 3.4% for the Meuse, which is small compared to the relative standard deviation of 9.7% that was found for the HBV simulations with the 50% parameter set, using different weather generator series. For the Rhine the relative standard deviation is 1.7%, compared to the 6.5% found for the HBV simulations with different weather generator series. This large difference in standard deviation is not immediately clear from the scatter in Figure 7.4 and Figure 7.6 which is due to the dependence between the return level estimates for the various jackknife series in Figure 7.4. As mentioned earlier, Eq. (1) accounts for this dependence.

From the row for the Meuse in Table 7.1 it can be seen that the Meuse discharges almost monotonously increase with the “quantile index” of the HBV parameter combination. This monotony would also be expected from the selection procedure of the five representative HBV-parameter sets. For the Rhine, however, such a monotonic behaviour is not seen in Table 7.1. In particular, the 1250-year discharge is for the 95%-parameter set lower than for the 5%- parameter set. This less pronounced monotony for the Rhine may originate from multiple major sub-basins contributing to the discharge at Lobith. The peaks that come from these major sub-basins typically do not perfectly coincide when they meet downstream. Therefore lower and wider peaks may amplify more when they meet downstream than higher and smaller peaks, simply because the chance that they (partly) coincide is larger. The combination of the parameter sets with the largest discharge peaks in the major sub-basins does not necessarily result in the largest discharge peaks downstream at Lobith. It should further be noted that the selection procedure of the five representative HBV-parameter combinations for the Rhine differs from that for the Meuse. For the Rhine it was based on a relatively small discharge quantile, i.e. the 10-year return level (Section 4.3.3). For the Meuse the 100-year return level was used (Section 4.3.2) and this may be more representative of the 1250- to 4000-year return levels that GRADE is primarily intended for. Though the use of a less representative discharge quantile for the selection of the 5 HBV parameter sets may lead to non-monotony at long return periods, the non-monotonicity for the Rhine is already observed at low and moderate return periods (see Figure 7.6).

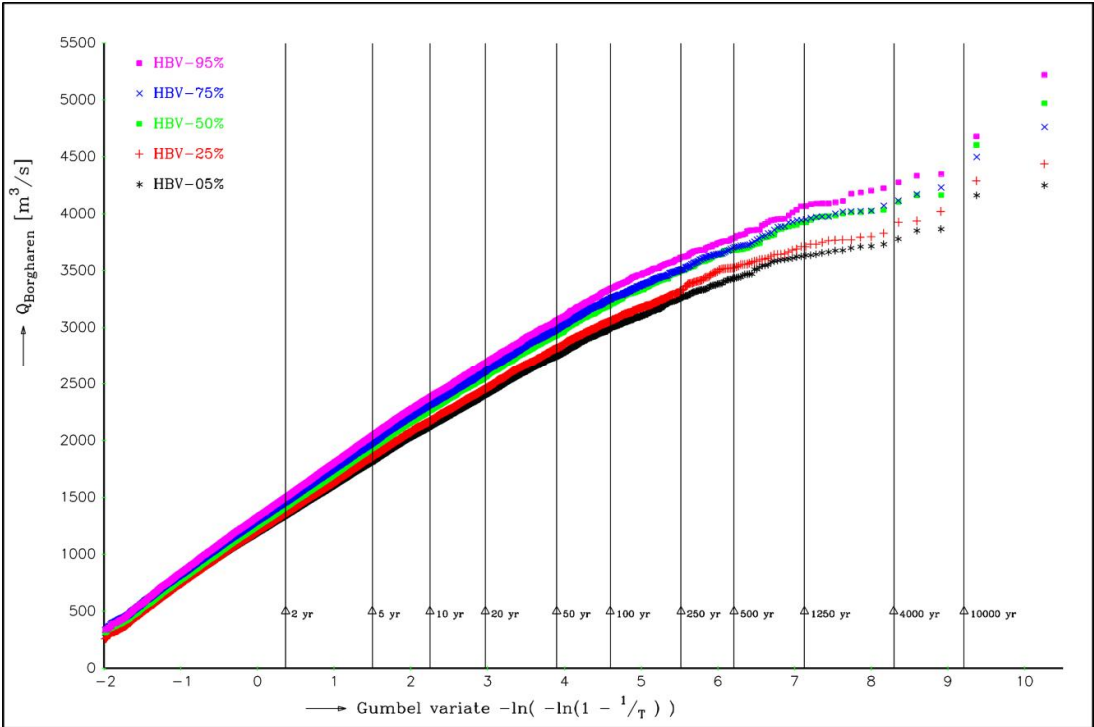


Figure 7.5 Frequency discharge curves for the river Meuse at Borgharen for the five representative HBV parameter combinations using the first 20,000 years of the reference weather generator series for the Meuse

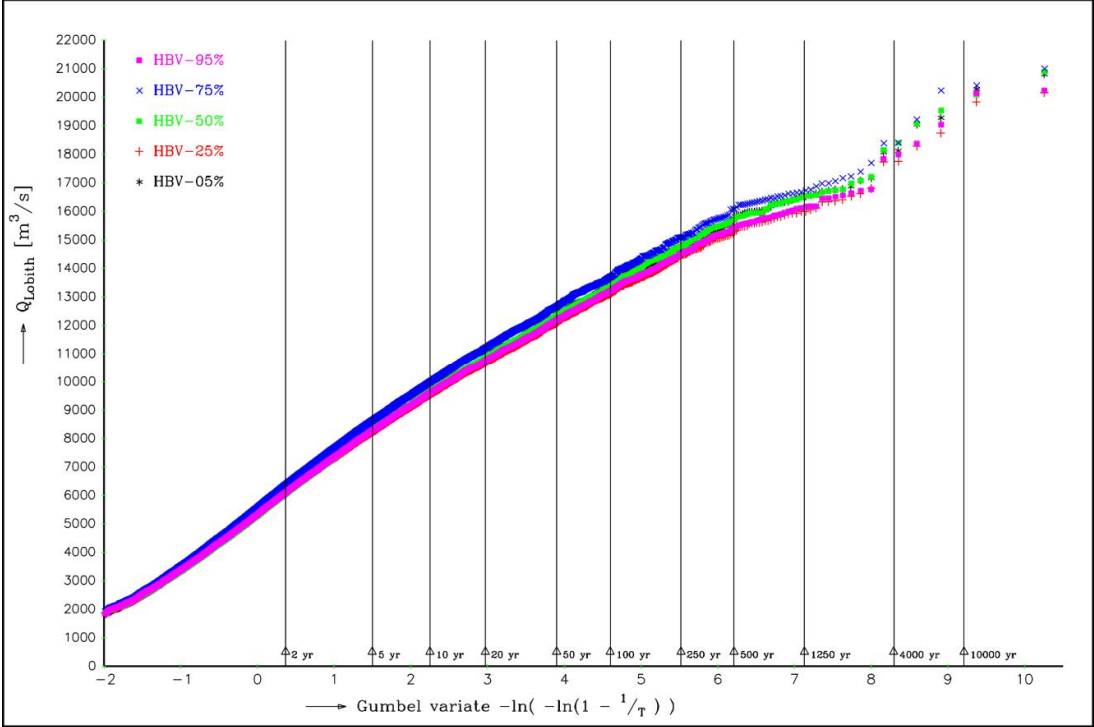


Figure 7.6 Frequency discharge curves for the river Rhine at Lobith for the five representative HBV parameter combinations using the first 20,000 years of the reference weather generator series for the Rhine

7.3 Uncertainty in hydrodynamic modelling

7.3.1 Uncertainty in Sobek

Just as in the other GRADE components several sources of uncertainty are present in the Sobek models for the Rhine and Meuse. These may be located in the model schematization, and/or consist of uncertainties in various model parameters (e.g. in the bed roughness, or in hydraulic structures, or in flooding mechanisms), and/or structural uncertainties due to various other (conceptual, algorithmic, numerical) errors in the modelling. Such uncertainties in the Sobek models should formally also be taken into account in a GRADE uncertainty analysis. Presently this has not yet been done. In the case of no flooding it is expected that ignoring the uncertainties in the hydrodynamic models does not significantly affect the results of the 'overall' GRADE uncertainty analysis. The nature of the hydrodynamic modelling then implies that the uncertainty in the discharges computed by Sobek is largely due to uncertainties in its input in the form of the lateral inflows produced by the hydrological (HBV) models of the contributing sub-basins.

7.3.2 Uncertainty in flooding

The assumption that the uncertainty in the Sobek models is relatively small may not be valid when flooding is included in the modelling. In Section 5.3 the impact of flooding due to overtopping and/or levee breaches in the upstream part of the river Rhine has already been considered. The results appear very sensitive to the variations in the dike height, which suggests that uncertainties in this flooding parameter may significantly affect the overall uncertainty of extreme discharges at Lobith in GRADE. The magnitude of the variations depicted in Figure 5.3 are not yet realistically representing the flooding induced uncertainties in the discharge at Lobith, because (physically) maximum variations of a flooding parameter were applied simultaneously for each location along the river. As a consequence flooding parameter induced uncertainty is overestimated in Figure 5.3.

7.4 Combining uncertainties

This section deals with the combination of the uncertainties in the weather generator component and the HBV parameters. Therefore, GRADE simulations for all possible mutual combinations of a synthetic weather series and a representative HBV parameter set were conducted. Each of these simulations yields a 20,000-year synthetic discharge series from which the annual maximum discharges associated with a particular return period can be obtained. From this set of return levels an overall estimate of the uncertainty in the discharge maximum must be derived. "Overall" here means the total uncertainty in the maximum discharge due to the two sources of uncertainty.

7.4.1 Reduction of computation time

Within GRADE the Sobek calculations are computationally most demanding, Although Sobek is used only for the simulation of annual maxima within the total simulation period (Section 5.1), its computation time remains substantial. In order to avoid the many (i.e. 55 for the Rhine and 120 for the Meuse) 20,000-year Sobek calculations required for the uncertainty analysis, a regression formula was derived to convert HBV estimates of extreme discharges to corresponding Sobek values. In this way, without doing all possible Sobek calculations, Sobek representative results could be obtained, which were used in the uncertainty analysis.

The regression formula is derived from the Sobek and HBV results of the 50.000-year reference GRADE simulation. The regression formula is calibrated on the 50,000 pairs of annual discharge extremes (according to GRADE with only HBV, and according to GRADE with HBV and Sobek). It is assumed that this regression is also valid for the HBV results obtained with the other synthetic weather series and the HBV-parameter sets that are used in the uncertainty analysis.

For the Rhine two regression formulae were derived, for the Sobek model with and without flooding. For the Meuse only one regression formula was derived since only one Sobek model (without flooding) is used. See Van den Boogaard et al. (2014) for more details about the regression formulae.

Figure 7.7 shows for the Rhine the regression of the Sobek annual maxima at Lobith (the version with flooding) on those simulated with HBV. The non-linear relation is well captured by the regression.

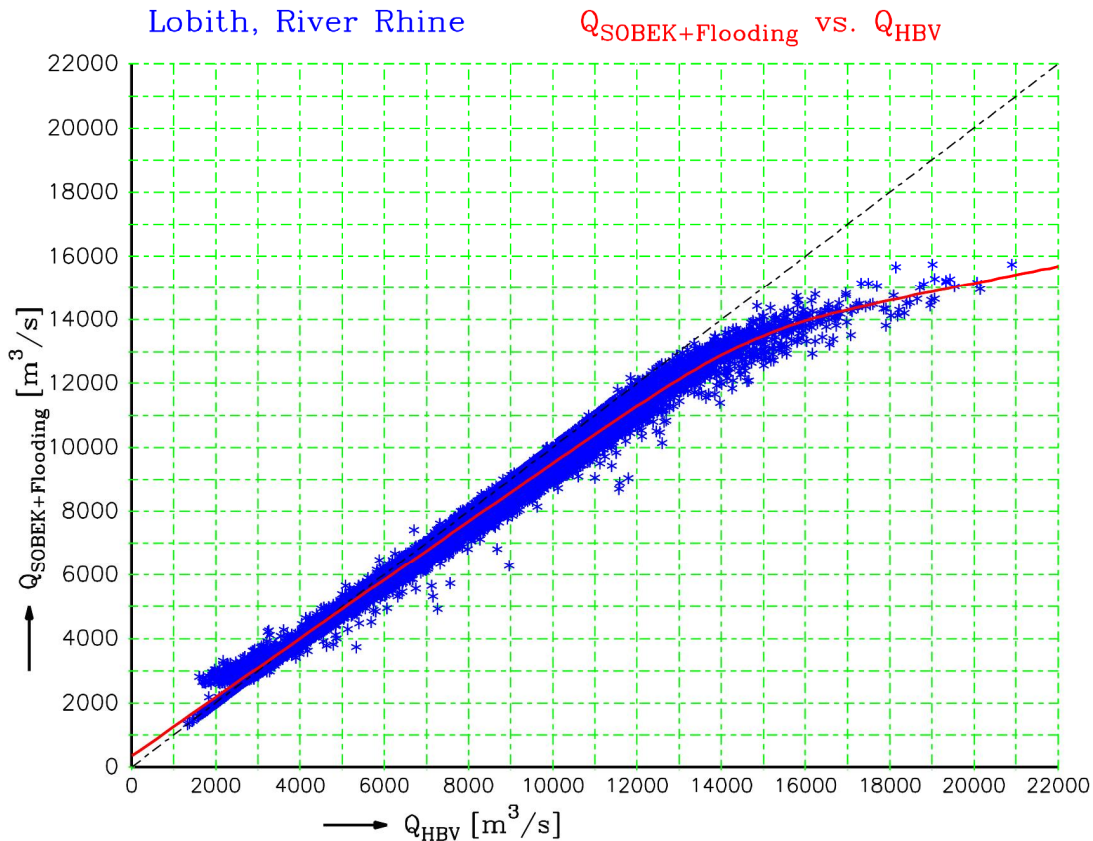


Figure 7.7 Scatterplot of Sobek and HBV calculated annual maximum discharges of the river Rhine at Lobith, computed in a GRADE simulation of length 50,000 years (Sobek version with flooding). The solid red curve represents the regression line

7.4.2 Procedure for combining uncertainties

By means of a specific example the (mathematical/numerical) procedure for the combination of the uncertainties in the two GRADE components is demonstrated.

Table 7.2 presents the set of annual maximum discharges for the Rhine at Lobith associated with a return period of 4000 years. They were derived from 11×5 GRADE simulations for the river Rhine (the eleven jackknife variations of the weather series combined with the five HBV-parameter sets). For ease of notation and reasoning the discharge found for the i -th synthetic weather series (WG i , with $1 \leq i \leq 11$) and the j -th HBV-parameter set ($1 \leq j \leq 5$) is denoted by $Q(i,j)$. In the table these $Q(i,j)$ are listed within the area with **light blue background**. In the GRADE simulations in this specific example the Sobek version with flooding was used. The other entries in Table 7.2 (marked with blue and red) denote various quantities that are derived from the $Q(i,j)$ matrix within the combination procedure of uncertainties (therefore Table 7.2 is also referred to as an *uncertainty matrix*). The meaning and the numerical recipes for the computation of these entries are now briefly described.

- i. The entries along the five columns in the rows with label “WG Mean” and “WG Spread” give the mean and standard deviation for each of the five HBV-parameter sets. These quantities are derived from Eqs. (1) and (2) by replacing $Q_{WG}(i)$ by $Q(i,j)$. WG Spread measures the uncertainty in the discharge *due to solely the uncertainty in the weather series*. From the table it can be seen that this spread varies from 362 to 446 m^3/s and thus to some extent depends on the HBV-parameter set that is used.
- ii. Similarly the entries in the last two columns of Table 7.2 (with labels “Mean HBV” and “Spread HBV”) give the mean and spread of the $Q(i,j)$ over the five HBV-parameter sets for each of the 11 synthetic weather series. These quantities are derived from Eqs. (3) and (4) by using $Q(i,j)$ instead of $Q_{HBV}(j)$. The spread then measures the uncertainty in the discharge *due to solely the uncertainty in the HBV-model parameters*. From the table it can be seen that this spread varies from 61 to 109 m^3/s . This relatively large range for the spread reflects a significant sensitivity to the different weather series. On the other hand, compared to the spreads found in (i) these values are about 4 times smaller, confirming that the uncertainty in the climate contributes more heavily to the uncertainty in the extreme discharges than the uncertainty in the hydrological models.
- iii. The overall mean m and standard deviation s are calculated from the mean and standard deviation for each HBV parameter set, taking into account the weights w_j :

$$m = \sum_{j=1}^5 w_j m_{WG}(j) \quad (5)$$

$$s = \sqrt{\sum_{j=1}^5 w_j [m_{WG}(j) - m]^2 + \sum_{j=1}^5 w_j s_{WG}^2(j)} \quad (6)$$

where $m_{WG}(j)$ and $s_{WG}(j)$ are the estimated mean and standard deviation for each HBV-parameter set derived in step i. The overall variance s^2 is thus a superposition of a variance in the ‘marginal’ means $m_{WG}(j)$ on the one hand, and a weighted mean of the marginal variances $s_{WG}^2(j)$ on the other hand. The overall mean and overall standard deviation that are thus derived from all the 11×5 estimates $Q(i,j)$ are listed in the second row from the bottom of Table 7.2. In this case they are 14,807 m^3/s and 414 m^3/s respectively.

Table 7.2 GRADE uncertainty matrix for the annual maximum discharge for the river Rhine at Lobith for a return period of 4000 years, according to Sobek with flooding

HBV ►	1 st Par. Comb (5%)	2 nd Par. Comb. (25%)	3 rd Par. Comb. (50%)	4 th Par. Comb. (75%)	5 th Par. Comb. (95%)	Mean HBV (m_{HBV})	Spread HBV (s_{HBV})
WG 1	14875	14737	14983	14967	14802	14892	102
WG 2	14845	14777	14898	14912	14774	14855	61
WG 3	15022	14818	14958	15024	14878	14939	79
WG 4	14915	14676	14926	14873	14701	14825	106
WG 5	14952	14811	14928	15013	14817	14912	81
WG 6	14738	14620	14736	14764	14618	14702	63
WG 7	14962	14764	15032	14971	14802	14920	109
WG 8	14586	14425	14603	14653	14522	14566	85
WG 9	14575	14447	14625	14694	14521	14588	93
WG 10	14784	14684	14918	14879	14683	14815	102
WG 11	14895	14754	14931	14932	14775	14869	80
Mean WG (m_{WG})	14832	14683	14867	14880	14717		
Spread WG (s_{WG})	446	409	436	378	362		
Overall mean (m): 14,807 [m³/s] Overall standard deviation (s): 414 [m³/s]							

The overall standard deviation s is used to construct a (pointwise) 95% confidence band for the frequency discharge curve (see Section 7.5).

In the present example of the description of the uncertainty analysis the discharge at Lobith associated with a return period of 4000 years was considered. The procedure can however be applied generally and the $Q(i,j)$ may be any value computed with GRADE. The procedure can thus be applied for any return period, any discharge (either from HBV or from Sobek, with or without flooding) and any location along the Rhine and Meuse.

In the next section the construction of the frequency discharge curve with uncertainty band for the Rhine with upstream flooding is presented. All frequency discharge curves with uncertainty bands are presented in Chapter 8.

7.5 Frequency discharge curve with uncertainty band

For the frequency discharge curve and its uncertainty two types of GRADE simulations were carried out for both river basins:

1. The 50,000-year reference GRADE simulation. In this simulation the reference synthetic weather series (based on all available historic weather data) is combined with the 50% HBV-parameter set.
2. A set of 20,000-year “uncertainty simulations”. In these GRADE simulations each of the jackknife based synthetic weather series is combined with each of the five HBV-parameter sets. For the Rhine this involves 11x5 and for the Meuse 24x5 20,000-year GRADE uncertainty simulations.

The frequency discharge curve is based on the annual maximum discharges from the reference simulation in 1. The simulations in 2. are used to construct a confidence band for the frequency discharge curve. The width of the confidence band is based on the overall standard deviations of the estimated return levels of extreme discharges from Eq. (6). For each return level, a confidence interval is obtained as $Q_T \pm z_{\gamma} s$, where Q_T is the estimate from the 50,000-year reference GRADE simulation and $z_{\gamma} = 1.96$ for a 95% confidence interval. All these symmetric 95% confidence intervals¹⁰ together constitute a pointwise 95% confidence band for the frequency discharge curve.

As an example Figure 7.8 shows the frequency discharge curve with 95% confidence band for the Rhine at Lobith where upstream flooding in Germany is taken into account. This uncertainty band represents the uncertainties owing to resampling from historical precipitation and temperature records of limited length and uncertain parameters in the HBV rainfall-runoff model. Uncertainties in flooding parameters and other uncertainties in the weather generator and the HBV model are discarded. The true uncertainty may therefore be larger than indicated by the confidence band. All frequency discharge curves, including that for the Rhine without flooding and that for the Meuse are presented in the next chapter.

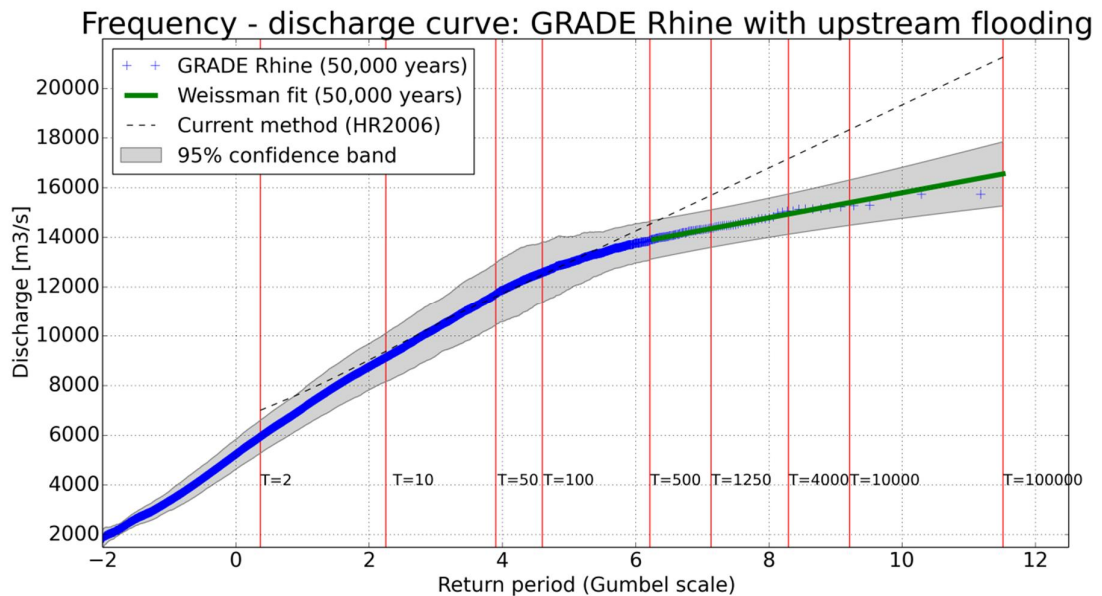


Figure 7.8 Frequency discharge curve for the Rhine at Lobith with 95% confidence band according to GRADE, including flooding in Germany

7.6 Limitations of the uncertainty analysis

With regard to the present representation and combination of uncertainties in GRADE the following limitations and/or issues for further investigation or improvement of the uncertainty analysis can be mentioned:

¹⁰ In theory such a symmetric confidence interval is only valid if for the estimated return level a Gaussian distribution can be assumed. For the extreme return levels this may not be true and even the assumption of a symmetric distribution is doubtful. Skew confidence intervals would then provide a better representation of the uncertainty. To obtain reasonably accurate skew confidence intervals GRADE computations for a much larger number of variations of the synthetic weather series and/or HBV-parameter sets will be required. This was not feasible within the present work.

- 1 For the determination of uncertainties in return levels of extreme multi-day rainfall and extreme river discharge a jackknife method was used. The accuracy of the jackknife estimate S_{WG} (see Eq. (1) in Section 7.1) is known to be low. For the Rhine basin a second set of 11 jackknife series was formed by leaving out different 5-year blocks from the baseline series (Schmeits et al., 2014a). Though the results were similar for the standard deviations of the estimated return levels of the 4-day and 10-day precipitation maxima, marked differences were found for the 20-day precipitation maxima. This demonstrates that the standard deviations of the estimated return levels are uncertain. This uncertainty may explain a large part of the differences found between the relative standard deviations for the Rhine and Meuse basins.
- 2 The uncertainty analysis in the hydrological models is limited to the uncertainty in the parameters of the HBV models of the sub-basins. Structural uncertainties referring to errors in the conceptual modelling have not been considered. For hydrological models such as HBV this structural uncertainty might be significant due to the highly schematized representation and approximations of complex rainfall-runoff processes.
- 3 In the hydro-dynamical Sobek models no uncertainties have been taken into account. It has been assumed that (as long as flooding is not included in the modelling) these uncertainties are small compared to the uncertainties in the other GRADE components. However, uncertainties in flooding parameters, primarily the height of dikes, may significantly contribute to the overall uncertainty in the discharges. To verify this quantitatively, probability distributions must be assigned to the flooding parameters of interest and GRADE simulations have to be carried out for various variations of the flooding parameters.

8 Final results of the GRADE simulations

This chapter summarizes all results of the GRADE simulations in the form of figures and tables. The frequency discharge curves with confidence bands and frequency discharge tables for the Meuse and Rhine are given in Section 8.1. For comparison, the frequency discharge curves for the current method (HR2006) are also presented. In Section 0 the GRADE flood hydrographs with uncertainty bands are presented and compared with the hydrographs for the current method (HR2006). For a fair comparison the latter are scaled to the 1250-year peak discharges from the GRADE simulations.

8.1 Frequency discharge curves

The frequency discharge curve for the Meuse with 95% confidence band up to a return period of 100,000 years is presented in Figure 8.1. In Table 8.1 the results are given for specific return periods. The ordered observed annual maxima fall within the 95% confidence band. The confidence band becomes relatively wide at long return periods. The relative width is 26% at $T = 10$ years, 36% at $T = 1250$ years and 72% at $T = 100,000$ years.

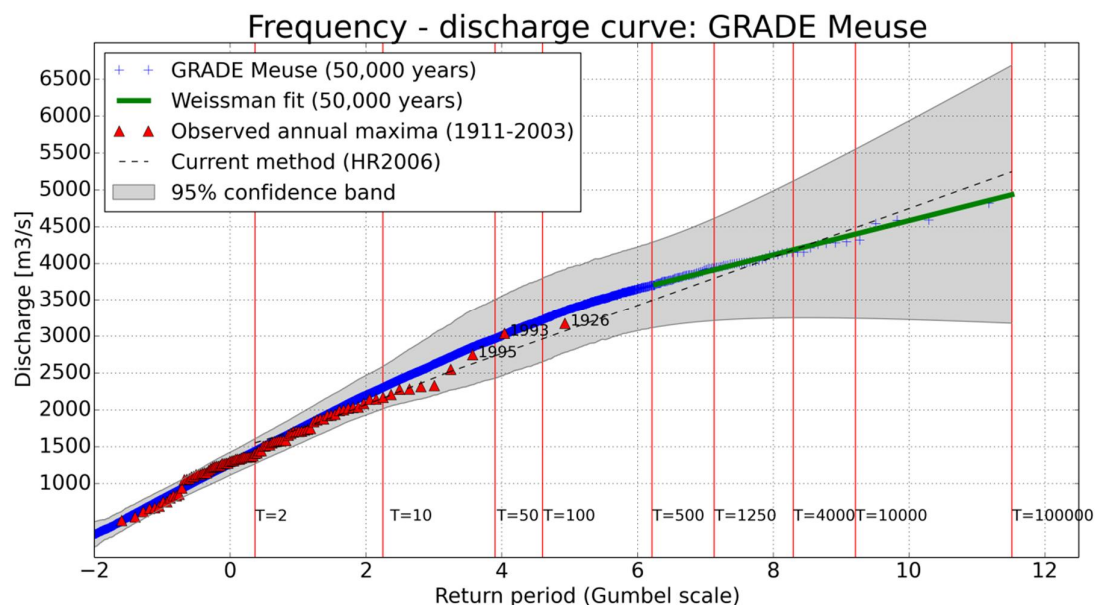


Figure 8.1 Frequency discharge curve with 95% confidence band for the Meuse at Borgharen

Table 8.1 Frequency discharge table for the Meuse at Borgharen

Return Period [years]	Discharge at Borgharen [m^3/s]	Width 95% confidence band [m^3/s]
5	1970	470
10	2300	588
50	2970	1098
100	3220	1137
250	3520	1137
500	3700	1176
1250	3910	1411
4000	4180	1882
10,000	4400	2313
100,000	4930	3528

The frequency discharge curve for the Rhine at Lobith with upstream flooding up to a return period of 100,000 years is presented in Figure 8.2. The discharges corresponding to specific return periods are listed in Table 8.2.

As a result of the upstream flooding, there is no strong increase of the width of the 95% confidence band at long return periods (Figure 8.2). In fact, the width of the uncertainty band first decreases after which it starts to increase again. This can be explained as follows. Between $T \approx 100$ and 500 years the width of the uncertainty band reduces as a result of flooding¹¹. Beyond $T = 500$ years the width of the uncertainty band is determined by the standard deviation of the Weissman fit which gradually increases with increasing T at long return periods.

The relative width of the uncertainty band is 21% at $T = 10$ years, 11% at $T = 1250$ years and 16% at $T = 100,000$ years. The uncertainty of flooding parameters is not included in these figures. The ordered observed annual maximum discharges all fall within the confidence band.

¹¹ In particular, flooding reduces large discharge peaks (larger than $\approx 12,000 m^3/s$) but since the uncertainty is presented as a symmetric confidence band both the upper- and lower limit of the confidence band are equally affected.

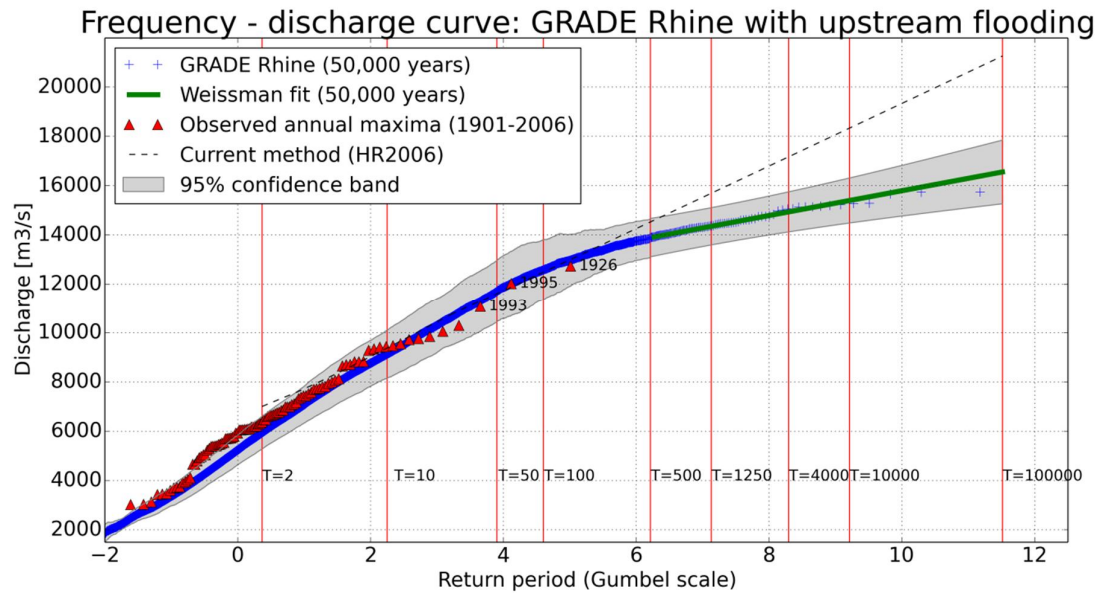


Figure 8.2 Frequency discharge curve with 95% confidence band for the Rhine at Lobith, with upstream flooding

Table 8.2 Frequency discharge table for the Rhine at Lobith, with upstream flooding

Return Period [years]	Discharge at Lobith [m ³ /s]	Width 95% confidence band [m ³ /s]
5	7970	1725
10	9130	1960
50	11,710	2509
100	12,580	2470
250	13,390	1646
500	13,890	1568
1250	14,350	1529
4000	14,940	1620
10,000	15,400	1842
100,000	16,560	2587

8.2 Flood hydrographs

Figure 8.4 gives the 1250-year hydrograph for the Meuse at Borgharen, which has a peak of 3910 m³/s. The hydrograph is based on all hydrographs with peak discharges > 3500 m³/s. In grey, the pointwise 95% uncertainty band is given.

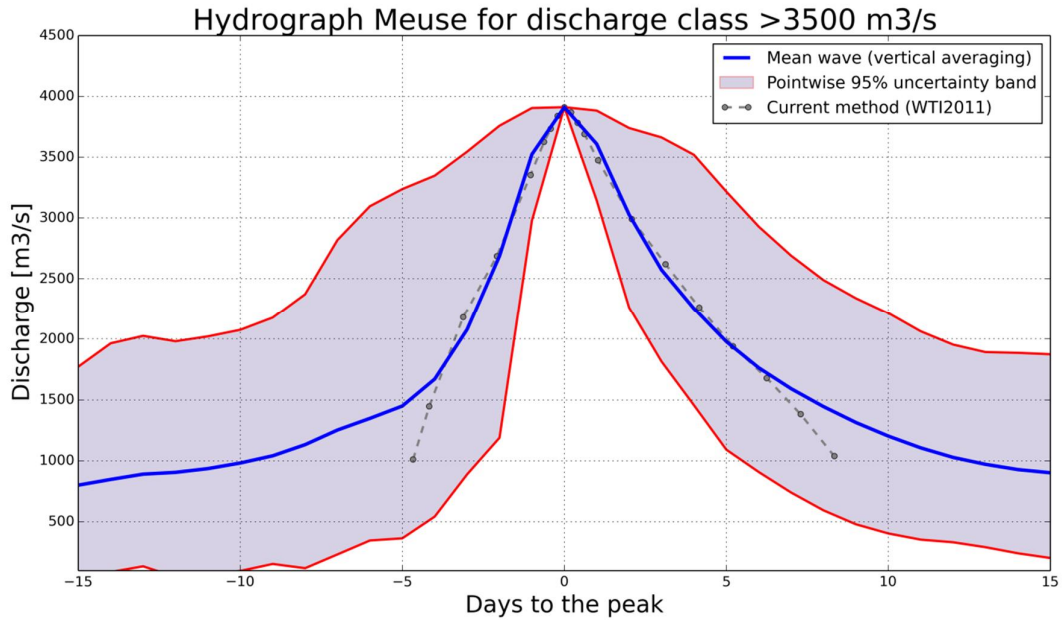


Figure 8.4 Flood hydrograph with pointwise 95% uncertainty band for the Meuse at Borgharen. The peak corresponds with the 1250-year discharge of 3910 m³/s

Figure 8.5 gives the 1250-year hydrograph for the Rhine at Lobith with upstream flooding, which has a peak of 14,350 m³/s. The hydrograph is based on all hydrographs with peak discharges > 14,000 m³/s. In grey, the pointwise 95% uncertainty band is given.

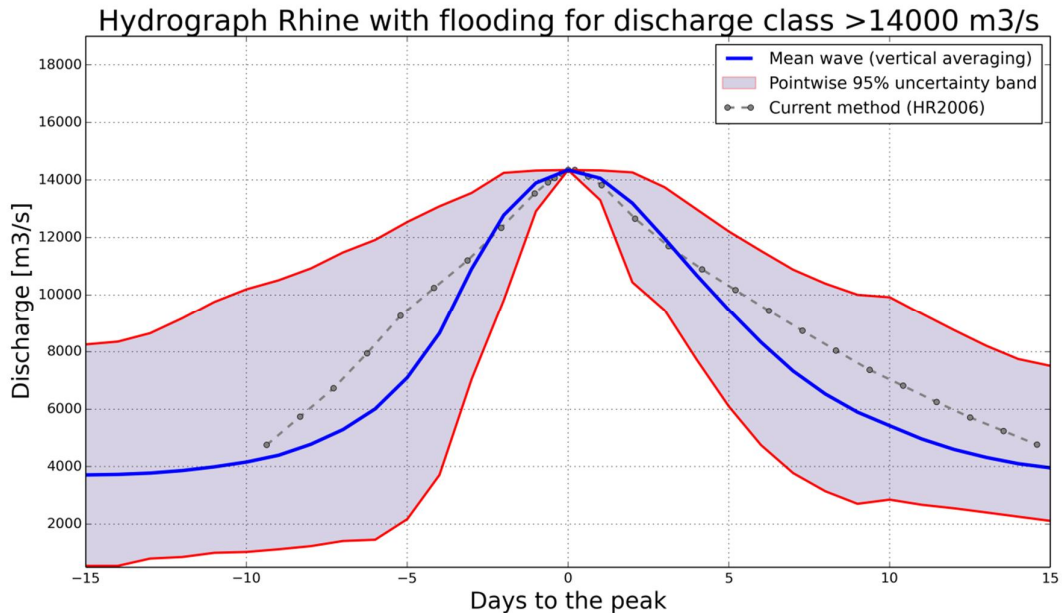


Figure 8.5 Flood hydrograph with pointwise 95% uncertainty band for the Rhine at Lobith with upstream flooding. The peak corresponds with the 1250-year discharge of 14,350 m³/s

Figure 8.6 presents the 1250-year hydrograph for the Rhine at Lobith without upstream flooding, which has a peak of 16,560 m³/s. The hydrograph is based on all hydrographs with peak discharges > 15,500 m³/s. In grey, the pointwise 95% uncertainty band is given. The flood hydrograph is smaller than in the case of upstream flooding.

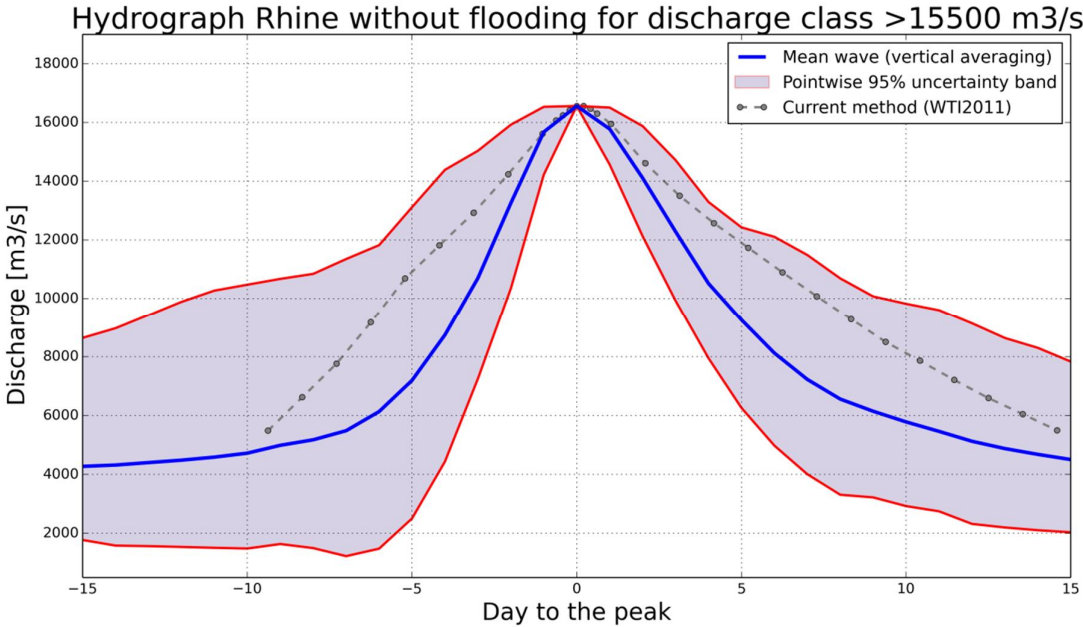


Figure 8.6 Flood hydrograph with pointwise 95% uncertainty band for the Rhine at Lobith **without** upstream flooding. The peak corresponds with the 1250-year discharge of 16,560 m³/s

9 Conclusions

Grade is an instrument that consists of a stochastic weather generator, a rainfall – runoff model and a hydrodynamic model. The output is a discharge series of 50,000 years for the river Rhine or Meuse. This time series is used to derive the probability distribution of the annual maximum discharge and corresponding flood hydrographs.

Overall conclusions:

- The current version of GRADE is ready to be used for the determination of the design discharge and corresponding shape of the flood hydrograph.
- GRADE provides satisfactory results for the simulation of discharge extremes. For the range where measurements are available, the GRADE results describe the distribution of the observed extremes well. For higher discharges, the effect of upstream flooding along the Rhine is included in GRADE. This leads to a reduction of the discharge compared to the situation without flooding. This reduction is not accounted for in the current method.
- GRADE provides more realistic flood hydrographs than the current method. Unlike the current method, it takes into account the influence of the height of the peak on the width of the peak. Upstream flooding leads to wider flood hydrographs.

Quality of the GRADE components:

- The weather generator in GRADE which is based on multi-site nearest-neighbour resampling reproduces the distribution of the extreme multi-day rainfall in the winter half-year well.
- The HBV rainfall-runoff model in GRADE satisfactorily simulates the discharges of the Rhine and the Meuse including the (major) sub-basins. For some (small) sub-basins the performance is less well. This can be attributed to geological and anthropogenic influences or to a lag time shorter than 1 day.
- Although the routing modules in GRADE do not cover the most upstream parts of the rivers, GRADE simulates the discharges at Lobith and Borgharen well.

Uncertainties in GRADE:

- The uncertainties in the extreme discharges owing to the individual components are separately analyzed.
- The uncertainty in the extreme discharges owing to the limited length of the historical precipitation and temperature series used in the weather generator dominates the uncertainty associated with the parameter uncertainty of the HBV rainfall-runoff model. Uncertainties in the HBV model concept and schematization (i.e. structural uncertainties of HBV) are not included.
- The uncertainties owing to resampling from historical precipitation and temperature series of limited length and uncertain HBV parameters are reduced in the case of upstream flooding. The uncertainty bands in GRADE do not account for the uncertainty in flooding parameters yet. For the river Rhine at Lobith however it was found that the impact of upstream flooding is particularly sensitive to variations in the dike height along parts of the river stretches in Germany.

Possible other applications of GRADE:

- With the present GRADE instrument it is possible to make ‘what-if’ scenario analyses, such as the impact of climate change, changes in land use, impacts of river works and temporary measures during flood events (such as e.g., placing of sandbags).
- Although the focus in the application of GRADE is placed on the border gauging locations of Lobith and Borgharen, GRADE also provides information for other locations along the main branches upstream of Lobith and Borgharen, and may also be used for the main tributaries of the Rhine.

Acknowledgements

Over the past years, many people and institutes contributed to the development of GRADE by either developing the method and models, or by delivering the necessary information and data to build and calibrate the models.

In particular, we are grateful to Robert Leander, Erwin Wolters, and Maurice Schmeits who contributed at KNMI to the present weather generators for the Rhine and Meuse basins.

At Deltares, Nienke Kramer, Willem van Verseveld and Hessel Winsemius had a significant role in the hydrological and hydraulic modelling, as well as in the (statistical) analysis of the GRADE results.

At Rijkswaterstaat, Hendrik Buiteveld and Rita Lammersen provided us with the necessary information and useful feedback.

The German Federal Institute for Hydrology (BfG) has been partner in the project and has made essential contributions. The hydrological and hydraulic models were developed within the cooperation between the BfG and Rijkswaterstaat (WVL).

The HYRAS 2.0 precipitation dataset that was used in the weather generator for the Rhine basin was made available by the German Weather Service (DWD) via the BfG. The E-OBS precipitation and temperature dataset was developed in the framework of the EU-FP6 project ENSEMBLES (<http://ensembles-eu.metoffice.com>). We acknowledge the meteorological institutes that provided the data for these gridded data sets.

The daily precipitation and temperature data for the weather generator for the Meuse basin were supplied by Météo France and the Royal Meteorological Institute of Belgium (RMIB). The precipitation and temperature records of Aachen were obtained from the DWD website. RMIB provided also area-average daily precipitation and potential evapotranspiration data for sub-basins in the Belgian part of the Meuse basin.

The historical discharge records for the Walloon part of the Meuse basin were supplied by MET-Sethy. The discharge data for the French part of the Meuse basin were taken from the hydrological databank Banque Hydro (<http://www.hydro.eaufrance.fr/>).

The historical discharge records for the Rhine basin have been provided by the BfG and by the International Commission for the Hydrology of the Rhine Basin (CHR), except for the Swiss part of the basin where the discharge records were provided by the Federal Office for the Environment (FOEN).

The schematization of the hydrological model for the Rhine basin has been made available by the BfG. The schematization of the lakes in Switzerland was provided by FOEN.

The hydraulic models for the Rhine were provided by the BfG and Landesamt für Natur, Umwelt und Verbraucherschutz Nordrhein-Westfalen (LANUV NRW). Hessisches Landesamt für Umwelt und Geologie (HLUG), Landesanstalt für Umwelt, Messungen und Naturschutz Baden-Württemberg (LUBW), Landesamt für Umwelt, Wasserwirtschaft und Gewerbeaufsicht Rheinland-Pfalz gave expert advice on incorporating the effects of flooding behind the dikes in the Sobek model for the Rhine.

HKV Consultants performed calculations with the GRADE instrument to obtain the sensitivity to the flooding parameters in the Sobek model of the Rhine and performed a first analysis of the effects of flooding of the Meuse around Liège.

Relevant GRADE reports

- Beersma, J.J., Buishand, T.A. and Schmeits, M.J., 2014. Technical description of the KNMI rainfall generators for the Rhine and Meuse basins. Technical Report, TR-345, KNMI, De Bilt, The Netherlands.
- Buishand, T.A. and Leander, R., 2011. Rainfall generator for the Meuse basin: Extension of the base period with the years 1999-2008. KNMI publication 196-V, KNMI, De Bilt, The Netherlands.
- Hegnauer, M., 2013. Technical documentation GRADE part III: Models Meuse. Deltares report 1207771-003-ZWS-0015, Deltares, Delft, The Netherlands.
- Hegnauer, M., 2014. Improvements of the (coupling of) routing components in Fews-GRADE Rhine. Deltares report 1209424-004-ZWS-0005, Deltares, Delft, The Netherlands.
- Hegnauer, M. and Becker, A., 2013. Technical documentation GRADE part II: Models Rhine. Deltares report 1207771-003-ZWS-0013, Deltares, Delft, The Netherlands.
- Hegnauer, M. and Van Verseveld, W., 2013. Generalised likelihood uncertainty estimation for the daily HBV model in the Rhine Basin, Part B: Switzerland. Deltares report 1204290-005-ZWS-0002, Deltares, Delft, The Netherlands.
- Kramer, N., 2012. GRADE 2012: Procedure to derive the design hydrograph – phase 1. Deltares report, Deltares, Delft, The Netherlands.
- Kramer, N. and Schroevers, R., 2008. Generator of rainfall and discharge extremes (GRADE): Part F. Report of project Q4424, Deltares, Delft, The Netherlands.
- Kramer, N., Beckers, J. and Weerts, A., 2008. Generator of rainfall and discharge extremes (GRADE): Part D&E. Report of project Q4424, Deltares, Delft, The Netherlands.
- Kramer, N., Winsemius, H.C.W. and De Keizer, O., 2010. GRADE 2009. Deltares report 1202382-005-VEB-0002, Deltares, Delft, The Netherlands.
- Schmeits, M.J., Wolters, E.L.A., Beersma, J.J. and Buishand, T.A., 2014a. Rainfall generator for the Rhine basin: Description of simulations using gridded precipitation datasets and uncertainty analysis. KNMI publication 186-VII, KNMI, De Bilt, The Netherlands.
- Schmeits, M.J., Beersma, J.J. and Buishand, T.A., 2014b. Rainfall generator for the Meuse basin: Description of simulations with and without a memory term and uncertainty analysis. KNMI publication 196-VI, KNMI, De Bilt, The Netherlands.
- Van den Boogaard, H.F.P., Beersma, J.J., and Hegnauer, M., 2014. GRADE uncertainty analysis. Deltares report 1209424-004-ZWS-0003, Deltares, Delft, The Netherlands.
- Winsemius, H.C.W., van Verseveld, W., Weerts, A. and Hegnauer, M., 2013. Generalised likelihood uncertainty estimation for the daily HBV model in the Rhine Basin, Part A: Germany. Deltares report 1207771-003-ZWS-0018, Deltares, Delft, The Netherlands.

Literature

- Aalders, P., Warmerdam, P.M.M. and Torfs, P.J.J.F., 2004. Rainfall generator for the Meuse basin: 3,000 year discharge simulations in the Meuse basin. Report No. 124, Sub-department Water Resources, Wageningen University, Wageningen, The Netherlands.
- Beersma, J.J. and Buishand, T.A., 2007. Drought in the Netherlands – Regional frequency analysis versus time series simulation. *Journal of Hydrology*, 347, 332-346.
- Beersma, J.J., 2011. Rainfall generator for the Rhine basin: Sensitivity to the composition of the feature vector and passive simulations. KNMI publication 186-VI, KNMI, De Bilt, The Netherlands.
- Belz, J.U., Brahmmer, G., Buiteveld, H., Engel, H., Grabher, R., Hodel, H., Krahe, P., Lammersen, R., Larina, M., Mendel, H.-G., Meuser, A., Müller, G., Plonka, B., Pfister, L., and Van Vuuren, W., 2007. Das Abflussregime des Rheins und seiner Nebenflüsse im 20. Jahrhundert, Analyse, Veränderungen und Trends. CHR report I-22, International Commission for the Hydrology of the Rhine Basin (KHR/CHR), Lelystad, The Netherlands.
- Berglöv, G., German, J., Gustavsson, H., Harbman, U., and Johansson, B., 2009. Improvement HBV model Rhine in FEWS, Final report. Hydrology report, No. 112, SMHI, Norrköping, Sweden.
- Beven, K.J., 2001. *Rainfall - Runoff Modelling: The Primer*, Wiley Chichester, England.
- Beven, K.J. and Binley, A.M., 1992. The future of distributed models: model calibration and uncertainty prediction. *Hydrol. Process.*, 6, 279–298
- BfG, 2008. Erstellung, Kalibrierung und Validierung des Sobek-Modells für die Rheinstrecke zwischen den Pegeln Andernach und Lobith. Report No. 1593, Bundesanstalt für Gewässerkunde (BfG), Koblenz, Germany.
- Booij, M.J., 2002. Appropriate modelling of climate change impacts on river flooding. PhD thesis, University Twente, Enschede, The Netherlands.
- Booij, M.J., 2005. Impact of climate change on river flooding assessed with different spatial model resolutions. *Journal of Hydrology*, 303, 176-198.
- Bos, H., 1993. Verloop daggemiddelde afvoer Borgharen, periode 1911-1991 (in Dutch). RIZA werkdocument 92.112X. Rijkswaterstaat RIZA, Lelystad, The Netherlands. Unpublished document.
- Brandsma, T. and Buishand, T.A., 1999. Rainfall generator for the Rhine basin: Multi-site generation of weather variables by nearest-neighbour resampling. KNMI publication 186-II, KNMI, De Bilt, The Netherlands.
- Buishand, T.A., 2007. Estimation of a large quantile of the distribution of multi-day seasonal maximum rainfall: the value of stochastic simulation of long-duration sequences. *Climate Research*, 34, 185-194.
- Buishand, T.A. and Brandsma, T., 2001. Multi-site simulation of daily precipitation and temperature in the Rhine basin by nearest-neighbour resampling. *Water Resources Research*, 37, 2761 – 2776.
- Buishand, T.A. and Leander, R., 2011. Rainfall generator for the Meuse basin: Extension of the base period with the years 1999-2008. KNMI publication 196-V, KNMI, De Bilt, The Netherlands.
- De Joode, A., 2007. WAQUA-Model Niederrhein von Andernach nach Lobith, Aufbau, Kalibrierung und Verifizierung des WAQUA-Modells für 1995 und 2005. im Auftrag von RWS-RIZA projectnummer 10244 / 4500052750 (also available in Dutch), Meander Advies en Onderzoek, Utrecht, The Netherlands.

- Dewals, B., Huismans, Y., Archambeau, P., De Keizer, O., Detrembleur, S., Buiteveld, H., and Pirroton, M., 2012. Hydraulic modelling of the Meuse: Hydraulic modelling from Amspin to Maaseik. WP1 report action 6 Amice, EPAMA, Liège, Belgium. Unpublished document.
- De Wit, M., 2008. Van Regen tot Maas, Grensoverschrijdend waterbeheer in droge en natte tijden, Veen Magazines, Diemen, Nederland.
- Diermanse, F.L.M., van Kappel, R.R., Ogink, H.J.M. and Heynert, K.V., 2000. Analysis of the instrumentation for computing design discharges. WL | delft hydraulics, Delft, The Netherlands.
- Disse, M. and Engel, H., 2001 Flood events in the Rhine basin: genesis, influences and mitigation. *Nat. Hazards*, 23, 271–290, doi:10.1023/a: 1011142402374.
- Eberle, M., Buiteveld, H., Beersma, J., Krahe, P. and Wilke, K., 2002. Estimation of extreme floods in the Rhine basin by combining precipitation-runoff modelling and a rainfall generator. In: *Proceedings International Conference on Flood Estimation*, Berne, 2002 (M. Spreafico and R. Weingarter, Eds.), 459-468. CHR report II-17. International Commission for the Hydrology of the Rhine Basin (KHR/CHR), Lelystad, The Netherlands.
- Eberle, M., Buiteveld, H., Krahe, P. and Wilke, K., 2005. Hydrological modelling in the Rhine basin, Part III: Daily HBV model for the Rhine basin. Report No. 1451, Bundesanstalt für Gewässerkunde (BfG), Koblenz, Germany.
- Haylock, M.R., Hofstra, N., Klein Tank, A.M.G., Klok, E.J., Jones, P.D. and New, M., 2008. A European daily high-resolution gridded data set of surface temperature and precipitation for 1950-2006. *Journal of Geophysical Research*, 113, D20119, doi: 10.1029/2008JD010201.
- Hegnauer, M., 2013. Technical documentation GRADE part III: Models Meuse. Deltares report 1207771-003-ZWS-0015, Deltares, Delft, The Netherlands.
- Hegnauer, M., 2014. Improvements of the (coupling of) routing components in Fews-GRADE Rhine. Deltares report 1209424-004-ZWS-0005, Deltares, Delft, The Netherlands.
- Hegnauer, M. and Becker, A., 2013. Technical documentation GRADE part II: Models Rhine. Deltares report 1207771-003-ZWS-0013, Deltares, Delft, The Netherlands.
- Hegnauer, M. and Van Verseveld, W., 2013. Generalised likelihood uncertainty estimation for the daily HBV model in the Rhine Basin, Part B: Switzerland. Deltares report 1204290-005-ZWS-0002, Deltares, Delft, The Netherlands.
- HKV, 2011. Sobek-Models Rhine for Hval and GRADE including flood areas behind dikes. HKV report PR2140.10, Lelystad, The Netherlands.
- Kramer, N., 2012. GRADE 2012: Procedure to derive the design hydrograph – phase 1. Deltares report, Deltares, Delft, The Netherlands.
- Kramer, N. and Schroevers, R., 2008. Generator of rainfall and discharge extremes (GRADE): Part F. Report of project Q4424, Deltares, Delft, The Netherlands.
- Kramer, N., Beckers, J. and Weerts, A., 2008. Generator of rainfall and discharge extremes (GRADE): Part D&E. Report of project Q4424, Deltares, Delft, The Netherlands.
- Kramer, N., Winsemius, H.C.W., and De Keizer, O., 2010. GRADE 2009, Deltares report 1202382-005-VEB-0002, Deltares, Delft, The Netherlands.
- Lammersen R., 2004. Grenzüberschreitende Auswirkungen von extremem Hochwasser am Niederrhein, final report, Deutsch-Niederländische Arbeitsgruppe Hochwasser, Düsseldorf, Germany (also available in Dutch, Arnhem, The Netherlands).
- LANUV NRW, 2010. Hydraulische Studie zur Abfluss- und Strukturverbesserung am Niederrhein – HyStAT. HKV Hydrokontor for LANUV, Projekt Nr. P09.006, Aachen, Germany.

- Leander, R. and Buishand, T.A., 2004a. Rainfall generator for the Meuse basin: Inventory and homogeneity analysis of long daily precipitation records. KNMI publication 196-II, KNMI, De Bilt, The Netherlands.
- Leander, R., and Buishand, T.A., 2004b. Rainfall generator for the Meuse basin: Development of a multi-site extension for the entire drainage area. KNMI publication 196-III, KNMI, De Bilt, The Netherlands.
- Leander, R., Buishand, T.A., Aalders, P. and de Wit, M.J.M., 2005. Estimation of extreme floods of the Meuse using a stochastic weather generator and a rainfall-runoff model. *Hydrological Sciences Journal*, 50, 1089-1103.
- Leander, R. and Buishand, T.A., 2007. Resampling of regional climate model output for the simulation of extreme river flows. *Journal of Hydrology*, 332, 487-496.
- Leander, R. and Buishand, T.A., 2008. Rainfall generator for the Meuse basin: Description of 20,000-year simulations. KNMI publication 196-IV, KNMI, De Bilt, The Netherlands.
- Leander, R. and Buishand, T.A., 2009. A daily weather generator based on a two-stage resampling algorithm. *Journal of Hydrology*, 374, 185-195.
- Lindström, G., Johansson, B., Persson, M., Gardelin, M. and Bergström, S., 1997. Development and test of the distributed HBV-96 hydrological model. *Journal of Hydrology*, 201, 272-288.
- Meijer D.G., 2009. Aktualisierung des SOBEK-Modells Iffezheim/Maxau – Andernach; Erstellung der BASELINE-Datensätze und der SOBEK-Modelle, hydraulische und morphologische Modellkalibrierung und –verifizierung, Interner Bericht, Bundesanstalt für Gewässerkunde (BfG), Koblenz, Germany.
- Ministerie van Verkeer en Waterstaat, 2007. Hydraulische Randvoorwaarden primaire waterkeringen. Ministerie van Verkeer en Waterstaat, Augustus 2007, ISBN: 978-90-369-5761-8, Den Haag, Nederland.
- Paarlberg, A.J. and Barneveld, H.J., 2013. GRADE: Gevoeligheidsanalyse naar het effect van de mijnverzakkingsgebieden bij Luik op de topafvoer en de golfvorm bij Eijsden. HKV report PR2479.20, Lelystad, The Netherlands.
- Parmet, B.W.A.H. and Van Bennekom, A., 1998. Bemessungsabfluß in den Niederlanden; menschliche Einflüsse und andere Unsicherheiten. Rijkswaterstaat RIZA, Lelystad, The Netherlands.
- Parmet, B.W.A.H., Buishand, T.A., Brandsma, T. and Mülders, R., 1999. Design discharge of the large rivers in the Netherlands - towards a new methodology. In: *Hydrological Extremes: Understanding, Predicting, Mitigating* (L. Gottschalk, J.-C. Olivry, D. Reed and D. Rosbjerg, Eds.), 269-272. IAHS Publication No. 255, IAHS Press, Institute of Hydrology, Wallingford, UK.
- Passchier, R.H., 1996. Evaluation hydrological model packages. Delft Hydraulics report Q2044, Delft, The Netherlands.
- Patzke, S., 2007. GRADE. WL | Delft Hydraulics report Q4424, Delft, The Netherlands
- Rauthe, M., Steiner, H., Riediger, U., Mazurkiewicz, A. and Gratzki, A., 2013. A central European precipitation climatology – Part I: Generation and validation of a high resolution gridded daily data set (HYRAS). *Meteorologische Zeitschrift*, 22, 235-256.
- Schmeits, M.J., Wolters, E.L.A., Beersma, J.J. and Buishand, T.A., 2014a. Rainfall generator for the Rhine basin: Description of simulations using gridded precipitation datasets and uncertainty analysis. KNMI publication 186-VII, KNMI, De Bilt, The Netherlands.
- Schmeits, M.J., Beersma, J.J. and Buishand, T.A., 2014b. Rainfall generator for the Meuse basin: Description of simulations with and without a memory term and uncertainty analysis. KNMI publication 196-VI, KNMI, De Bilt, The Netherlands.
- Steinrücke, J., Fröhling, B. and Weißhaupt, R., 2012. HYMOG - Hydrologische Modellierungsgrundlagen im Rheingebiet. KHR Bericht I-24, Internationale Kommission für die Hydrologie des Rheingebietes (KHR/CHR), Lelystad, The Netherlands.

- Tu, M., 2006. Assessment of the effects of climate variability and land use change on the hydrology of the Meuse river basin. PhD Thesis, UNESCO-IHE, Delft, The Netherlands.
- Udo, J. and Termes, P., 2013. Bepalen variatie dijkverstromingsparameters. Memorandum HKV, PR2479.30, 4 Oktober 2013, Lelystad, The Netherlands. Unpublished document.
- Ulbrich, U. and Fink, A., 1995. The January 1995 flood in Germany: Meteorological versus hydrological causes. *Phys. Chem. Earth*, 20, 439–444.
- Van den Boogaard, H.F.P., Beersma, J.J., and Hegnauer, M., 2014. GRADE uncertainty analysis. Deltares report 1209424-004-ZWS-0003, Deltares, Delft, The Netherlands.
- Van der Veen, R., Lammersen, R., Kroekenstoel, D.F. and Brinkmann, M., 2004. Grenzüberschreitende Auswirkungen von extremem Hochwasser am Niederrhein, Teilbericht Eingabedaten für das DSS Niederrhein-Rheinzeige. Deutsch-Niederländische Arbeitsgruppe Hochwasser, Düsseldorf, Germany (also available in Dutch, Arnhem, The Netherlands).
- Van Deursen, W., 2004. Afregelen HBV model Maasstroomgebied. Rapportage aan RIZA, Carthago Consultancy, Rotterdam, The Netherlands. Unpublished document.
- Van Vuuren, W., 2003. Evaluatie HBV-simulaties voor het stroomgebied van de Ourthe in de periode 1968 t/m 1998. Rijkswaterstaat RIZA Memo WSR 2002-22, Lelystad, The Netherlands. Unpublished document.
- Waterloopkundig Laboratorium en EAC-RAND, 1993a. Toetsing uitgangspunten rivierdijkversterkingen, deelrapport 2: maatgevende belastingen. Emmeloord/Delft, The Netherlands.
- Waterloopkundig Laboratorium en EAC-RAND, 1993b. Toetsing uitgangspunten rivierdijkversterkingen, aanvullend deelrapport 2: werklijn Rijn en Maas. Emmeloord/Delft, The Netherlands.
- Weissman, I., 1978. Estimation of parameters and large quantiles based on the k largest observations. *Journal of the American Statistical Association*, 73, 812-815.
- Winsemius, H.C.W., van Verseveld, W., Weerts, A. and Hegnauer, M., 2013. Generalised likelihood uncertainty estimation for the daily HBV model in the Rhine Basin Part A: Germany. Deltares report 1207771-003-ZWS-0018, Deltares, Delft, The Netherlands.
- Wijbenga, J.H.A., Paarlberg, A.J., Vieira da Silva, J. and van Wijk, G.P., 2008. Grenzüberschreitende Abstimmung von Hochwasserreduzierende Maßnahmen – 2-D Berechnungen mit WAQUA. Report HKV consultants for RWS- Waterdienst, PR1350 (also available in Dutch), Lelystad, The Netherlands.